COO-3253-5

NOTICE

PORTIONS OF THIS REPORT ARE ILLEGIBLE. It has been reproduced from the best available copy to permit the broadest possible availability.

Research Proposal

to

U. S. Energy Research and Development Administration

"INTEGRO-DIFFERENTIAL EQUATION ANALYSIS AND RADIOISOTOPE IMAGING SYSTEMS"

[Continuation of E(11-1)-3253]

Prof. Hiram Hart

THE CITY COLLEGE OF
THE CITY UNIVERSITY of NEW YORK

MASTER

DISTRIBUTION OF THIS DOCUMENT IS UNLIMITED

DISCLAIMER

This report was prepared as an account of work sponsored by an agency of the United States Government. Neither the United States Government nor any agency Thereof, nor any of their employees, makes any warranty, express or implied, or assumes any legal liability or responsibility for the accuracy, completeness, or usefulness of any information, apparatus, product, or process disclosed, or represents that its use would not infringe privately owned rights. Reference herein to any specific commercial product, process, or service by trade name, trademark, manufacturer, or otherwise does not necessarily constitute or imply its endorsement, recommendation, or favoring by the United States Government or any agency thereof. The views and opinions of authors expressed herein do not necessarily state or reflect those of the United States Government or any agency thereof.

DISCLAIMER

Portions of this document may be illegible in electronic image products. Images are produced from the best available original document.

Research Proposal

to

U. S. ENERGY RESEARCH AND DEVELOPMENT ADMINISTRATION

"INTEGRO-DIFFERENTIAL EQUATION ANALYSIS AND RADIOISOTOPE IMAGING SYSTEMS

[Continuation of E(11-1)-3253]

submitted jointly by

The City College
The City University of New York
Convent Avenue at 138th Street
New York, N. Y. 10031
(212)281-0470

- and -

Research Foundation of
The City University of New York
1411 Broadway
New York, N. Y. 10018
(212)354-2228
(FISCAL AGENT)

Desired Starting Date: June 1, 1976

Duration: One (1) Year

Amount Requested: $41, 591

Hiram Hart DATE: 3/9/76
Hiram Hart - Principal Investigator
Professor - Department of Physics
The City College
[redacted]
(212)690-6896

Eric Erlbach DATE: 3/9/76
E. Erlbach - Chairman
Department of Physics
The City College
(212)690-6832

Morton F. Kaplon DATE: 3/15/76
Morton F. Kaplon - Vice Provost
The City College
(212)690-6679

Morton M. Pavane DATE: 3/15/76
Morton M. Pavane - Director
City College Office of
Research Foundation of The City
University of New York
(212)281-0470

NOTICE
This report was prepared as an account of work sponsored by the United States Government. Neither the United States nor the United States Energy Research and Development Administration, nor any of their employees, nor any of their contractors, subcontractors, or their employees, makes any warranty, express or implied, or assumes any legal liability or responsibility for the accuracy, completeness or usefulness of any information, apparatus, product or process disclosed, or represents that its use would not infringe privately owned rights.

MASTER

DISTRIBUTION OF THIS DOCUMENT IS UNLIMITED

I. Abstract

Our five probe focussing collimator coincidence scanning system recently fitted with new collimators and slightly modified electronics will be further tested using a variety of phantoms and several different isotopes. The three dimensional depth dependent point source response functions which now exhibit a F.W.H.M. of 7.5 mm will be used to deconvolute the data obtained with phantoms using both matrix methods and a newly devised direct iterative approach. The analysis should make it possible to detect cold lesions considerably less than 1 cm^3 so long as they are within several inches of the surface. If the system performance continues to be encouraging, animal scan and possibly selected clinical scans will be carried out. The practical application of tracer analysis of the data from multi-probe single gamma and coincidence systems will be continued in collaboration with groups at the Montefiore Hospital and Medical Center and the Edward J. Hines Veteran's Administration Hospital. Diffusion-interaction analysis of biological systems will be continued and application for some of the mathematical methods of analysis to environmental and ecological models will be considered as well. Characterization of the classes of experiments necessary for complete theoretical solutions of multi-compartment systems will also be considered.

II. Background for the Research

Analysis of radioisotope tracer data has often involved assuming complete compartmentalization of the biological system being studied. If the experimenter has access to all compartments of a truly N compartment system, complete determination of all rates and volumes of steady state and non-steady state systems is possible by simultaneous measurments of N-1 different isotopes (1, 2, 3). Completely accessible steady state systems can also be solved by appropriate analysis of the tracer concentration time dependencies of a single isotope (4). When all compartments are not accessible, a solution or range of solutions may still be obtained by studying the various constraints imposed by the physical nature of the problem (5, 6). Perturbation methods can also be combined with tracer determinations (24).

The point of view emphasized in the above treatment finds expression mathematically principally in terms of systems of coupled first order linear differential (or difference) equations in which the classical mathematical program is reversed. Instead of finding the solution (i.e., concentration curves) from the equations and boundary conditions, the objective is rather to determine that system of equations which gives rise to the experimentally observed specific activity curves. It was recognized, however, that the integrated values alone of the specific activity curves might, in some cases, provide enough information to solve a multi-compartment system (7), (i.e. determine rates and volumes) an approach recently extended (8, 9) to various, partly accessible, special multi-compartment topologies for which systems of

differential equations did not necessarily apply since non-continguities and therefore time lags could exist. This latter development suggested that general multi-compartment analysis might not have to be restricted to contiguous topologies at all and that integral equation approaches previously principally restricted either to two-compartment systems, vascular flow treatments, and individual parameter (i.e. volume) determinations (10, 11, 12, 13, 14, 15), or focussed essentially on the inverse problem of predicting the tracer time dependencies from known transfer characteristics (16) could in fact be adapted to solve steady-state, non-contiguous, multi-compartment systems (17, 18) in the sense that all the actually determinable intercompartment transfer properties of generally injectable systems could be specified. While the resulting integral equation approach permitted analysis of many previously rather intratable systems, two difficulties remained. Since the method focussed on transport from one compartment to another, flows of material leaving a measurement compartment and subsequently reentering the same compartment without having been in any measured site in the interim, could not be treated readily in the analysis. Secondly, the data obtained from compartments which were measurable but not injectable was not easily incorporated into the formalism. The integro-differential equation approach was devloped in an effort to deal with these difficulties (19, 20, 21).

The integro-differential equation approach is probably applicable to all of the many situations in which a realistic representation of the tracer data curves can be made in terms of decaying exponentials. There are,

however, situations in which sufficiently accurate measurements of the early points are not really feasible. Also any curve in which "bumps" appear is difficult to effectively represent exponentially.

Discrete analogs of the integral and integro-differential equation approaches have been developed to deal with these difficulties. The discrete method avoids all analytic curve fitting and simply makes use of the counts sequentially recorded in successive time intervals. The inherent simplicity of the formalism made possible, to our knowledge, a novel analysis of mono-compartment randomized date (22). In collaboration with medical investigators a discrete integral equation approach has been used in studying calcium metabolism. The rate of absorption of calcium from the gut into the vascular system is determined by correlating the results of external probe measurements following i.v. and oral administration of Ca^{47} (25). The method may have direct clinical applicability in diagnosing hyperparathyroidism (26).

Our research in the field of diffusion-interaction analysis is fundamentally motivated by the importance of this area to cell metabolism and to antibody-antigen systems. A diffusion-interaction equation for the reaction $A + B \rightleftarrows C$ has been derived by the group (23), and the rate of thermal dissociation calculated for an antigen-antibody-antigen like system (27).

By applying many of the same physical principles used in the thermal dissociation calculation a theory has now been developed which appears to predict in a reasonably quantitative way those antibody, antigen and particulate concentrations at which flocculation will occur (Appendix I.). To our knowledge this is the first general theory of antigen-antibody-latex flocculation and perhaps flocculation in general in which the very significant role played by dissociation is quantitatively treated. Mr. K. Chak is the graduate student actively engaged in this aspect of our research.

Complete determination of a multi-compartment contiguous system by means of tracer measurements was, of course, demonstrated over 20 years ago. The method initially proposed involved injection into one compartment and measurement in all compartments. Subsequently it has been demonstrated that a solution can also be obtained by a series of injections in all N compartments with the repeated measurements restricted to a single compartment. Characterization of the general sets of N injections and measurements necessary for complete determination of an N compartment system has until recently not been possible. A solution to this rather classic type of problem has now been obtained principally by Ms. P. Spetsieris and appears in Appendix II.

Research on F.C.C.S. has been carried out for quite a few years beginning with the original experiments at Brookhaven National Laboratory 28, 29, 30. A manuscript relating to work of the last two years and detailing the extent to which multi-millimeter resolution is possible with this technique has been accepted for publication in the IEEE Transactions on Biomedical Engineering (Appendix III.).

The 5 probe F.C.C.S. system described in last year's report has now been fitted with more suitable collimators and active testing of the system is currently going on. A description of the modifications made, the results obtained and work currently in progress, carried out principally by Mr. P. Zacuto, appears in Appendix IV. Based upon the latest system and straight-forward minimal projections, the F.C.C.S. approach seems to be particularly well suited for detecting small cold lesions(considerably less than $1cm^3$) within a well defined limited volume. It is probably not likely to be as useful as a general purpose screening type instrument because the overall count rates are significantly lower than those obtainable with other approaches. For cold lesion detection within small organs or for re-scanning suspicious regions seen using other larger scale scanning techniques, F.C.C.S. is extremely promising. It may also be useful in obtaining some kinds of tomographic kinetic data.

III. Description of Proposed Research

The program of research proposed for the next year represents in large measure a continuation of the on going work described immediately above.

The work falls into two broad categories which are, however, often closely related.

1. Basically General Techniques and Approaches

a) Development of analytic techniques and algorithms for interpreting the results of tracer and perturbation - tracer kinetic experiments involving multi-compartment systems and multi-probe data acquisition.

b) Analysis of optimal interpretation techniques in radioisotope scanning

and gamma camera applications including tomographic approaches (31, 32).

c) Theoretical investigation of diffusion-interaction phenomena in biologically related systems.

d) Studying the extent to which diffusion-interaction theory can be applied to environmental and ecological models.

e) Continuing tissue distribution studies in animals, in collaboration with Prof. B. Rosoff, of radioisotope compounds suitable for F.C.C.S. applications.

2. Basically Direct Applications

Further testing of the current 5 probe system. Selecting methods for best reconstructing the known Phantoms from experimental data. Installing a moving computer controlled table so that animal and possibly selected patient scans can be carried out.

REFERENCES

1. Sheppard, C.W. and A.S. Householder, J. App. Physics 22, 510, 1951.
2. Landahl, H.D., Bull. Math. Biophysics 16, 151, 1954.
3. Hart, H.E., Bull. Math. Biophysics 19, 61, 1957.
4. Hart, H.E., ibid. 17, 87, 1955.
5. Berman, M. and R. Schoenfeld, J. App. Physics 27, 1361, 1956.
6. Berman, M., Ann, N.Y. Acad. of Sci. 108, 182, 1963.
7. Hearon, J.A., ibid. 108, 36, 1963.
8. Gurpide, B., J. Mann. and S. Liebermann, J. CLin. Endo. 23, 1155, 1963.
9. Gurpide, B.J. and J. Mann. Bull. Math. Biophysics 27, 389, 1965.
10. Stephenson, J.L. ibid. 10, 117, 1948.
11. Branson, H., Cold Springs Symp. Quant. Biol. 13, 35, 1948.
12. Zierler, K.L., Ann. N.Y. Acad. Sci., 108, 106, 1963.
13. Sheppard, C.W., Basic Principles of the Tracer Method, J. Wiley Sons 1962.
14. Berkowitz, J.M., J.L. Sherman and H.E. Hart, Ann. N.Y. Acad. Sci. 108, 250, 1963.
15. Bergner, P., 10th Annual Symp. O.R.I.N.S. 1966.
16. Stephenson, J.L., Bull. Math. Biophysics 22, 113, 1960.
17. Hart, H.E., ibid., 27, 329, 1965.
18. Hart, H.E., ibid. 28, 261, 1966.
19. Hart, H.E., Second International Biophysics Congress, Vienna, 1966.

20. Hart, H.E., Proc. Symp. on Compartments, Pools and Spaces in Medical Physiology, Oak Ridge Inst. Nuclear Studies 11, 145, 1966.

21 Hart, H.E., Bull. Math. Biophysics 29, 319, 1967.

22. Hart, H.E. and J. Sondheimer, Comput. Biol. Med. 1, 59-74, 1970.

23. Hart, H.E., D. Sugarman and D.I. Shelupsky, Bull. Math. Biophysics 32, 377, 1970.

24. Hart, H.E., U. Mallik and D. Sugarman, Bull. Math. Biophysics, 34, 377, 1970.

25. Hart, H.E. and H. Spencer, Proc. Exp. Biol. and Mod. 126, 365, 1967.

26. Barzel, U.S. and H. Hart, Nephron 10: 174-87 (1973)

27. Sugarman, D. and H.E. Hart, Bull. Math. Biol. 35, 219-235, 1973.

28. Hart, H.E. Radiology 84, 126, 1965.

29. Hart, H.E. Trans. N.Y. Acad. Sci., 30, 580, 1968.

30. Hart, H.E., K. Rider, J. Korenthal, P. Spetsieris and A. Bachman. Trans. in Nuclear Science. NS-21, 665-677, 1974.

31. Rider, K.L., S. Rudin and H.E. Hart, Biomed. Trans. IEEE, 32, 377-390, 1972.

32. Rudin, S., K.L. Rider and H.E. Hart, Radiology 102, 371, 1972.

JOINT APPLICANT STATEMENT

The Research Foundation of The City University of New York is designated as fiscal agent for grants and contracts awarded to The City College. Payment for the Grant/Contract, if awarded, should be made to the:

Research Foundation of
The City University of New York
1411 Broadway
New York, New York 10018
Attention: Controller - Mr. Paul Segall
(212) 354 - 2228

BUDGET CERTIFICATION

"I certify that the distribution of costs between direct and indirect categories as shown in the proposal conforms to the usual accounting practices of the institution for all Federally supported or sponsored research."

Morton M. Pavane DATE: 3/15/76

Morton M. Pavane
Director - City College Office
Research Foundation of
The City University of New York
Tel. No. (212) 281 - 0470

Proposal Title: Integro-Differential Equation Analysis and Radioisotope Imaging System 3/3/76

Principal Investigator: Prof. Hiram Hart

THE CITY COLLEGE
New York, N.Y. 10031

BUDGET
June 1, 1976 - May 31, 1977

Continuation E(11-1)-3253

A-II(a) Reimbursable or Cost Sharing Portion

1. Salaries and Wages

Scientific Personnel

Principal Investigator - Prof. Hiram Hart	
Academic Yr. (20% effort x 37,613)	$7,523
Summer-1 mo.-Full Time (1/9 x 37,613)	4,179
Graduate Research Assistant	
Academic Year, Half Time (10 mos. @ $450/mo)	4,500
Summer Full Time (2 mos. @ $900/mo)	1,800
Support Personnel	
Secretarial Assistance	1,000
Total Salaries and Wages	$19,002

2. Indirect Costs

53% of Salaries and Wages (Provisional rate established by DHEW - Effective 7/1/75)	10,071

3. Supplies and Materials
Significant Items of a Special Nature

Specialized Radio Isotopes, Computer tapes Film, Books, Hand Tools	3,000

4. Equipment

a) Nuclear Detection equipment, Time to Amplitude Converter, Components for a Heavy Duty traverse Collinator	($5,000)	
b) Tectronix 7000 series/accessories	($5,000)	
		10,000

5. Publication and Communication Costs	600
6. Travel	400

7. Other

Consultants (Principally P. Bardfeld, B. Rosoff and S. Rudin - see vita enclosed)	($3,000)	
Fringe Benefits		
27% x $ 7,523 =	$2,031	
20% x $10,300 =	2,060	
		7,091
	GRAND TOTAL	$50,164

It is requested that ERDA provide 82.91% of the A-II(a) portion, or $41,591.

A-II(b) -Items Excluded from Cost Sharing to be Furnished by University

NONE

A-II(c) University Contribution of Principal Investigator

~~College Contribution of Principal Investigator included in A-II(a).~~

None

CURRICULUM VITAE

NAME HIRAM HART COLLEGE The City College of New York

RECOMMENDATION FOR

Appointment _____ Promotion _____

Reappointment _____ Reappointment with Tenure _____

Other _____

TITLE Professor DEPARTMENT Physics

EFFECTIVE DATE _____ SALARY RATE _____

HIGHER EDUCATION

A. Degrees

Institution	Dates Attended	Degree and Major	Dates Conferred
The City College		B.S., Physics	1943
New York University		Ph.D., Physics	1952

B. Additional Higher Education and/or Education in Progress

Institution	Dates Attended	Courses, Etc.

EXPERIENCE

A. Teaching

Institution	Dates	Title	Department
High Schools, Board of Education, N.Y.C.	9/46-6/53	Teacher	Physics
The City College	9/53-1957	Instructor	Physics
The City College	1957-1962	Asst. Prof.	Physics
The City College	1962-1968	Assoc. Prof.	Physics
The City College	1968-	Professor	Physics

EXPERIENCE (continued)

B. Research

Institution	Dates	Title
New York University	2/50-9/51	Graduate Student
Montefiore Hospital and Medical Center	5/52-1962	Physicist, Neoplastic Division
Montefiore Hospital	1962-1968	Head, Medical Physics Laboratory
The City College	12/60-1965	Princeipal Investigator (NIH Grant) (Study of Zone Plates)
Brookhaven National Lab.	1964-67,1971-	Research Collaborator
The City College	1968-	Principal Investigator (A.E.C. Grant) Tracer Analysis
Montefiore Hospital and Medical Center	1968-	Chief Physicist

C. Administrative

Institution	Dates	Title
Montefiore Hospital and Medical Center	1962-1968	Head, Medical Phys. Lab.

ACADEMIC AND PROFESSIONAL HONORS

Sigma Xi
Office of Naval Research, Research Fellow, N.Y.U., 1950-1951
American Men of Science, 1957
N.S.F. Science Faculty Fellow, Department of Biophysics, Yale, 1959-1960
Chairman, Section of Physical Sciences, New York Academy of Science, 1961-1962
Who's Who in the East, 1962
Affiliate, Royal Society of Medicine, 1965
Fellow, New York Academy of Science, 1964
World's Who's Who in Science, 1966
Chairman, Fourth and Final Session on General Mathematical Theories, Second International Biophysics Congress, Vienna, 1966
President Radiological and Medical Physics Society, 1968-1970
Associate Editor - Bulletin of Mathematical Biology, 1973 –
Editorial Board - Journal of Biological Physics, 1973 –
Fellow, American Physical Society
Chairman of the Session on Biophysics, Annual Meeting American Physical Society 1976.

PUBLICATIONS (Last five years only)

(a) Books and Contributions to Books:

Section in Clinical Scintillation Scanning, Edited by L.M. Freeman and Philip Johnson, Hoeber Medical Division of Harper and Row (1969).
Lesion Detection Characteristics of a Focusing Collimator Gamma Camera Coincidence System, (with co-authors), IEEE 1973 - Nuclear Science Symposium.

PUBLICATIONS (continued)

(b) Articles in Standard Journals:

"Concentration Equations for the Diffusion of a Reversible Reacting Substance in Gel-Like Media", (with D. Sugerman and D. Shelupsky), Bull. Math. Biophysics 32, 377 (1970).

"Discrete Formulation and Error Minimization in Applying the Integro-Differential Equation Approach to Monocompartment Data", (with J. Sondheimer), Computers in Biology and Medicine 1, 59 (1970).

"Fate of Intravenously Administered Zinc Chelates in Man", (with B. Rosoff, A.H. Methfessel and H. Spencer), J. of App. Physiology 30, 12 (1971).

"Use of Magnifying Multihole Collimator in the Gamma Ray Camera System", (with S. Rudin and P. Bardfeld), J. Nuc. Med. 12, 831 (1971).

"Determination of Reaction Rate Constants in the Mammillary System", (with U. Mallik and D. Sugerman), Bull. Math. Biophysics 34, 87 (1972).

"Resolution Characteristics of Tomographic Rotating Collimator Systems", (with K. Rider and S. Rudin), IEEE Transactions on Biomedical Engineering Vol. BME-19, 186 (1972).

"A Tomographic Magnifying Collimator System for the Gamma Camera", (with S. Rudin and K. Rider), Radiology 102, 371 (1972).

"Thermal Dissociation of Antigen-Antibody-Antigen Like Systems", (with D. Sugerman), Bull. Math. Biology 35, 219-35, (1973).

"Initial Entry of Calcium into the Gastrointestinal Tract in Hyperparathyroidism and in a Case of Renal Tubular Acidosis", (with U.S. Barzel), Nephron 10, 174-187 (1973).

(c) Abstracts, Research Reports and Other:

Hiram Hart

MEMBERSHIP IN PROFESSIONAL SOCIETIES

American Physical Society
American Association of Physics Teachers
A.A.A.S.
Biophysical Society
New York Academy of Science
Health Physics Society
American Association of Physicists in Medicine
Society of Nuclear Medicine
President RAMPS (Radiological and Medical Physics Society) 1968-1970
Member National Executive Board AABM American Association of Physicists in Medicine - December 1968-December 1970

REFERENCES

CHAIRMAN'S REPORT

Hiram Hart

1. COLLEGE AND COMMUNITY SERVICES

Invited lectures at Oak Ridge National Laboratory (2), Brookhaven National Laboratory, Sloan Kettering Institute (2), Wayne State University, New York Academy of Science, The City College - Sigma Xi, Hines V.A. Hospital, University of Chicago (2), Rockefeller University

Member, The City College Research Committee 1964-

Secretary, The City College Research Committee 1966-1970

Chairman, The City College Research Committee, 1973

Member, Physics Department Appointments Committee 1963-1964; 1968-1971

Member, General Faculty Council 1962-1965

Member, Building Committee 1962-1966

Member, First-Year Professional Courses Committee 1966

Member, Terminal Introductory Courses Committee 1966

Member, Ph.D. Doctoral Committee for Gerald Kent (Civil Engineering) - Plasma Physics, Joseph Cataldo (Civil Engineering) - Plasma Physics, James Slevin (Physics), M. Margulies (Physics)

Member, City College Honors Committee 1971-

Chairman, City College Medical Health Sciences Committee, 1971-1972

Member, Advisory and Search Committee for Dean of City College School of Nursing, 1972

Member, City University Biomedical Physics-Biomedical Engineering Committee, 1970-

Member, City University Research Awards Committee (Physics) 1970-1972

Member, City University Committee on Admissions and Awards (Physics) 1971-

Member, C.C.N.Y.-Mt. Sinai Committee on the Appointment of a Director of Nursing and Dean of the School of Nursing, 1972

Member, Policy Committee for the City College Center for Biomedical Education 1972-

Consultant, International Commission Radiological Units and Measurements (Tracer Kinetics). New grant obtained - U.S.A.E.C.

3. GRANTS AND CONTRACTS AWARDED

Agency: Atomic Energy Commission
Period: 1968-1969
Amount: $16,200
Title of Grant:

Agency: Atomic Energy Commission
Period: 1969-1970
Amount: $16,000
Title of Grant:

Agency: Atomic Energy Commission
Period: 1970-1971
Amount: $12,000
Title of Grant:

Agency: Atomic Energy Commission
Period: 1971-1972
Amount: $12,000
Title of Grant:

Agency: Atomic Energy Commission
Period: 1973-1976
Amount: $12,000 for 1/31/73-1/31/74

Title of Grant:

Agency: ERDA
Period: 2/1/74 - 5/31/75
Amount: $12,000
Title of Grant:

Agency: ERDA
Period: 6/1/75 - 5/31/76
Amount: $15,967
Title of Grant:

Agency:
Period:
Amount:
Title of Grant:

Hiram Hart

RECORD AT COLLEGE

Dates	Rank	Salary Rate

PERSONAL DATA

Address 3450-25 Wayne Avenue, Bronx, New York 10467

Telephone Number (212) 798-8338

Military Status

Social Security Number [redacted]

Date of Birth [redacted]

Date Submitted to BHE:

4. COURSES TAUGHT

Physics 3,4,7,8,	General Physics
Physics 9	Mechanics I
Physics 13	Thermodynamics
Physics 54	Biophysics
Physics 64	Biophysics Laboratory
Elec. Eng. 128	

Post Doctoral Medical Physics Retraining Course - Bio-Medical Program

5. PUBLICATION RECORD PRIOR TO THE LAST FIVE YEARS

(a) Books and Contributions to Books:

Multicompartment Analysis of Tracer Experiments, (Editor), New York Academy of Science 108, 1-338 (1963).

Distribution of Y^{90} Upon Systematic and Intercavitary Administration and its Modification by Chelating Agents, (with co-authors), Proceedings of the Radioisotope Conference, Oxford, p. 125, July 19-23 (1954).

Biological Studies on Calcium, Strontium, Lanthanum and Yitrium, (with co-authors), International Conference on the Peaceful Uses of Atomic Energy (1955).

Modification of Distribution and Excretion of Rare Earths by Chelating Agents, Conference Volume on Rare Earths in Biochemical and Medical Research, Oak Ridge Institute of Nuclear Studies; O.R.I.N.S. 12, 118 (1955).

Multicompartment Analysis of Steady State and Non-Steady State Systems, 10th Annual Symposium Oak Ridge Institute of Nuclear Studies (1966).

5. PUBLICATION RECORD PRIOR TO THE LAST FIVE YEARS (continued)

(b) Articles in Standard Journals:

"Regular Meson Potentials in Low Energy Proton-Proton Scattering", (with R.D. Hatcher), Phys. Rev. 87, 375 (1952).

"Modification of the Distribution and Excretion of Radioisotopes by Chelating Agents", (with D. Laszlo), Science 118, (No. 3053), 24 (1953).

"Distribution of Y^{90} in Ascites Tumor Mice following Intraperitoneal Administration of Yttrium Chloride", (with co-authors), Science 119, (No. 3103) 880 (1954).

"Biological Studies on Stable and Radioactive Rare Earth Compounds: III Distribution of Radioactive Yttrium in Normal and Ascites-Tumor-Bearing Mice, and in Cancer Patients with Serous Effusions", (with co-authors), J. of the National Cancer Institute 15, (No. 1) 131 (1954).

"Analysis of Tracer Experiments in Nonconservative Steady-State Systems", Bull. of Mathematical Biophysics 17, (No. 2), 87 (1955).

"Metabolism of Lanthanum and Yttrium Chelates", (with co-authors), J. of Laboratory and Clinical Medicine 46, No. 2), 182 (1955).

"Radioyttrium (Y^{90} O) for the Palliative Treatment of Effusions due to Malignancy", (with co-authors), J.A.M.A. 161, 499 (1956).

"Strontium ^{85} Metabolism in Man and Effects of Calcium on Strontium Excretion", (with co-authors), Proc. Soc. Exp. Biol. and Med. 91, 155 (1956).

"Excretion of Yttrium and Lanthanum Chelates of Cyclohexane 1, 2 - Trans-Diamine Tetrascetic Acid and Diethylenetriamine Pentascetic Acid in Man", (with co-authors), Nature 180, 919 (1957).

"Analysis of Tracer Experiments: II. Non-Conservative, Non-Steady State Systems", Bull. Math. Biophysics 19, 61 (1957).

"Interaction of Yttrium Compounds with Serum and Serum Constituents in Vitro", (with co-authors), Archives of Biochemistry and Biophysics 78, 1 (1958).

"Decontamination Studies", (with co-authors), Advanced in Radiobiology, p. 298 (1958).

"Analysis of Tracer Experiments: III. Homeostatic Mechanicsm of Fluid Flow Systems", Bull. Math. Biophysics 20, 281 (1958).

"Effect of Excess Chelating Agents on Rare Earth Decontamination", Ann. N.Y. Acad. Sci. 88, 486 (1960).

"Analysis of Tracer Experiments: IV. The Kinetics of General N Compartment Systems", Bull. Math. Biophysics 22, 41 (1960).

"Determination of Body Spaces and Renal Clearances with Yttrium Chelates in Man", (with co-authors), International J. of Applied Radiation and Isotopes 8, 198 (1960).

"Effect of Chelating Agents on the Removal of Yttrium and Lanthanum from Man", (with B. Rosoff, S. Ritter, K. Sullivan, H.E. Hart and Herta Spencer-Lazzlo), Health Physics 6, 177 (1961).

"The Rate of Decarboxylation of Mevalonic Acid-1-C^{14} in Man", (with J. Berkowitz, J. Sherman and H.E. Hart), Ann. N.Y. Acad. Sci. 106, 250 (1963).

5. PUBLICATION RECORD PRIOR TO THE LAST FIVE YEARS (continued)

(b) Articles in Standard Journals:

"Perturbation Tracer Analysis", Ann. N.Y. Acad. Sci. 108, 23 (1963).
"Recent Developments in Multi-Compartment Tracer Analysis", (with C.A. Waller), Transactions of the N.Y. Acad. Sci. 26, 64 (1963).
"Analysis of Tracer Experiments V: Integral Equations of Perturbation-Tracer Analysis", Bull. Math. Biophysics 27, 417 (1965).
"Determination of Equilibrium Constants and Maximum Binding Capacities in Complex Vitro Systems, I. The Mammillary System", Bull. Math. Biophysics 27, 87 (1965).
"Analysis of Tracer Experiments VI: Determination of Partitioned Initial Entry Functions", Bull. Math. Biophysics 27, 329 (1965).
"Evaluation of the Radioisotope Renogram in Experimental Renal Artery Stenosis", (with H. Haimovici, N. Maier, Y. Hisnida), Journal Cardiovascular Res. 6, 152 (1965).
"Analysis of Tracer Experiments VII: General Multi-Compartment Systems Imbedded in Non-Homogeneous Inaccessible Media", Bull. Math. Biophysics 28, 261 (1966).
"Diffraction Characteristics of a Linear Zone Plate", (with J.B. Scrandis, R. Mark and R.D. Hatcher), Journal of Optical Society 56, 1018 (1966).
"Consideration of Mortality in Certain Chronic Diseases", (with B. Zumoff, H.E. Hart and L. Hellman), Annals of Internal Medicine 64, 595 (1966).
"Analysis of Tracer Experiments VIII. Integro-Differential Equation Method", Bull. Math. Biophysics 29, 319 (1967).
"Geometric Efficiency and Other Performance Characteristics of Focusing Collimators", (with H.E. Hart, B. Warshaw and H. Stoller), Bio-Medical Abstracts I.E.E.E. 14, 96 (1967).
"Rate of Initial Entry of Ca^{47} and Sr^{85} from the Intestine into the Vascular Space", (with H. Spencer), Proc. Soc. Biol. and Med. 126, 365 (1967).
"Comparative Resolution of Single Gamma Counting and Counting Coincidence Counting in Focusing Collimator Scanning Systems", Trans. N.Y. Acad. Sci. 30, 580 (1968).

CURRICULUM VITAE

Betty Rosoff Ph.D.
150 East 18th Street
New York, N.Y. 10003

Tel. No. 212 475-8454

EDUCATION:	Ph.D.	City University of New York	February, 1967
	M.A.	Hunter College	June 1960
	B.A.	Hunter College	June 1942

PROFESSIONAL EXPERIENCE:

Professor	Stern College	1974-
Associate Professor	Stern, College, Yeshiva University	1968-1974
Adjunct Associate Professor	Hunter College	1970-1974
Associate Professor	Paterson State College	1967-1968
Lecturer	Hunter College	1961-1967
Instructor	Bronx Community College	1964-1965
Research Associate	Montefiore Hospital	1952-1962
Research Chemist	National Aniline	1943-1948

Courses taught:

Last two years, Cell Physiology, Endocrinology, Vertebrate Physiology, Graduate Mammalian Physiology, General Biology, Anatomy and Physiology for Nurses, Histology

Previously (in addition to the above)
Comparative Physiology, Zoology, Comparative Anatomy, Hematology and Clinical Techniques

Publications: see attached list

PROFESSIONAL SOCIETIES: American Physiology Society
New York Academy of Sciences
Sigma Xi
Phi Sigma
AAAS

CURRENT RESEARCH INTERESTS AND PROFESSIONAL ACTIVITIES:

The effect of pituitary hormones, especially prolactin on the growth, development and zinc uptake of the prostate glands of the rat; The relationship of prolactin to prostatic pathology (hyperplasia and cancer).

Zinc metabolism; the role of zinc in the male reproductive system; the possible relationships of zinc nutrition to the development of prostatic pathology.

Member of the Working Cadre of the National Prostatic Cancer Project, National Cancer Institute.

PUBLICATIONS

Rosoff, B. and H. Spencer. The Distribution and Excretion of 99Mo in Mice. Health Physics. 25: 173 - 175, 1973

Rosoff, B. and C.R. Martin. The Influence of Thymectomy and Sham Operation on Prostate Gland Responses of Hooded Rats to Conadotrophins. Gen. & Compar. Endocrinol. 16: 484-491, 1971. (Selected for Republication in Gonadotrophins, I: by the Smithsonian Science Information Exchange 1974)

Rosoff, B., H. Hart, A.H. Methfessel and H. Spencer. Fate of Intravenously Administered Zinc Chelates in Man. J. Appl. Physiol. 30: 12 - 16, 1971

Rosoff, B. and C.R. Martin. Effect of Gonadotrophins and of Testosterone on Organ Weights and Zinc-65 Uptake in Male Rats. Gen. & Compar. Endocrinol. 10: 75 - 84, 1968.

Spencer, H., B. Rosoff, I. Lewin, and J. Samachson. Studies of Zinc-65 Metabolism in Man. Edited by A.S. Prasad, Springfield, Ill., Charles C. Thomas, 1966.

Spencer, H. and B. Rosoff. Effect of Chelating Agents on the Removal of Zinc-65 in Man. Health Physics 12: 475 - 480, 1966.

Spencer, H. and B. Rosoff. Removal of Scandium-46 in Man. Health Physics 11: 1181 - 1185, 1965.

Rosoff, B. and H. Spencer. Tissue Distribution of Zinc-65 in Tumour Tissue and Normal Tissue in Man. Nature 27: 652 - 653, 1965.

Rosoff, B. and H. Spencer. Metabolism of Scandium - 46 in Man. Int. J. Appl. Radiat. Isotopes 16: 479 - 485, 1965.

Spencer, H., B. Rosoff, A. Feldstein, S. H. Cohn and R. Gusmano. Metabolism of Zinc-65 in Man. Rad. Res. 24: 432 - 445, 1965.

Rosoff, B. and H. Spencer. Fate of Molybdenum-99 in Man. Nature 202: 410- 411, 1964.

Spencer, H. and B. Rosoff. Effects of Chelating Agents in Man. In: Chelation Therapy. Edited by A. Soffer. Springfield, Ill., Charles C. Thomas, 1964.

Cohn, S., B. Rosoff, V. Gusmano and H. Spencer. Cesium-137 in Man; Total Body Counting. Rad. Res. 19: 655 - 658, 1963.

Rosoff, B., S. Cohn and H. Spencer. Metabolism of Cesium-137. Rad. Res. 19: 643 - 654, 1963.

Spencer, H. and B. Rosoff. Metabolism and Removal of Rare Earths in Man. In: Diagnosis and Treatment of Radioactive Poisoning. IAEA. Vienaa, 1963.

PUBLICATIONS

Rosoff, B., E. Siegel, G.L.Williams and H. Spencer. Distribution and Excretion of Radioactive Rare Earth Compounds in Mice. Int. J. Appl. Radiat. Isotopes. 14:129-135, 1963.

Stand, F., B. Rosoff, G.L.Williams and H.Spencer. Tissue Distribution Studies of Ionic and Chelated Zinc-65 in Mice. J. Pharmacol. Exp. Ther. 138:399-404, 1962.

Stevens,E., B.Rosoff, M.Weiner and H.Spencer. Metabolism of the Chelating Agent Diethylenetriamine Pentaacetic Acid (C-14 DTPA). Proc. Soc. Exp. Biol. Med.111: 235 - 238, 1962.

Rosoff, B. The interaction of Yttrium Chelates with Serum Constituents. Ann. New York Acad. Science 88:479 - 485, 1960.

Rosoff, B. , S. Ritter, K. Sullivan, H. Hart and H.Spencer. Effect of Chelating Agents on the Removal of Yttrium and Lanthanum from Man. Health Physics 6:177 - 182, 1961

Greenwald, E., H.Hart, B.Rosoff, H.Spencer and D. Laszlo. Determination of Body Spaces and Renal Clearances with Yttrium Chelates in man. Int. J. Appl. Radiat. Isotopes.8:198 - 204, 1960.

Rosoff, B., R.Lewin, H.Hart, G.L.Williams and D. Laszlo. Interaction of Yttrium Compounds with Serum and Serum Constituents in vitro. Arch. Biochem. Biophysics 78:1 - 9, 1958.

A. B. [illegible]

Rosoff, B. and C.R. Martin. Effect of Surgery on Response to Gonadotrophins. Int'l Union of Physiol. Sciences. Vol. 7, 1968

Martin, C.R., B.Rosoff and L.A.Miller. Effect of Age on the Ventral Prostate Gland Response to Thymectomy. The Physiologist 10:243, 1967.

Rosoff, B. and C.R.Martin. Gonadotrophic and Thyroid Influences on Growth of Accessory Reproductive Structures in the Rat. Abstr. Endocrine Society. 153,1967

Rosoff, B. and C.R.Martin. Influence of Gonadotrophins on Zinc-65 Uptake and Organ Weights in Rats. Fed. Proc. 25, 1966

Rosoff, B. , F.Stand, and H.Spencer. Tissue Distribution of Zinc-65 in Man. Fed. Proc. 22, 1963

Rosoff, B., F.Stand and H.Spencer. Rare Earth Binding to Serum Proteins and Nucleic Acids. Fed. Proc. 21, 1962

Rosoff,B., A.Feldstein, F. Stand, G.L.Williams and H.Spencer. Cesium-137 Excretion and Distribution in Man. Rad. Res. 14, 1961.

Rosoff, B., A.Feldstein, E.Stevens and H.Spencer. Excretion and Distribution of Sc-46 in Man and its removal by Chelating Agents. Fed.Proc. 20, 1961.

Rosoff, B., E.Siegel, G.L.Williams and H.Spencer. Tissue Distribution of Rare Earth Isotopes in Mice. Fed. Proc. 19, 1960

Rosoff, B., S. Ritter, K. Sullivan and H.Spencer. Yttrium Chelate Excretion and Decontamination in Man. Fed. Proc. 18, 1959.

Rosoff, B., H.Hart, G.L.Williams and R.Lewin. Interaction of Yttrium Compounds with Serum Constituents. Fed. Proc.17, 1958.

Rosoff, B., R.Lewin, H. Hart and K.G.Stern. Interaction of Yttrium Compounds with Serum Proteins. Fed. Proc. 15, 1956.

RECENT ADDITION:

Weinstein, E. and B. Rosoff. Effect of Prolactin on Prostatic Weight and Zinc-65 Uptake in Castrated Rats. Fed. Proc. 31. 1972

CURRICULUM VITAE

Name: Philip A. Bardfeld, M.D.

Date of Birth: [redacted]

S. S.: [redacted]

Place of Birth: Bronx, N. Y.

Citizenship: U. S.

Education:

A.B.	New York University University College Bronx, N. Y.	1954
M.D.	State University of New York Downstate Medical Center	1961

Honors: Dean's List - 4 years at NYU

Experience:

Associate Professor of Radiology Albert Einstein College of Medicine	1975 -
Assistant Professor of Radiology Albert Einstein College of Medicine	1968 - 1975
Head, Section of Nuclear Medicine Department of Oncology, Montefiore Hospital and Medical Center	1968 - present
Residency in Internal Medicine Montefiore Hospital and Medical Center	1967 - 1968
Fellowship in Nuclear Medicine Johns Hopkins Hospital, Baltimore, Md.	1965 - 1967
Internist, USAF Hospital, Perrin AFB, Texas	1963 - 1965
Residency in Internal Medicine Jewish Hospital of Brooklyn	1962 - 1963
Internship Mt. Sinai Hospital of Cleveland	1961 - 1962

Service:

USAF Medical Corps, Internist — July 1963 - July 1965

Membership in Professional Societies:

Society of Nuclear Medicine (Treasurer of Greater N. Y. Chapter, 1973-1976)
Association of University Radiologists
American Association for the Advancement of Science
Council on Cardiovascular Radiology of the American Heart Association
American Federation for Clinical Research

Certification:

The American Board of Nuclear Medicine 1972

Hiram Hart

2. WORK IN PROGRESS

Biophysics

Tracer Analysis: (Theoretical)

One of the most useful ways of determining the distribution of certain metabolites in the body, as well as the reaction rates governing transformations from one metabolite to another, is by means of tracer analysis. The research is oriented towards developing a mathematical technique, based on coupled integro-differential equations, which would permit one to extract information about reaction rates and transport topologies from the experimental data. A new equation has been derived characterizing diffusion of a material through a reversibly reactive medium. Various applications of the theory are being explored. Practical methods of improving radioisotope imaging are also under investigation.

"Three Dimensional Imaging of Multimillimeter Sized Cold Lesions by Focusing Collimator Coincidence Scanning (F.C.C.S.)", (with S. Rudin), submitted for publication.

Hiram Hart

CHAIRMAN'S REPORT (continued)

STUDENT EVALUATION

PUBLICATIONS

1. Stein, I., Bakst, A., Caginalp, N. and Bardfeld, P. A.: Clinical experiences with the implanted internal pacemaker in complete atrioventricular dissociation with Stokes-Adams disease. Vas Dis. 1:144-155, 1964.

2. Bardfeld, P. A.: A controlled double-blind study of trimethobenzamide, prochlorperazine and placebo. JAMA 196:796-798, 1966

3. Wagner, H. N., Jr. and Bardfeld, P. A.: Evaluation of structure and function of spleen with radioactive tracers. JAMA 199:202-206, 1967.

4. Bardfeld, P. A., Lopez-Majano, V., and Wagner, H. N., Jr.: Measurement of the regional distribution of arterial blood flow in the human forearm and hand. J. Nucl. Med. 8:542-550, 1967.

5. Bardfeld, P. A. and Holmes, R. A.: Pertechnetate accumulation in the choroid plexus. Am. J. Med. Sc. 254:176-182, 1967.

6. Bardfeld, P. A., Levine, J. and Shulman, K.: Accumulation of Rhenium-188 in choroid plexus of cat. Abstract. Clin. Res. 17: 616, 1969.

7. Rudin, S., and Bardfeld, P. A.: New system for replacing polaroid with rapidly processed 35mm film for radioisotope scan display. Radiology 100:180-182, 1971.

8. Rudin, S., Bardfeld, P. A. and Hart, H. E.: Use of magnifying multi-hole collimators in the gamma ray camera system. J. Nucl. Med. 12:831-834, 1971.

9. Carter, T. E., Bardfeld, P. A. and Shulman, K.: The uptake of Rhenium-188 in the choroid plexus and its effect on CSF production. Published in Cisternography and Hydrocephalus: A Symposium, ed. by John C. Harbert, M.D., Charles C. Thomas, Publisher, 1972.

10. Bardfeld, P. A.: Radionuclide techniques in pediatric hematology. Seminars in Nuclear Medicine 3:81-88, 1973.

11. Veith, F. J., Koerner, S. K., Attai, L. A., Bardfeld, P. A., Boley, S. J., Bloomberg, A., Everhard, M., Anderson, J., Pollara, B., Steckler, R., Nagashima, H., Siegelman, S., Lalezari, P. and Gliedman, M. L.: Single lung transplantation in emphysema. The Lancet 1: 1138, 1972.

12. Torres, M., Koerner, S. K., Raines, E., Bardfeld, P. A., Siegelman, S., Chandler, P., Goldring, I., Takaro, T. and Veith, F. J.: Single lung transplantation in experimental emphysema. Surg. Forum 23:227-229, 1972.

13. Bardfeld, P. A., Rudin, S.: The use of the magnifying or converging collimator in brain scanning. J. Nucl. Med. 14:834-836, 1973.

PUBLICATIONS (continued)

14. Bardfeld, P. A., Rudin, S.: Comparative study of instant technetium from various commercial suppliers. J. Nucl. Med. 14:880, 1973.

15. Veith, F. J., Koerner, S. K., Siegelman, S. S., Torres, M., Bardfeld, P. A., Attai, L. A., Boley, S. J., Takaro, T., and Gliedman, M. L.: Single lung ttansplantation in experimental and human emphysema. Ann. Surg. 178:463-476, 1973.

16. Sachs, B. A., Bardfeld, P. A., Bodian, J. E., Sugarman, L. A. and Hellman, L.: The liver scan in hyperlipoproteinemia. JAMA 227: 907-910, 1974.

17. Veith, F. J., Koerner, S. K., Torres, M., Bardfeld, P. A., Siegelman, S. S., Kaufman, S., Gliedman, M. L. and Takaro, T.: Single lung transplantation in experimental emphysema. Bull. Soc. Int. Chir. 1:37-39, 1975.

18. Bardfeld, P. A. and Shulman, K.: The transport and distribution of Rhenium-188 in the central nervous system. Experimental Neurology 50:1-13, 1976.

19. Bardfeld, P. A. and Shulman, K.: Rhenium-188 therapy of Experimental hydrocephalus. Experimental Neurology. (In Press)

20. Bardfeld, P. A., Yipintsoi, T., Koerner, S. K., Crane, R., Hagstrom, J. W. C., and Veith, F. J.: ^{131}I-fibrinogen in the detection of pulmonary allograft rejection. Surgery (In Press)

21. Bardfeld, P. A., Chervu, L. R., and Murty, V. R. K.: The organ distribution of ^{131}I-tyrosyl somatostatin. British Journal of Radiology, Letter to the Editor (In Press)

CURRICULUM VITAE

PERSONAL

NAME:	Stephen Rudin
ADDRESS:	11 Nassau Road Yonkers, New York 10710
TELEPHONE:	(914) 793-5351
BIRTH DATE:	September 30, 1943
MARITAL STATUS:	Married, no children

EDUCATION

City University of New York (CUNY)
Ph.D., September, 1975, medical physics
University of Chicago 1964-1968
M.S., September 1965, low temperature solid state physics
University of Chicago 1960-1964
B.S., June 1964, physics

EMPLOYMENT

Montefiore Hospital and Medical Center, Bronx, N.Y.
Nuclear Medicine Section and Medical Physics Laboratory
physicist, 1968-present (full-time)
City College of CUNY, New York, N.Y.
Department of Physics
adjunct lecturer, 1974
General Electric Company, Schnectady, N.Y.
Knolls Atomic Laboratory
technician, summer 1964

CERTIFICATION

American Board of Radiology, Medical Nuclear Physics, June 9, 1972
American Board of Health Physics, eligible for 1976 examination

MEMBERSHIP IN PROFESSIONAL SOCIETIES

American Association of physicists in Medicine
Health Physics Society
Institute of Electrical and Electronic Engineers:
Nuclear Science, Bio-engineering, and Ultrasonic Societies
Radiological and Medical Physics Society (RAMPS)
Society of Nuclear Medicine

PROFESSIONAL SERVICE

Radiological Physics Examination (RAPHEX) Committee of RAMPS, 1972-1974
Nuclear Medicine Committee of RAMPS, 1974-present

HONORS

Guest Scientist, Brookhaven National Laboratory, Medical Division, 1972-1975
Member Faculty Tomography Symposium of Society of Nuclear Medicine, 1972
National Science Foundation Graduate Fellow, University of Chicago, 1964-1968
Bell and Howell Undergraduate Scholar, University of Chicago, 1961-1964

PUBLICATIONS

Sherman, A.A., Rudin, S., McDougall, R.S.: Dose measurement of mixed beta and gamma fields of a homogeneously distributed isotope using powder and solid TLD's (abstract). Phys. Med. Biol. 15: 376-377, 1970.

McDougall, R.S. and Rudin,S.: Thermoluminescent dosimetry of aluminum oxide. Health Physics 19: 281-283, 1970.

Rudin, S. and Hart, H.E.: Monitor for ^{133}Xe contamination of air, letter to the editor. J. Nucl. Med. 12: 145-146, 1971.

Rudin, S. and Bardfeld, P.A.: New system for replacing Polaroid with rapidly processed 35mm film for radioisotope scan display. Radiology 100: 180-182, 1971.

Rudin, S., Bardfeld, P. A., Hart, H.E.: Use of magnifying multi-hole collimators in the gamma-ray camera system. J. Nucl. Med. 12: 831-834, 1971.

Rudin,S., Rider, K.L., Hart, H.E.: A tomographic magnifying collimator system for the gamma camera. Radiology, 102: 371-373, 1972.

Rider, K.L., Rudin, S., Hart, H.E.: Resolution characteristics of tomographic rotating collimator systems. IEEE Trans. on Biomed. Engin. BME-19: 186-193, 1972.

Rudin, S., Bardfeld, P.A., Hart, H.E.: Authors' Reply to letter to the editor, J. Nucl. Med. 13: 574, 1972.

Bardfeld, P.A. and Rudin, S.: Use of the magnifying or converging collimator in brain scanning. J. Nucl. Med. 14: 834-836, 1973.

Bardfeld, P.A. and Rudin, S.: Comparative study of instant technetium from various commercial suppliers, letter to the editor, J. Nucl. Med. 14: 880-881, 1973.

Rudin, S., Rider, K.L., Hart, H.E.: Gamma camera magnifying collimator systems. Chapter 8 of Tomographic Imaging in Nuclear Medicine, edited by Gerald S. Freedman, Soc. of Nucl. Med., New York, N.Y. 1973.

Hart, H.E. and Rudin,S.: Appendix A of Lesion detection characteristics of a focusing collimator gamma camera coincidence system. IEEE Trans. on Nucl. Sci. NS-21: 670-1, 676-7, 1974.

Hart, H.E. and Rudin, S.: Three dimensional imaging of multi-millimeter sized cold lesions by focusing collimator coincidence scanning (FCCS), in preparation.

Rudin, S.: Three dimensional radioisotope imaging using gamma ray coincidence scanning, Ph.D. thesis, Dept. of Physics, City College of CUNY, 1975.

Rudin, S.: Book Review. Medical Physics 2: 39, Jan./Feb., 1975.

PHYSICS DEPARTMENT

GRADUATE RESEARCH ASSISTANT

Name: Ki-Chuen Chak

Education:

B. S.	Chungchi College, Hong Kong	1967
Grad. Student	C.C.N.Y.	1971 - present

Experience:

Instructor	St. Stevens College, Hong Kong	1968-1970

PHYSICS DEPARTMENT GRADUATE RESEARCH ASSISTANT

Name: Phoebe Spetsieris

Education:

B.S. (Physics)	University of Athens Greece	1968
M.A. (Physics)	The City College of N.Y.	1970

Experience:

Teaching Asst.	C.C.N.Y.	1968-to present
Research Asst.	C.C.N.Y.	1970-to present

Academic Honors:

N.Y. State Regents Scholarship	1962
First in Ph.D. Qualifying Exam (CUNY)	Feb. 1971

PHYSICS DEPARTMENT

GRADUATE RESEARCH ASSISTANT

Name: Philip Zacuto

Education:

B.S. (Physics)	The City College of N.Y.	1963
M.A. (Physics)	The City College of N.Y.	1966

Experience:

Teacher	N.Y.C. High Schools	1962-1965
Teaching Asst.	C.C.N.Y.	1965-1967
Research Asst.	C.C.N.Y.	1967-1970
Teacher	N.Y.C. High Schools	1971-1972
Lecturer, Part Time	C.C.N.Y.	1972-

APPENDIX I

Theory of Antigen-Antibody Interaction in Agglutinating Systems

I. Introduction

Agglutination of red cells or latex particles is a widely used method for detecting and quantitating antigen-antibody interactions. Although numerous mathematical analyses of cellular and particulate antigen-antibody induced aggregation have been proposed, there is yet no general accepted quantitative treatment of this broad class of phenomenon. This may be due in part to the incomplete information available and partly to the complexity involved in the calculations.

The gross features of the agglutination process are well known. If a red cell or particle suspension which has been coated with antigen is then mixed with antiserum, the antibodies become bound to the surface antigens. Agglutination takes place when sufficient intercellular bonds or bridges are formed to bind the red cells or particles together in a multi-element aggregate. In attempting a quantitative theory, however, many factors have to be considered. The negative surface charge of the red cells limits the likelihood of antibody binding. The density of antigen sites on the surface, the strength and specificity of antigen-antibody bond, the number and length of the antibody molecule and chemical or physical parameters such as pH, temperature, ionic strength and dielectric constant of the medium have also been demonstrated to affect the final aggregations.

Since a complete general theory of antigen-antibody particle aggregation

involved would be extremely complex, most analyses have tended to concentrate upon one or a few factors only, quantitatively or qualitatively. Pollack's[1] theoretical model of agglutination emphasize the important effect of the zeta potential and the dielectric constant of the bulk medium. Greenbury[2] discussed the binding effect of 7S antibody on red cells. Singer[3] calculated the number of antibodies needed per latex particle in agglutination while Leikola[4] and Hoyer[5] emphasized the significance of antigen sites in studying hemagglutination. Girob[6] showed that the uptake of IgG was pH and ionic strength dependent and was influenced by the proportion of cells to IgG present during reaction. Greenwalt[7] evaluated the red blood cell concentration in effecting the percentage of agglutination and antiserum concentration as well as the temperature effect. Areview of the general features of the antigen-antibody interaction is given by Singer[8].

In the above theories, either the effect of antinbody concentration(in many cases, only the relative concentration expressed in terms of titre is given) or the antigen concentration is examined. In the present work, the combined role of antibody antigen and cellular concentrations will be described in terms of a reasonable unified theory of antigen-antibody induced agglutination; under the assumptions that factors such as the pH, temperature, ionic strength and dielectric constant are kept constant and that the effects of surface charge can be estimated in terms of a parameter of closest inter particle approach. This theory is effective in describing the onset of

aggregation over a broad range of concentrations of the three reacting elements.

In section II, the kinetics of an isolated monomer-dimer system are studied and an equation for the equilibrium concentrations of monomers and dimers derived. In section III the significance of the monomer-dimer equilibrium concentration equation in predicting higher order aggregation will be discussed. In section IV, detailed calculations of the values and concentration dependences of the parameters of the equilibrium equation will be given.

II. Reversible Monomer-Dimer System

The various particulate agglutination tests will be idealized for the purposes of analysis in the following way:

1) The particles (or cells) are assumed to be identical rigid spheres
2) Only a single species of antibody is present in all reactions. The antibody molecule is assumed to be a loose, inelastic string with a single binding site at each end.
3) The antigen molecule provides only one binding site for an antibody.

In addition, it will be assumed initially in the system of investigation, only monomers and dimers are present.

Let:

n_o be the number of monomers per unit volume

n_1 n_2 --- n_j be the number of dimers per unit volume connected by a single antibody bond, double bond, --and j fold bond respectively.

Then $c_o = n_o + 2(n_1 + n_2 + \ldots + n_j + \ldots)$ is the total number of spherical particles per unit volume. Also let fn_o^2 be the number of unbound particle

pairs per unit volume where for each pair of these monomers the center to center separation is less than a distance say L (i.e. the reaction distance) Let r be the dissociation rate of a single antigen-antibody bond and s_i be the average binding rate of the i-th bond between the two particles when they are within the reaction distance r be the dissociation rate of one antigen-antibody pair. Since each dimer consists of two particles, the rate of decrease of monomers by forming a n_1 type dimer is $2Sfn_o^2$, while the rate at which monomers reappear as a result of n_1 type dimer dissociation is $2rn_1$. The rate at which the antibody bridges from between higher order multiple bound dimer formations and dissociations occur is difficult to predict, since some of the antibody bridges may be more vulnerable to dissociation than others for geometrical re asons. However, it is convenient to assume that even for higher order dimers, all of the antibody bridges are a prior equally and independently likely to form or dissociate. It follows that the kinetics of formation and dissociation of the monomer and different dimer species is given by a set of first order differential equations:

$$\dot{n}_0 = 2s_1 f n_0^2 + 2rn_1 \tag{1}$$

$$\dot{n}_1 = s_1 f n_0^2 - rn_1 - s_2 n_1 + 2rn_2 \tag{2}$$

$$\dot{n}_2 = s_2 n_1 - 2rn_2 + 3rn_3 - s_2 n_2 \tag{3}$$

$$\dot{n}_3 = s_3 n_2 - 3rn_3 + 4rn_4 - s_4 n_3 \tag{4}$$

.....

$$\dot{n}_j = s_j n_{j-1} - jrn_j + (j+1)rn_{j+1} - s_{j+1} n_j \tag{5}$$

where n_j stands for $\frac{dnj}{dt}$,

Adding all the equations up, one gets:

$$\dot{n}_0 + 2(\dot{n}_1 + \dot{n}_2 + \cdots + \dot{n}_j + \cdots) = 0$$

and

$$n_0 + 2(n_1 + n_2 + \cdots + n_j) = C_0$$

as expected.

The general analytic time dependence of n_i is not obtainable due to the non-linearity in n_o^2. However, by setting all $\dot{n}_j = o$ in equations (1) to (5), equilibrium values of n_j can be readily obtained. For example, if only species of n_o, n_1 and n_2 are present, the equilibrium values for n_o is given by:

$$n_0^2 + \frac{1}{2fE} n_0 - \frac{C_0}{2fE} = 0 \qquad (6)$$

where $E = \frac{S_1}{r} + \frac{S_1 S_2}{2r^2}$

Letting $g = 1 - \frac{n_0}{C_0}$ equation (6) can be written as

$$g[2fC_0(1-g)^2]^{-1} = E \qquad (6\text{-}a)$$

If a maximum of n_j fold binding of the dimers occurs, the general form can be written as:

$$g[2fC_0(1-g)^2]^{-1} = \frac{S_1}{r} + \frac{S_1 S_2}{2!\, r^2} + \frac{S_1 S_2 S_3}{3!\, r^3} + \cdots + \frac{S_1 S_2 \cdots S_j}{j!\, r^j} \qquad (7)$$

It can be seen that each term on the right hand side of equation (7) arises from the presence of the j-th order dimer n_j. This makes it possible to estimate the relative concentration of the different order dimers under various equilibrium conditions.

III. Significance of the Doubly Bound Dimers

The initial pathways in agglutination are diagramed in figure 1 :

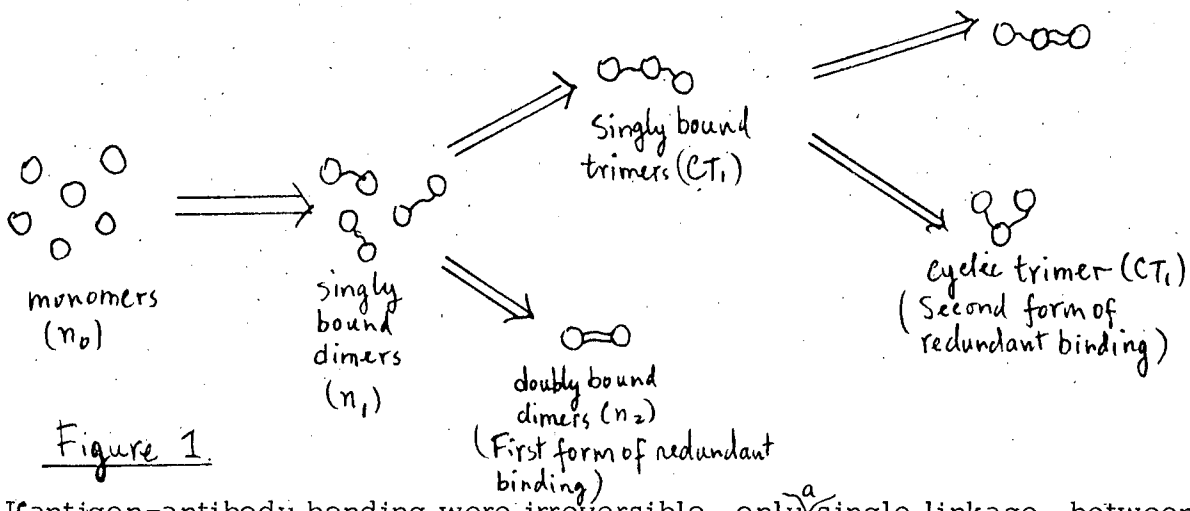

Figure 1.

If antigen-antibody bonding were irreversible, only a single linkage between the particles would be required for gradual formation of large scale aggregates. Since, in fact, thousands of antibody molecules per particle are required for agglutination to occur,[9][4] it is apparent that dissociation of the antigen-antibody bond serves to limit the rate of aggregation and so affect the conditions for agglutination. As indicated in figure 1 above, there exists elementary aggregates, the doubly bound dimer (n_2) and the cyclic trimer (CT_1), for which dissociation of one bond will not significantly alter the configuration of the particles. For such configurations, antigen-antibody reformation is much favoured over nonredundantly bound aggregates. If a break occurs in either bond of the non-cyclic trimer (T_1), the aggregate is itself dissociated and the likelihood of reformation grossly reduced. The redundant binding in n_2 and CT_1 therefore very much stabilizes the mini-aggregate.

It seems reasonable, therefore, that the conditions necessary for the formation of large scale aggregation must first be suitable for the effective production of one or both of the stable mini-aggregates n_2 and/or CT_1.

In order to more effectively estimate the minimum concentration of antibody required for large scale aggregation, it will be useful to compare the probabilities of formation and the partial and complete dissociation and the reconstruction of n_2, T_1 and CT_1.

A) Formation:

1) The average rate of forming a doubly bound dimer from a singly bound one has already been defined as S_2. If the number of singly bound dimer is n_1, the total formation rate is: $R_{N_2} = n_1 S_2$

2) In trimer formation, it is necessary to find the number of pairs of dimers and monomers which are close enough for the antibody molecule to form a bridge. If each monomer is of radius R and the antibody length ℓ is much less than R, then the accessible volume for the center of the monomer within which a linkage to a dimer is possible, is shown as V_{ac} in figure 2.

This volume can be readily calculated

$$V_{ac} \simeq 24 \pi R^2 \ell$$

For n_o monomers and n_1 dimers per unit volume, the number of such possible reacting pairs will be :

$$n_o n_1 V_{ac}$$

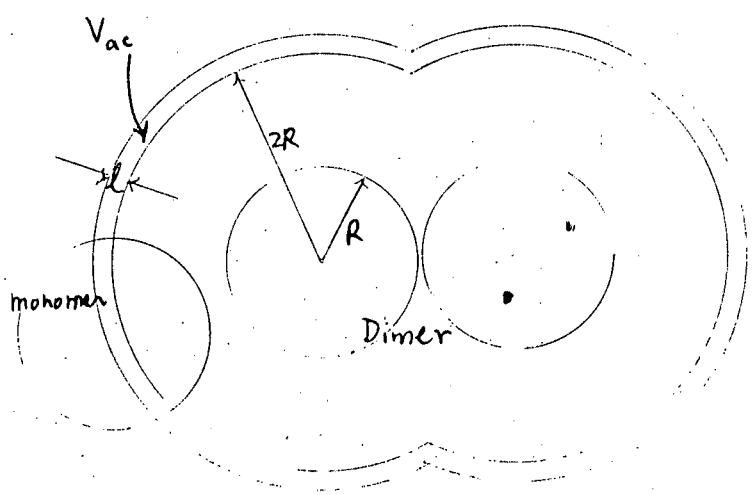

Figure 2.

Thus, the total formation rate of T_1 will then be: $R_{T_1} = S_1 n_o n_1 V_{ac}$

The ratio of the rate of formation of doubly bound dimer to that of a singly connected

trimer is therefore

$$\frac{R_{N_2}}{R_{T_1}} = \frac{n_1 S_2}{n_1 S_1 n_0 V_{ac}} = \frac{S_2}{S_1 n_0 V_{ac}}$$

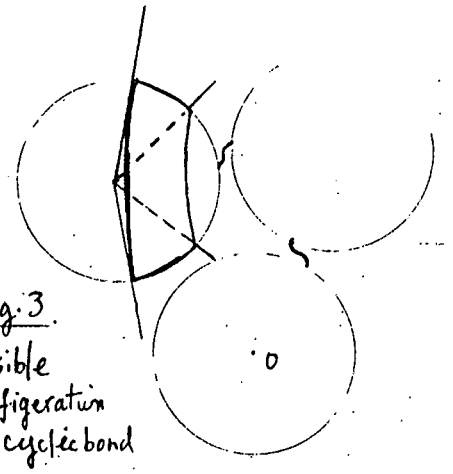

Fig. 3. possible configeration for cyclic bond

3) As shown in figure 3 only a small fraction of the T_1 trimers are geometrically available for the formation of cyclic bonds. Calculated to the lowest order of $\frac{\ell}{R}$, this fraction is $\sqrt{\frac{\ell}{R}}$. The ratio of formation of doubly bound dimer to that of potentially cyclic trimer is thus: $\frac{R_{N_2}}{R_{CT_1}} = \frac{S_2}{S_1 n_0 V_{ac}} \left(\frac{\ell}{R}\right)^{-1/2}$

In almost all practical cases of red cell or big latex particles (diameter $\sim \cdot 8\,\mu$) agglutinated by 7S antibody, these two expressions ($\frac{R_{N_2}}{R_{T_1}}$, $\frac{R_{N_2}}{R_{CT_1}}$) are much greater than one (*) showing in favour of the dimer double bound formation.

B) The chance of reformation

If one of the linkages of simply connected trimer is dissociated the likelihood of reformation is relatively small because in general the resulting dimer and monomer

*(If the volume of red cell is taken as $94\mu^3$, then $R = 2.82 \times 10^{-4}$ cm length of antibody is around 250 Å [10] while S_1, S_2 will be shown later in this text that are of the same order of magnitude. Then, even if n_0 is taken as high as 10^9 per cm^3 (about 10% suspension) $\frac{R_{N_2}}{R_{T_1}} \simeq 10^2$ and $\frac{R_{N_2}}{R_{CT_1}} \simeq 10^{+3}$)

will be rapidly separated. The chance of an initially n_2 dimer to reform its double bound, however, is very much greater since as long as the other bond remains unbroken (the chance of two bonds being broken simultaneously is considered small) the two particles are still close together. Cyclic trimer CT_1 reformation can be viewed in quite the same manner as that of n_2. However, as shown in figure 4, the probability of reformation is reduced by the rotation of sphere 0 about the z-axis. Thus, it is clear that of the two redundantly bound "stable" elementary aggregates, the n_2 is more rapidly bound and more stable than the CT_1. In order for the development of higher order aggregates to be favoured, it is apparent that the conditions for the initial formation of the doubly bound dimer must also be favorable. Viewed in this light, the idealized monomer-dimer analysis of section II examines therefore what would be the concentrations of multiply bound dimers for a given set of association and dissociation parameters and with the loss of dimer to higher particulate species (trimer, tetramers, etc) suppressed by the assumption of the model. If under the "equilibrium" condition, the concentrations of multiply bound dimers are extremely low, it is reasonable to suppose that higher order aggregations in fact will not occur, while for high "equilibrium" dimer concentrations, the conditions are clearly suitable for the formation of gross aggregates.

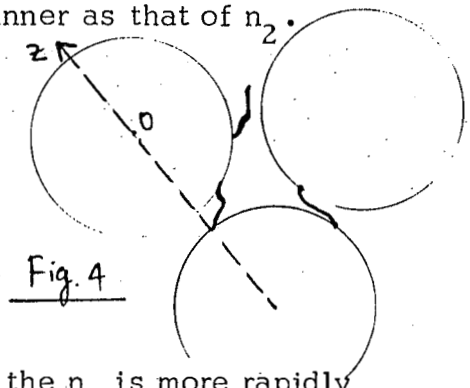

Fig. 4

IV Evaluation of the parameters f, r and S_i

A, Calculation of the proximity factor f

Consider N_o uniform spherical particles randomly distributed. Throughout a unit volume of fluid V_o. The likelihood that the center of a given particle will be within a distance of less than $2R+\ell$ from another particle is given by:

$$b = \frac{4\pi}{3}(N_o-1)\frac{(2R+\ell)^3-(2R)^3}{V_o - \frac{4\pi}{3}(N_o-1)(2R)^3}$$

where R is the radius of particles and

ℓ is the length of the antibody

Considering all N_o particles, the number of such pairs is:

$$P_N = \frac{1}{2}N_o(N_o-1)\frac{V_\ell}{V_1}$$

where

$$V_\ell = \frac{4\pi}{3}\left[(2R+\ell)^3-(2R)^3\right]$$

$$V_1 = V_o - \frac{4\pi}{3}(N_o-1)(2R)^3$$

for $N_o \gg 1$ and for dilute solution where fluid volume is much greater than particle volume;

$$P_N = \frac{2\pi N_o^2 \ell}{3V_o}(12R^2+6R\ell+\ell^2) \qquad (8)$$

The number of such pairs per unit volume is

therefore $$f = \frac{2\pi\ell}{3}(12R^2+6R\ell+\ell^2) \qquad (9)$$

In calculating this f, a purely random spatial distribution of N_o has been assumed. This will not be true for the initial non-equilibrium stage in which n_1 is increasing at the expense of those pairs of monomers which are close together. At equilibrium detailed balancing predicts that the dissociation of n_1 supplies as many closely spaced monomer pairs as are being removed by n_1 formation ‡

‡ (Since the production of N_1 can occur for a range of antibody configurations while the dissociation of n_1 occurs only when the antibody is fully stretched, the production and removal of N_o pairs occurs at slightly different spatial separations).

B, Representation of the dissociation rate r

The dissociation rate of a single antigen-antibody pair, assuming a loose string model, has been calculated to be [11]

$$r = \frac{D}{\ell}\sqrt{\frac{kT}{m}}\,\mathrm{erfc}\sqrt{\frac{E_B}{kT}} \qquad (10)$$

where:

ℓ is the length of the antibody molecule

k is the Boltzman constant

t is in absolute temperature

m is the mass of the spherical particle of radius R

E_B is the energy required to break the antigen-antibody binding

D is a constant with values:

$D = 1.67$ when $\ell \ll R$

$D = 0.72$ when $\ell > 2R$

C, Evaluation of the formation rate of the i-th bond S_i

Let $s_i = s^t{}_g h_i$ where s represents the average formation rate between an antibody already attached to particle 1 and an antigen on the surface of particle 2, t_g is the factor reflecting the number of antigen sites inside an effective area a_{ef} while the remaining factor h_i is related to the possibility that one or more such potential antigen-antibody pairs exists.

1, Calculation of the factor h_i

a) The concept of effective areas:

The probability of an antibody attached on particle 1 combining with an antigen on the surface of particle 2 depends upon the geometric configurations.

Let ℓ be the length of the antibody molecule. When the minimum distance q between the two identical particles of radius R is less than ℓ.

There is an effective area A_{ef} on each of the spherical surfaces where antibody bridges can be formed.

From figure 5, this area is:

$$A_{ef} = 2\pi R^2 (1-\cos\theta)$$

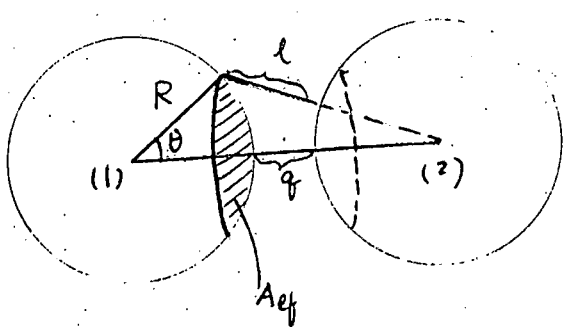

Figure 5

The effective area A_{ef} can also be expressed in terms of the distance of closest approach q.

Since $(R + \ell)^2 = R^2 + (2R + q)^2 - 2R(2R + q)\cos\theta$

$$A_{ef} = \frac{\pi R(2R+\ell+q)(\ell-q)}{2R+q} \qquad (11)$$

Let $q = \epsilon\ell$; $\epsilon \leq 1$

and for case of $R >> \ell$

$$A_{ef} = \pi R(\ell - q) = \pi R\ell(1-\epsilon) \qquad (11.a)$$

Now suppose one end of the bond is fixed at any arbitrary point G on the effective area A_q on particle 1 while the other end is free to impinge upon the second sphere. It can be seen in figure 6 that this free end can cover a sub-area on surface 2 denoted as a^o_{ef} where

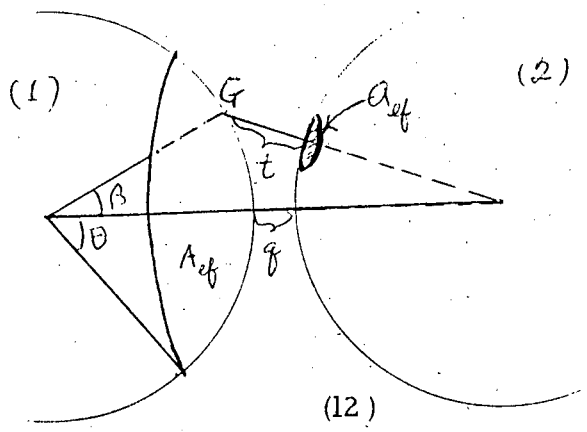

Fig. 6

$$a^o_{ef} = \frac{\pi R(\ell+t)(\ell-t)}{R+t} \qquad (12)$$

and t is the perpendicular distance from the point G to the spherical surface.

It can be shown from the geometry that $a^o_{ef} = \pi[\ell^2 - q^2 - 4Rq\mu - 4R^2\mu^2]$ (13)

where $\mu \equiv 1 - \cos\beta$

and a^o_{ef} is function of both q and the angular position B of point G. The probability of point G being anywhere on area A_{ef} is the same, while the probability of G being located at an angular position B is proportional to the annular ring $2\pi R^2 \sin\beta\, d\beta$

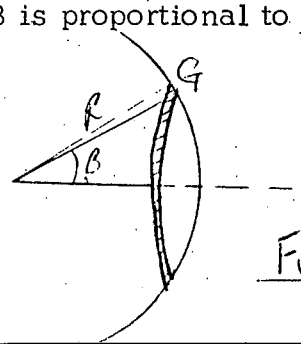

Fig. 7

Taking all values of β from 0 to Θ

into account, the average value

of a^{o}_{ef} is obtained:

$$a_{ef} = (a^{o}_{ef})_{ave} = \frac{\pi \int_0^{\theta} (\ell^2 - q^2 - 4Rq\mu + 4R^2\mu^2)\, 2\pi R^2 \sin\beta\, d\beta}{\int_0^{\theta} 2\pi R^2 \sin\beta\, d\beta}$$

$$\text{or} \quad a_{ef} = \frac{\pi \ell^2}{3}(2 - \varepsilon - \varepsilon^2) \qquad (14)$$

b) Distribution of antigens and antibodies within the effective areas. Having introduced the concept of an effective area A_{ef} and the effective sub-area a_{ef} it is now appropriate to examine the statistical distribution of antigens and antibodies within these areas.

Let $A = 4\pi R^2$ be the area of the sphere and assume that both antigen sites and antibodies are uniformly distributed over the surface. The probability of finding a particular antibody within an effective area A_{ef} is A_{ef}/A and the probability that this particular antibody is not inside is:

$(1 - A_{ef}/A)$

For a total number of N antibodies, the probability that any n of then will be inside A_{ef} is:

$$\omega(n) = \frac{N!}{n!(N-n)!}\left(\frac{A_{ef}}{A}\right)^n \left(1 - \frac{A_{ef}}{A}\right)^{N-n} \qquad (15)$$

The average value of such a distribution is $\nu = \frac{A_{ef}}{A} N$ and equation (15) can be rewritten in the form

$$\omega(n) = \frac{N!}{n!(N-n)!}\left(\frac{\nu}{N}\right)^n \left(1 - \frac{\nu}{N}\right)^{N-n} \qquad (16)$$

for n=o, N large and ν finite

$$\omega(0) = 1 - e^{-\nu} \qquad (17)$$

When the spheres are close together, there are two effective areas A_{ef}, one on each opposite surfaces. A bond is formed whenever an antibody from either one of the A_{ef} links with the other.

Let $W_b(n)$ be the probability of finding n antibodies inside the two effective areas $2A_{ef}$, then:

$$\omega_b(n) = \frac{2N!}{n!(2N-n)!}\left(\frac{2A_{ef}}{2A}\right)^n\left(1-\frac{2A_{ef}}{2A}\right)^{2N-n}$$

letting $N_b = 2N$

$\nu_b = 2\nu$

$$\omega_b(n) = \frac{N_b!}{n!(N_b-n)!}\left(\frac{\nu_b}{N_b}\right)^n\left(1-\frac{\nu_b}{N_b}\right)^{N_b-n} \qquad (18)$$

By exactly the same analysis, the probability of finding j antigens inside an effective area A_{ef} is :

$$\omega_g(j) = \frac{N_g!}{j!(N_g-j)!}\left(\frac{\nu_g}{N_g}\right)^n\left(1-\frac{\nu_g}{N_g}\right)^{N_g-j} \qquad (19)$$

where Ng is the total number of antigen on one sphere

and $\nu_g = \frac{a_{ef}}{A}\cdot N_g$

C) Determination of h_i

Assume that a pair of unbound particles are within the reaction distance, If there is only one antibody inside the combined effective areas 2Aef, the formation rate $S_1 = h_1 s = s$, and $h_1 = 1$. If there are two antibodies in 2Aef and assuming that the corresponding effective sub-areas a_{ef} do not overlap, each antibody will act independently and the formation rate will be doubled.*

* (If the concentration of antigen sites is large, the effect of the overlapping sub-areas is clearly minimized. If the antigen concentration is small, and the antigen sites widely separated, the likelihood of closely neighboring antibodies with significantly overlapping sub-areas would be extremely small.)

Thus the average value for h_1 can be written as:

$$h_1 = \sum_{n=1}^{N_b} \omega_b(n) \cdot n = \nu_b \tag{20}$$

Second bond formation after the first bond has been formed will be proportional to the number of unbridged antibodies present:

$$h_2 \propto \sum_{n=2}^{N_b} \omega_b(n)(n-1)$$

Since only the class of singly bound particles n_1 is now being considered, the two A_{ef}, of course, always contain at least one antibody and the case of zero antibody must be excluded. Including the appropriate normalization factor, the final expression for h_2 becomes

$$h_2 = \sum_{n=2}^{N_b} \omega_b(n)(n-1) \Big/ [1 - \omega_b(0)] \tag{21}$$

Defining

$$W_k \equiv 1 - \sum_{n=0}^{k-1} \omega_b(n) \tag{22}$$

The general expression for h_1 becomes :

$$h_i = \sum_{n=i}^{N_b} \omega_b(n)(n-i+1) \Big/ W_{i-1} \tag{23}$$

A variation of h_i with respect to ν_b is shown in figure 8.

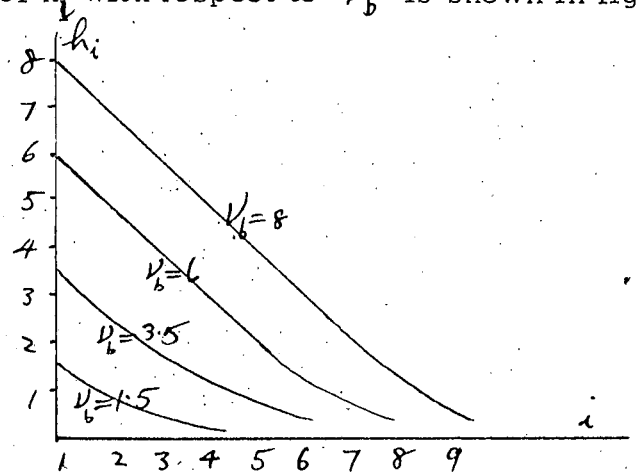

Figure 8

It is seen that for large values of ν_b, h_i is directly proportional to the average number of unbridged antibodies remaining. For smaller values of ν_b, however, the very existence of one or more antibody bridges tends to select a subset of particle pairs having an initially larger number antibodies than the general population-thus resulting in the non-linearity of the lower curves in figure 8.

2) The factor t_g

If the collision of the antibody on a_{ef} is random, one would expect the formation rate of the bond to be proportional to the number of sites. It would, therefore, be reasonable to equate t to the average number of antigen sites inside a_{ef}. (For low values of the average number of antigen sites ν_g, it is the same as the probability of finding any site inside a_{ef}, i.e. $1-e^{-\nu_g} \simeq \nu_g$)

3) The formation rate s

Consider a single unbridged antibody attached to particle 1 within the effective area A_{ef}. The average rate of antibody-bridge formation is determined principally by three factors :

i) The average frequency z_f at which the free end of the antibody impinges upon the opposite surface.

ii) The energy activation factor P_E

iii) The probability factor S_t arising from the relative orientations between the antibody and the antigen molecule inside the average effective sub-area a_{ef}

iv) Evaluation of z_f

In comparing the thermal motion of the much larger spherical particles to that of the antibody molecule, the spheres can be assumed to be quasi-

stationary, with the unbound antibody site free to move randomly in any direction. The average thermal velocity of this unbound site can be estimated from kinetic theory:

$$v_{th} = \frac{2}{3}\sqrt{\frac{8kT}{\pi m_{eq}}} \tag{25}$$

where m_q is the "effective mass of the particle" represented by the free end of the molecule. This effective mass will depend on details of its specific molecular structure-its mass distribution and flexibility and is difficult to determine accurately. It is reasonable, however, to assume this value is of the order of magnitude of the mass of the antibody molecule itself.

With one site bound at point G, an antibody molecule can have its free end anywhere inside a volume V_T as shown in figure 9 where

$$V_T = \frac{2\pi \ell^3}{3}\left(1 - \frac{3\ell}{8R}\right)$$

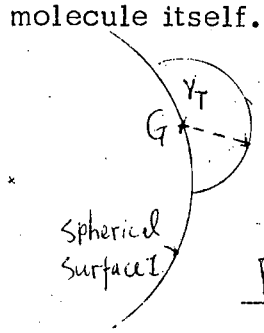

Fig. 9

In the presence of sphere 2 close to point G, the volume accessible to the free end would be reduced to $V_F = V_T - V_B$

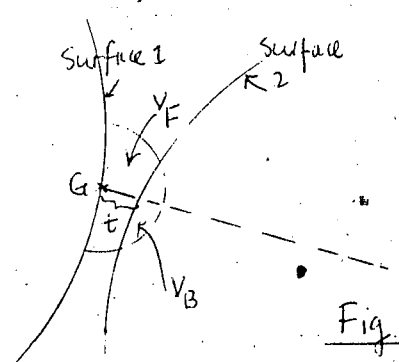

Fig. 10

As shown in figure 10, it can be shown that

$$V_B = \frac{\pi \ell^3}{3}\left\{(2+\varepsilon_1)(1-\varepsilon_1)^2 - \frac{3}{2}\left(\frac{\ell}{R}\right)\left(\frac{1-\varepsilon_1^2}{1+t/R}\right)\left[(1-\varepsilon_1) - \frac{1-\varepsilon_1^2}{2(1+\frac{t}{R})}\right] + \frac{3}{4}\left(\frac{\ell}{R}\right)^2 \frac{\varepsilon_1(1-\varepsilon_1^2)^2}{(1+t/R)^2}\right\} \tag{35}$$

where t is the perpendicular distance from G to surface 2 and $\varepsilon_1 = \frac{t}{\ell}$

The most probable value of t is given in Appendix 1.

In case $R >> \ell$

$$V_B = \frac{\pi \ell^3}{3}(2 - 3\epsilon_1 + \epsilon_1^3)$$

and thus:

$$V_F = \pi \ell^3 \left(\epsilon_1 - \frac{\epsilon_1^3}{3}\right) \tag{26}$$

Continuing to regard the unbound site as a free particle, with no preference in any particular direction, the number of "collisions" per second with the effective area a_{ef} on particle 2 is calculated in Appendix 2 and yields the result:

$$Z_f = \frac{v_{th} \cdot a_{ef}}{4 V_F}$$

$$= \frac{(2 - \epsilon - \epsilon^2)}{6(3\epsilon_1 - \epsilon_1^3)} \frac{1}{\ell} \sqrt{\frac{8kT}{\pi m_{ef}}} \tag{27}$$

(i) The factors of P_E and S_t are difficult to evaluate separately. Exact evaluation of S_t is extremely difficult because of the complexity of the molecular structures involved. So far no such determinations have been reported. In most experiments, measurements are made for the activation energy only. The value of this activation energy, however, seems to be higher than one would expect for such a biologically favored combinations (12, 13, 14) These high values may be interpreted as indicating the existence of severe steric constraints. The spatial configurations and orientations of the binding sites of colliding antigen-antibody pairs will usually be far from optimal. Higher collision energies would probably be required for binding under less favorable steric conditions. It seems reasonable to evaluate these two factors together, and introduce

$$B_{ET} = P_E S_T$$

Consider the Maxwell distribution for the velocity of the antibody molecules. (With antigen sites assumed at rest)

$$P(v) = \left(\frac{2}{\pi}\right)^{1/2} \left(\frac{m}{kT}\right)^{3/2} v^2 \exp\left(-\frac{mv^2}{2kT}\right) \tag{28}$$

The fraction of these molecules having a velocity v_A or greater is:

$$F = \int_{v_A}^{\infty} P(v)dv = A\int_{v_A}^{\infty} v^2 e^{-\alpha v^2} dv$$

with $A = \left(\frac{\pi}{2}\right)^{1/2}\left(\frac{m}{kT}\right)^{3/2}$; $\alpha = \frac{m}{2kT}$

Integrating : $$F = \frac{A}{2\alpha}\left[v_A e^{-\alpha v_A^2} + \frac{1}{2\sqrt{\alpha}} \operatorname{erfc}\sqrt{\frac{E_A}{kT}}\right] \tag{29}$$

where $E_A = \frac{1}{2} m v_A^2$

If E_A is a few K cal/mole, $E_A >> kT$ at room temperature and therefore

$$F \simeq \sqrt{\frac{2E_A}{\pi kT}} \exp\left(-\frac{E_A}{kT}\right) \tag{29.a}$$

If E_A stands for the activation energy, this would normally be interpreted as indicating that whenever an antibody molecule possesses an energy E_A or greater, and it meets an antigen site, a bond would form. But it must be noted that in this approach, E_A is an average combining energy reflecting both the minimal activation energy and the steric factors involved.

Let

$$B_{ET} = B_o F \tag{30}$$

where B_o is the probability of an antibody imp inging upon an antigen site when a collision on the sub-area a_{ef} has occurred. Now assume that there is a small effective region a_g (Not necessary the area of the antigen binding

site) such that whenever the center of an antibody binding site hits it a bond is possible (with sufficient energy $E > E_A$, of course) The probability of possible binding formation is therefore:

$$B_o = a_g / a_{ef}$$

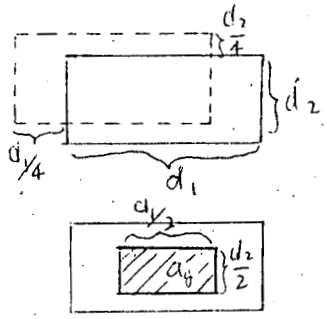

Fig. 11 Maximum dislocation for two sites and effective region a_g

The most probable value of a_g can be evaluated as follows Suppose the cross-sectional area of the binding site of the antibody is $d_1 \times d_2$. Taking the same value for the corresponding antigen site and assuming that the offset of the two binding sites can be up to one fourth of their corresponding sides, the center of the antibody binding site must strike on an area a_g equal to $\frac{d_1}{2} \times \frac{d_2}{2} = \frac{1}{4} d_1 \times d_2$ in order for a possible bondage to form.*

Referring back to equation (7) and letting $\chi = \frac{S}{r}$ the equation can be rewritten as:

$$g[2fc_o(1-g)^2]^{-1} = \sum_{j=1} \left(\prod_{i=1}^{j} h_i \right) \frac{(t_g \chi)^j}{j!} \tag{31}$$

* (Taking as an example an activation energy $E_A \sim 13.6$ K cal/mole, $E_B \sim 14.2$ K cal/mole

The antibody binding site dimensions $d_1 \times d_2 \sim 34 \times 12$ $\mathring{A}^2$ (q)

A calculation will give : $r \sim 10^{-7}\ s^{-1}$; $z_f \sim 6 \times 10^{7}\ s^{-1}$; $F \sim 6 \times 10^{-10}$; $B \sim 10^{-3}$ and $\chi = \frac{S}{r} \sim 10^2$)

All the quantities in equation (31) can be experimentally or theoretically evaluated. Equation (31) relates the particulate concentration (C_o), the antigen and antibody concentration (t_g and h_i) to the percentage of agglutination (given by g). Physico -chemical factors such as the activation and binding energies the temperature and zeta potential determining the particles distance of closest approach are contained implicitly in X and h_i.

Equation (31) can be used to predict the fractional amount of agglutination "g" or conversely from the measured value of "g" to determine "X", the ratio of the formation to dissociation rates

There is reasonably good agreement between the above theory and experiment. A summary of detailed calculations and comparisons is currently being prepared.

The most probable value of the distance t, between a point G on one spherical surface to the other.

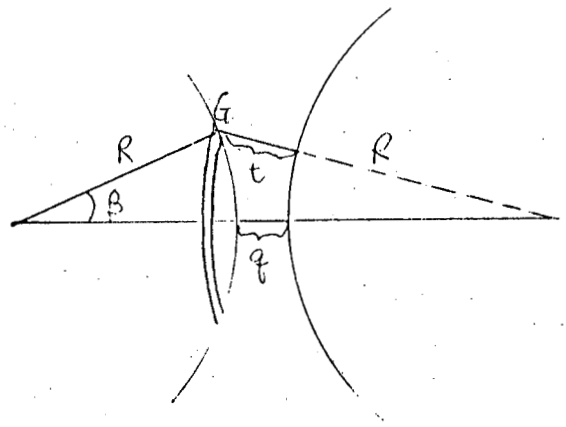

Fig A1

The value of t is a function of q and β. The most probable value of cos β can be evaluated as:

$$(\text{Cos } \beta)_{MP} = \frac{\int_0^\theta 2\pi R^2 \text{Sin } \beta \text{ Cos } \beta \, d\beta}{\int_0^\theta 2\pi R^2 \text{Sin } \beta \, d\beta}$$

$$= \tfrac{1}{2}(1 + \text{Cos } \theta)$$

where θ is the angle when $t = \ell$, the length of the antibody molecule

From the geometry of figure

$$(t+R)^2 = R^2 + (2R+q)^2 - 2R(2R+q) \cos \beta$$

inserting the most probable value of Cos β, and after simplifing;

$$t = \tfrac{1}{2}(2R+q)(1-\cos \theta) + q$$

yet (1-cos θ) can be readily calculated from the geometry to yield a value:

$$(1-\text{Cos } \theta) = \frac{\ell - q}{2R+q}$$

Thus $t = q + \frac{1}{2}(\ell - q)$

$$\simeq \tfrac{1}{2}(\ell + q)$$

$$= \frac{\ell}{2}(1+\epsilon)$$

Thus, for $\epsilon_1 = \frac{t}{\ell}$,

$$\epsilon_1 = \tfrac{1}{2}(1+\epsilon)$$

Appendix 2

To find the number of collision of one molecule with the wall of the container of arbitrary shape.

Let A_s be the total surface area of the container. Inside a volume V, a particle K moving with an average speed u, in time dt, will hit on an area dA when it is inside a volume equal to

$$u\ dt\ dA\ \cos\theta$$

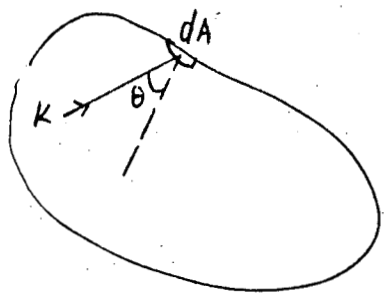

Thus, the probability $P_{dt\ dA}$ of a collision with dA in time dt is:

$$P_{dt\ dA} = \frac{u \cos\theta}{V}\, dt\ dA$$

Taking the normal to dA as the axis of polar axis, the probability of K approaching dA in direction θ and $\theta + d\theta$ will be proportional to the solid angle at dA subtended by these directions, and the chance that θ lies between θ and $\theta + d\theta$ is : $\frac{2\pi \sin\theta\, d\theta}{4\pi} = \frac{\sin\theta\, d\theta}{2}$

But collision of K on dA is possible only for values of $\theta \leq \frac{\pi}{2}$ when averaging out:

$$P_{dt\,dA} = \frac{u}{V}\, dt\, dA \int_0^{\frac{\pi}{2}} \frac{\sin\theta \cos\theta\, d\theta}{2}$$

$$= \frac{u}{4V}\, dt\, dA$$

Integrating over a surface of A,

$$P_{dt,A} = \frac{uA}{4V}\, dt$$

In a time At so that P = 1, ie certainty of a single collision then $\Delta t = \frac{4V}{uA}$

Supposing that the amount of time consumed in a collision is negligible, the total number of collision per unit time on area A is thus:

$$n_o = \frac{1}{\Delta t} = \frac{uA}{4V}$$

REFERENCES

1. Pollack, W., Hoger, H.J., Reckel, R., Toren, D.A., and Singher, H.O. Transf. 5:158 (1965)

2. Greenbury, C.L., Moove, D.H. and Nunn, L.A.C. Immunol. 6:421 (1963)

3. Singer, J.M., Oreskes, I., Hutterer, F. and Ernst, J. Ann. rheum. Dus. 22:424 (1963)

4. Leikola, J. and Pasaner, V.J. Int. Arch. Allergy Appl. Imm. 39:352 (1970)

5. Hoter, L.W. and Trabold, N.C. J. Clin. Invest. 49:87 (1970)

6. Grob, P.J., Frommel, D., Isliker, H.C. and Masouredis, S.P. Immunol. 13:489 (1967)

7. Greenwalt, T.J. and Steane, E.A. Brit. J. Haematology 19:691 (1970)

8. Singer, J.M. Bull. Rheumatic Disease 24:762 (73)

   Singer, J.M. Vekemans, F.C.A., Lichtenbelt, J.W.T., Hesselink, F.T. and Weinsema, P.H., J. Colloid and Interface Sci. 45:608 (1973)

9. Barrett, J.T. Textbook of Immunology, The C.V. Mosby Comp. (1970)

10. Almeido, J., Cinader, B. and Howatson, A.J. Exp. Med. 118:327 (1963)

11. Sugerman, D. and Hart, H.E. Bull. Math, Bio. 35:219 (1973)

12. Hughes-Jones, N.C., Gardner, B. and Telford, R. Biochem. J. 88:435 (1963)

13. Cann, J.R. and Clark, E.W. J. Immunol. 72:463 (1954)

14. Economidou, J., Hughes-Jones, N.C., Gardner, B. Immunol. 13:227 (1967)

APPENDIX II

Current Research in Multicompartment Tracer Analysis

In attempting to identify a linear multi-compartment model for a steady-state biological system using tracer mehods, appropriate experimental data must be obtained. It is of interest that the necessary set of experimental measurements capable of providing enough information to completely define the system is not unique in that the choice of injections and measurements to be performed can be specified in several seemingly unrelated ways. The general principle underlying what constitutes a complete set of experimental measurements that can determine such a multicompartment system is now being investigated.

In section I it is proposed that the existence of a properly defined reference compartment is a necessary condition for establishing the completeness of a set of measurements and a general algebraic approach for studying the problem is outlined. In section II it is shown that the existence of a reference compartment is a necessary and sufficient condition for solution of an n compartment system if the n measurements to be performed are chosen from 2 columns or rows of the transition matrix. In section III the equations and corresponding conditions for solution when measurements are selected from 3 and 4 columns are compared. A general mathematical expression for the necessary condition for solution for any n measurements is derived in section IV and a pictorial analogue with the resulting representations of several solvable and non-solvable cases are presented in section V.

General Algebraic Considerations

Consider the n compartment linear system described by the vector eqn. (1), where the components $x_i(t)$, $(i=1,\ldots,n)$ of the vector $\underline{x}(t)$ are the concentrations of labeled material in each compartment i and $\underline{\underline{a}}$ is an (nxn) constant matrix composed of the n^2 transfer rates a_{ij} $(i,j=1,\ldots,n)$.

$$\dot{\underline{x}}(t) + \underline{\underline{a}}\,\underline{x}(t) = 0 \tag{1}$$

It has been shown by H. Hart (ref. 1) that the matrix $\underline{\underline{a}}$ defining the system (1) can in general be specified by measuring the concentrations $x_i(t)$ in all compartments i for sufficiently long periods of time, assuming constant initial conditions.

$$x_i(t) = \sum_{k=1}^{n} A_{ik}\, e^{\lambda_k t}, \qquad i=1,\ldots,n \tag{2}$$

The values $a_{ij}(i,j=1,\ldots,n)$ can be expressed in terms of the parameters $\lambda_k(k=1,\ldots,n)$ and $A_{ik}(i,k=1,\ldots,n)$ of the solutions (2) which best fit the experimental data.

$$a_{ij} = \begin{vmatrix} A_{11} & A_{21} & \cdots & A_{j-1,1} & \lambda_1 A_{i1} & A_{j+1,1} & \cdots & A_{n1} \\ A_{12} & A_{22} & & A_{j-1,2} & \lambda_2 A_{i2} & A_{j+1,2} & & A_{n2} \\ \vdots & \vdots & & \vdots & \vdots & \vdots & & \vdots \\ A_{1n} & A_{2n} & & A_{j-1,n} & \lambda_n A_{in} & A_{j+1,n} & & A_{nn} \end{vmatrix} \div |A| \tag{3}$$

where $|A|$ is assumed $\neq 0$. (This requirement is always satisfied (ref. 5)

Thus measurement of the concentrations $x_i(t)$ in all compartments i, subject to constant initial conditions, constitutes a complete set of measurements capable of defining the system.*

The general solution to the system (1) for initial concentrations $\underline{x}(0)$ can be written in matrix form as follows: (ref. 2,3)

$$\underline{X}(t) = \underline{\underline{T}}(t) \cdot \underline{X}(0) \tag{4a}$$

or

$$\begin{pmatrix} X_1(t) \\ X_2(t) \\ \vdots \\ X_n(t) \end{pmatrix} = \begin{pmatrix} T_{11} & T_{12} & \cdots & T_{1n} \\ T_{21} & T_{22} & & T_{2n} \\ \vdots & & & \\ T_{n1} & T_{n2} & & T_{nn} \end{pmatrix} \begin{pmatrix} X_1(0) \\ X_2(0) \\ \vdots \\ X_n(0) \end{pmatrix} \tag{4b}$$

where $\underline{\underline{T}}(t)$ is the (nxn) state transition matrix whose elements

$$T_{ij}(t) = \sum_{k=1}^{n} A_{ik}^{j} e^{\lambda_k \cdot t} \tag{5}$$

represent the tracer concentration in the ith compartment at time t subsequent to unit injection in the jth compartment at time t=0. It follows from the previous discussion that measurement of a complete column j of the transition matrix constitutes a complete set of measurements from which the n^2 parameters a_{ij} or equivalently all the elements of the transition

* A complete set of measurements capable of defining a system is a set of injections and measurements which will in general permit determination of all a_{ij}. We are not considering the effect of any special relationship that may exist between the a_{ij} of a particular system.

matrix can be determined. Knowledge of a single row i of the transition matrix is also sufficient to uniquely define the model (ref. 4). Physically the measurement of a single row i of the transition matrix implies that injections are made in each of the n compartments separately and the activity of the ith compartment is measured after each injection. In addition to any complete row or column certain other combinations of n elements of the transition matrix are sufficient to describe the system. As will be verified, if any set of n elements of $\underline{T}$ (do not) constitute a complete set capable of defining the matrix $\underline{\underline{a}}$ then the corresponding elements of the transposed matrix also (do not) constitute a complete set. While only the n elements of a row or a column in general <u>uniquely</u> define the system, we are here referring to those other sets of n elements for which the numerical values of all n^2 elements a_{ij} can be determined subject to a residual ambiguity in assigning the values.

Equation (3) can be written in matrix form

$$\underline{\underline{a}} = \underline{\underline{A}}\,\underline{\underline{\lambda}}\,\underline{\underline{A}}^{-1}, \qquad \underline{\underline{\lambda}} = \begin{pmatrix} \lambda_1 & & & 0 \\ & \lambda_2 & & \\ & & \ddots & \\ 0 & & & \lambda_n \end{pmatrix} \tag{6}$$

where the diagonal elements of $\underline{\underline{\lambda}}$ are the eigenvalues of $\underline{\underline{a}}$ and the eigenvectors are the columns of $\underline{\underline{A}}$. The n eigenvalues λ_i (i=1,...,n) can be determined from the measurement of any element T_{ij} of the transition matrix over a long enough time t and the parameters λ_i then define the invariants of the matrix (trace, determinant, etc.). For a two compartment system consideration of the invariants leads to two equations in four unknowns:

$$a_{11} + a_{22} = \lambda_1 + \lambda_2 \qquad \text{(trace)} \tag{7a}$$

$$a_{11} a_{22} - a_{12} a_{21} = \lambda_1 \lambda_2 \qquad \text{(Det.)} \tag{7b}$$

Since measurement of any element T_{ij} is also sufficient to determine the corresponding element a_{ij} of the matrix $\underline{\underline{a}}$ (ref. 5), it is evident that the system of equations (7) can be solved if the elements of any row or column of $\underline{\underline{T}}$ and, therefore, also of $\underline{\underline{a}}$ are known. It is also apparent that a solution can be obtained if T_{12} and T_{21} are measured (i.e. a_{12} and a_{21} determined). Note however, that the set of diagonal elements T_{11} and T_{22} does not result in a complete solution for the 2x2 matrix $\underline{\underline{a}}$ since only the product of a_{12} and a_{21} can be specified (fig. 1).

For a three compartment system each element T_{ij} permits a_{ij} and the cofactor of a_{ji} to be determined. Another invariant, the trace of the adjoint of $\underline{\underline{a}}$ (i.e. the sum of the cofactors of the diagonal elements of $\underline{\underline{a}}$) can be expressed in terms of the λ's. Generally, for every n elements of $\underline{\underline{T}}$ (nxn) known, a system of n^2 non-linear algebraic equations (ref.5) can be set up for the n^2 a_{ij}'s but if the n elements are not in the same column or row these equations may not all be independent and only partial solutions can be obtained.

The seventeen physically different ways of selecting the three elements T_{ij} for n=3 are indicated in fig.2 where any matrix resulting from a simple relabeling of rows or columns is considered equivalent and is not shown. Sets of elements of $\underline{\underline{T}}$ whose transpose elements are physically different but have equivalent algebraic solutions are noted by the superscript $^{\tau}$.

It can be seen from fig.2 that with the exception of #17 all of the cases leading to partial solutions fall into two categories:

1) Two or more measured elements are on the diagonal of $\underline{\underline{T}}$ (#'s 10,11,13,16)

2) No measured element appears from one of the columns and none from one of the rows of $\underline{\underline{T}}$. (#'s 8,9,12-15)

Upon examination, the sets of complete injection-measurements fall into two classes, corresponding in a sense, to the two basic solutions of one complete column or one complete row of the transition matrix. The column sets of transition matrix elements reflect experiments in which one compartment is injected and all of the n compartments are measured. The injected compartment can be viewed as a "reference compartment" with respect to which all n measurements are being taken. Generalizing this concept a set of transition matrix elements such as T_{11}, T_{21}, T_{32} may also be viewed as exhibiting a reference compartment. Clearly T_{11} and T_{21} refer to the common reference injection compartment 1. However, compartment 3 also refers to the injection compartment 1 albeit indirectly through compartment 2. Thus T_{11}, T_{21} and T_{32} form a complete set whereas for example T_{11}, T_{21} and T_{23} would not. The corresponding generalization applies for the common reference measurement compartment. For many sets of transition elements more than one common reference compartment is operative (n=2, #3), (n=3, #'s 5,6 and 7). In case 7, all three compartments can be viewed as the reference compartment. Viewing compartment 1

Elements of T known		Elements of that can be determin
	n=2	complete solution
1)	T_{11}, T_{21} $\begin{pmatrix} \circ & \\ \circ & \end{pmatrix}$	$a_{11}, a_{12}, a_{21}, a_{22}$ $\begin{pmatrix} \circ & \circ \\ \circ & \circ \end{pmatrix}$
2) (1^{τ})	T_{11}, T_{12} $\begin{pmatrix} \circ & \circ \\ & \end{pmatrix}$	
3)	T_{12}, T_{21} $\begin{pmatrix} & \circ \\ \circ & \end{pmatrix}$	
		partial solution
4)	T_{11}, T_{22} $\begin{pmatrix} \circ & \\ & \circ \end{pmatrix}$	a_{11}, a_{22} $\begin{pmatrix} \circ & \\ & \circ \end{pmatrix}$

fig. 1

---

n=3

		complete solution
1)	T_{11}, T_{21}, T_{31} $\begin{pmatrix} \circ & & \\ \circ & & \\ \circ & & \end{pmatrix}$	$a_{11}, a_{12}, a_{13}, a_{21}, a_{22}, a_{23}, a_{31}, a_{32}, a_{33},$ $\begin{pmatrix} \circ & \circ & \circ \\ \circ & \circ & \circ \\ \circ & \circ & \circ \end{pmatrix}$
2) (1^{τ})	T_{11}, T_{12}, T_{13} $\begin{pmatrix} \circ & \circ & \circ \\ & & \\ & & \end{pmatrix}$	
3)	T_{11}, T_{21}, T_{32} $\begin{pmatrix} \circ & & \\ \circ & & \\ & \circ & \end{pmatrix}$	
4) (3^{τ})	T_{11}, T_{12}, T_{23} $\begin{pmatrix} \circ & \circ & \circ \\ & & \\ & & \end{pmatrix}$	
5)	T_{12}, T_{21}, T_{31} $\begin{pmatrix} & \circ & \\ \circ & & \\ \circ & & \end{pmatrix}$	
6) (5^{τ})	T_{12}, T_{13}, T_{21} $\begin{pmatrix} & \circ & \circ \\ \circ & & \\ & & \end{pmatrix}$	
7)	T_{13}, T_{21}, T_{32} $\begin{pmatrix} & & \circ \\ \circ & & \\ & \circ & \end{pmatrix}$	
		partial solution
8)	T_{11}, T_{31}, T_{32} $\begin{pmatrix} \circ & & \\ & & \\ \circ & \circ & \end{pmatrix}$	$a_{11}\ a_{12}\ a_{31}\ a_{32}$ $\begin{pmatrix} \circ & \circ & \\ & & \\ \circ & \circ & \end{pmatrix}$
9) (8^{τ})	T_{11}, T_{13}, T_{23} $\begin{pmatrix} \circ & & \circ \\ & & \\ & & \circ \end{pmatrix}$	$a_{11}\ a_{13}\ a_{21}\ a_{23}$ $\begin{pmatrix} \circ & & \circ \\ \circ & & \circ \\ & & \end{pmatrix}$
10)	T_{11}, T_{22}, T_{31} $\begin{pmatrix} \circ & & \\ & \circ & \\ \circ & & \end{pmatrix}$	$a_{11}\ a_{13}\ a_{22}\ a_{31}\ a_{33}$ $\begin{pmatrix} \circ & & \circ \\ & \circ & \\ \circ & & \circ \end{pmatrix}$
11) (10^{τ})	T_{11}, T_{13}, T_{22} $\begin{pmatrix} \circ & & \circ \\ & \circ & \\ & & \end{pmatrix}$	$a_{11}\ a_{13}\ a_{22}\ a_{31}\ a_{33}$ $\begin{pmatrix} \circ & & \circ \\ & \circ & \\ \circ & & \circ \end{pmatrix}$
12)	T_{11}, T_{12}, T_{21} $\begin{pmatrix} \circ & \circ & \\ \circ & & \\ & & \end{pmatrix}$	$a_{11}\ a_{12}\ a_{21}\ a_{22}\ a_{33}$ $\begin{pmatrix} \circ & \circ & \\ \circ & \circ & \\ & & \circ \end{pmatrix}$
13)	T_{11}, T_{21}, T_{22} $\begin{pmatrix} \circ & & \\ \circ & \circ & \\ & & \end{pmatrix}$	$a_{11}\ a_{12}\ a_{21}\ a_{22}\ a_{33}$ $\begin{pmatrix} \circ & \circ & \\ \circ & \circ & \\ & & \circ \end{pmatrix}$
14)	T_{21}, T_{31}, T_{32} $\begin{pmatrix} & & \\ \circ & & \\ \circ & \circ & \end{pmatrix}$	$a_{21}\ a_{22}\ a_{31}\ a_{32}$ $\begin{pmatrix} & & \\ \circ & \circ & \\ \circ & \circ & \end{pmatrix}$
15)	T_{11}, T_{12}, T_{31} $\begin{pmatrix} \circ & \circ & \\ & & \\ \circ & & \end{pmatrix}$	$a_{11}\ a_{12}\ a_{31}\ a_{32}$ $\begin{pmatrix} \circ & \circ & \\ & & \\ \circ & \circ & \end{pmatrix}$
16)	T_{11}, T_{22}, T_{33} $\begin{pmatrix} \circ & & \\ & \circ & \\ & & \circ \end{pmatrix}$	$a_{11}\ a_{22}\ a_{33}$ $\begin{pmatrix} \circ & & \\ & \circ & \\ & & \circ \end{pmatrix}$
17)	T_{13}, T_{22}, T_{31} $\begin{pmatrix} & & \circ \\ & \circ & \\ \circ & & \end{pmatrix}$	$a_{11}\ a_{13}\ a_{22}\ a_{31}\ a_{33}$ $\begin{pmatrix} \circ & & \circ \\ & \circ & \\ \circ & & \circ \end{pmatrix}$

fig.2

as the reference entity, T_{21} indicates that 2 is being measured directly with respect to 1. T_{32} indicates that 3 is being measured with respect to 1 indirectly through 2. T_{13} indicates that 1 is being measured doubly indirectly first through 3 and then through 2.

In summary the observed necessary and sufficient condition for a complete solution when n=2 and n=3 is that:

(α) All n compartments must be either measured or injected with respect to a common reference compartment.

<u>Necessary Condition for the Completeness of a Set of Measurements in a General n Compartment System</u>

It will now be proven that statement (α) above is also the necessary condition for the completeness of a set of measurements in the <u>general</u> n compartment case.

From equations (4b) and (5) it is clear that the coefficients of the exponentials in the jth column of the transition matrix form an A_{ik} matrix (symbolized by $\underline{\underline{A}}^j$) corresponding to a unit injection in the jth compartment. Rewriting equation (6) in this new notation:

$$\underline{\underline{a}} = (\underline{\underline{A}}^j)\,\underline{\underline{\lambda}}\,(\underline{\underline{A}}^j)^{-1} \quad \text{where} \quad \underline{\underline{A}}^j \equiv \begin{pmatrix} A^j_{11} & A^j_{12} & \cdots & A^j_{1n} \\ \vdots & & & \\ A^j_{n1} & A^j_{n2} & \cdots & A^j_{nn} \end{pmatrix} \tag{8}$$

Since the matrix $\underline{\underline{A}}^j$ diagonalizes $\underline{\underline{a}}$, $(\underline{\underline{A}}^j)^{-1}\underline{\underline{a}}\,(\underline{\underline{A}}^j) = \underline{\underline{\lambda}}$, the corresponding eigenvector equations are :

$$\underline{\underline{a}}\,\underline{A}_k^j = \lambda_k \underline{\underline{I}}\,\underline{A}_k^j$$

$$\text{or} \qquad (\underline{\underline{a}} - \lambda_k \underline{\underline{I}})\underline{A}_k^j = 0 \quad , \quad \underline{A}_k^j = \begin{pmatrix} A_{1k}^j \\ A_{2k}^j \\ \vdots \\ A_{nk}^j \end{pmatrix} \tag{9}$$

where $\underline{A}_k^j$ is the eigenvector corresponding to the kth column of the matrix $\underline{\underline{A}}^j$.

Since corresponding columns k of any two matrices $\underline{\underline{A}}^j$ and $\underline{\underline{A}}^{j'}$ are eigenvectors of $\underline{\underline{a}}$ with the same eigenvalue λ_k the ratios of their components must be constant.

$$\frac{A_{ik}^j}{A_{ik}^{j'}} = \frac{A_{i'k}^j}{A_{i'k}^{j'}} \quad \text{or} \quad A_{ik}^j = \left(\frac{A_{i'k}^j}{A_{i'k}^{j'}}\right) A_{ik}^{j'} \quad ; \quad \begin{matrix} i \neq i' \\ j \neq j' \\ k = 1,\dots,n \end{matrix} \tag{10a}$$

The elements in equations (10a) are further related by the n^2 conditions:

$$T_{ij}(0) = \delta_{ij} \quad \text{or} \quad \sum_{k=1}^{n} A_{ik}^j = \delta_{ij} \quad ; (i,j = 1,\dots,n) \tag{10b}$$

It will be shown in the Appendix that unless exactly one element of T_{ij} is measured in each of the columns or rows, a complete solution is not generally obtainable. To further examine the requirement for a complete solution consider now an experimental design of n experiments in which one element (j') selected randomly for each row of the transition matrix is in fact measured.* From (10a) it follows that all of the unknowns can be expressed in terms

---

* Rewriting (10a) as $A_{ik}^j = \left(\frac{A_{ik}^{j'}}{A_{i'k}^{j'}}\right) \cdot A_{i'k}^j$ it is readily seen that the algebraic formalism is essentially identical when one element (j' selected randomly for each column) of the transition matrix is determined.

of the remaining $n(n-1)$ unknowns of the i' row.

The formal solution for these remaining unknowns will be complete if the $n(n-1)$ equations of (10b) relating to these unknowns are in fact independent. The independence of these equations for various cases will be examined in detail in the subsequent Sections.

Two Column Experimental Design

Consider the case where the n elements of the transition matrix are experimentally determined in two columns, s and t of $\underline{\underline{T}}$. For future reference, the 2 column configuration is designated as the case, m=2. Then we can define:

n_s : the number of measured elements in column s

n_t : the number of measured elements in column t

so that $n = n_s + n_t$

The rows of the measured elements in column s are labelled:

$\sigma_1, \sigma_2, \ldots, \sigma_{n_s}$

and the rows of the measured elements in column t are labelled:

$\tau_1, \tau_2, \ldots, \tau_{n_t}$

No two rows σ or τ can be the same since as indicated in the appendix all rows must be represented. In the above representation the measured elements of the transition matrix in columns s and t are respectively: $T_{\sigma s}$ ($\sigma = \sigma_1, \sigma_2, \ldots, \sigma_{n_s}$) and $T_{\tau t}$ ($\tau = \tau_1, \tau_2, \ldots, \tau_{n_t}$) and the corresponding experimentally determinable coefficients of the terms $e^{\lambda_k t}$ are $A^s_{\sigma k}$ and $A^t_{\tau k}$, (k=1,...,n). The remaining n unmeasured elements of $\underline{\underline{T}}$ in columns s and t are respectively $T_{\tau s}$ ($\tau = \tau_1, \tau_2, \ldots \tau_{n_t}$) and $T_{\sigma t}$ ($\sigma = \sigma_1, \sigma_2, \ldots, \sigma_{n_s}$) and the corresponding n^2 coefficients $A^s_{\tau k}$ and $A^t_{\sigma k}$,(k=1,...,n) are therefore unknowns.

It will be sufficient for the following analysis to examine the relations (10) for the two columns $j = s$ and $j = t$ alone. Choosing i' arbitrarily to be the fixed row σ_1 these are:

$$A^{s}_{\tau k} = \left(\frac{A^{s}_{\sigma_1 k}}{A^{t}_{\sigma_1 k}}\right) A^{t}_{\tau k}, \quad \begin{pmatrix}\tau=\tau_1,\tau_2,\ldots,\tau_{n_t}\\ k=1,\ldots,n\end{pmatrix} \qquad A^{t}_{\sigma k} = \left(\frac{A^{t}_{\sigma_1 k}}{A^{s}_{\sigma_1 k}}\right) A^{s}_{\sigma k}, \quad \begin{pmatrix}\sigma=\sigma_2,\sigma_3,\ldots,\sigma_{n_s}\\ k=1,\ldots,n\end{pmatrix} \tag{11a}$$

$n \cdot n_t$ equations $\qquad$ $n \cdot (n_s - 1)$ equations

$$\sum_{k=1}^{n} A^{s}_{\tau k} = \delta_{\tau s}, \quad (\tau=\tau_1,\tau_2,\ldots,\tau_{n_t}) \; ; \quad \sum_{k=1}^{n} A^{t}_{\sigma k} = \delta_{\sigma t}, \quad (\sigma=\sigma_1,\sigma_2,\ldots,\sigma_{n_s}) \tag{11b}$$

n_t equations $\qquad$ n_s equations

The relations (11a) and (11b) together constitute n^2 equations for determining the n^2 unknown coefficients in the n unmeasured elements of the s and t columns of the T_{ij} matrix. Substituting (11a) in (11b) the system of equations (12) consists of n equations for the n unknowns $A^{t}_{\sigma_1 k}$ (k=1,...,n) in the unknown element $T_{\sigma_1 t}$, in terms of which all other unknowns have been expressed in (11a).

$$\sum_{k=1}^{n} \left[\frac{A^{s}_{\sigma k}}{A^{s}_{\sigma_1 k}}\right] \left(A^{t}_{\sigma_1 k}\right) = \delta_{\sigma t}, \quad (\sigma=\sigma_1,\sigma_2,\ldots,\sigma_{n_s}) \tag{12a}$$

$$\sum_{k=1}^{n} \left[A^{s}_{\sigma_1 k} \cdot A^{t}_{\tau k}\right] \left(\frac{1}{A^{t}_{\sigma_1 k}}\right) = \delta_{\tau s}, \quad (\tau=\tau_1,\tau_2,\ldots,\tau_{n_t}) \tag{12b}$$

where known values appear in brackets and unknowns are in parentheses.

A complete solution for the $A^{t}_{\sigma_1 k}$ is not possible if all $\delta_{\sigma t}$ and $\delta_{\tau s}$ vanish. This is readily seen by deviding equations (12a)

by any unknown $A^{t}_{\sigma_1 K_p}$ and multiplying equations (12b) by the same unknown. The resulting equations will contain only the (n-1) ratios $\frac{A^{t}_{\sigma_1 K_q}}{A^{t}_{\sigma_1 K_p}}$ $(q \neq p)$ and a complete solution is therefore precluded. The necessary condition for a complete solution is therefore:

$\underline{n=2}$

$$\delta_{\sigma^* t} = 1 \qquad \text{or} \qquad \delta_{\tau^* s} = 1 \tag{13}$$

Either one of the unmeasured rows σ^* in column t is numerically equal to t (i.e. is a diagonal element of the T_{ij} matrix) or one of the unmeasured rows τ^* in column s is numerically equal to s (i.e. also a diagonal element). A complete solution is therefore clearly unobtainable if 2 of the n experimentally measured elements of the transition matrix occur on the diagonal. Alternatively, this means that a solution for $\underline{\underline{a}}$ can only be obtained if at least one of the injected compartments, for instance s, is measured after an injection in the other compartment t. Therefore, t can serve as the necessary "reference compartment" of statement (α).

If the measured elements of the transition matrix are restricted to two rows rather than to two columns, the above analysis follows exactly with appropriate subscript and superscript interchange** and the "reference compartment" requirement of statement (α) remains valid.

** If s and t now represent 2 rows of $\underline{\underline{T}}$ and the variables σ and τ are the columns of the measured elements in each row, all equations are valid if the subscripts σ and τ and the superscripts t and s are interchanged. For example, equations (12) become:

$$\sum_{K=1}^{n} \left[\frac{A^{\sigma}_{sK}}{A^{\sigma_1}_{sK}} \right] \left(A^{\sigma_1}_{tK} \right) = \delta_{\sigma t}, \quad (\sigma = \sigma_1, \sigma_2, \ldots, \sigma_{n_s})$$

$$\sum_{K=1}^{n} \left[A^{\sigma_1}_{sK} \cdot A^{\tau}_{tK} \right] \left(\frac{1}{A^{\sigma_1}_{tK}} \right) = \delta_{\tau s}, \quad (\tau = \tau_1, \tau_2, \ldots, \tau_{n_t})$$

Three and Four Column Experimental Design

Consider the cases where m compartments are injected and all n ($n \geq m$) compartments are measured for m=3 and m=4. Extending the notation of the previous section (m=2,case) to m=3 and m=4, the injected compartments are labelled r,s, and t for m=3 and r,s,t, and u for m=4. The number of measured elements in columns r,s,t,and u are n_r, n_s, n_t, and n_u^* respectively. Thus, $n = n_r + n_s + n_t + n_u$, where for m=3, $n_u = 0$.

The rows of measured elements in column				r	are labelled	$\rho_1, \rho_2, \cdots, \rho_{n_r}$
"	"	"	"	s	"	$\sigma_1, \sigma_2, \cdots, \sigma_{n_s}$
"	"	"	"	t	"	$\tau_1, \tau_2, \cdots, \tau_{n_t}$
"	"	"	"	u	"	$\upsilon_1, \upsilon_2, \cdots, \upsilon_{n_u}$

The n measured elements of $\underline{\underline{T}}$ are $T_{\rho r}, T_{\sigma s}, T_{\tau t}, T_{\upsilon u}$*

Thus, the n^2 experimentally determinable coefficients are:

$$A^r_{\rho K} \quad A^s_{\sigma K} \quad A^t_{\tau K} \quad \text{and} \quad A^u_{\upsilon K}{}^* \;, \quad (k=1,\ldots,n), \quad \begin{pmatrix} \rho = \rho_1, \rho_2, \cdots \rho_{n_r} \\ \sigma = \sigma_1, \sigma_2, \cdots \sigma_{n_s} \\ \tau = \tau_1, \tau_2, \cdots \tau_{n_t} \\ \upsilon = \upsilon_1, \upsilon_2, \cdots \upsilon_{n_u} \end{pmatrix}$$

All unknowns in columns r,s,t,and u (e.g. in column s these are $A^s_{\rho K}$, $A^s_{\tau K}$, and $A^s_{\upsilon K}$*) can be expressed using (10a) in terms of the (m-1)n such unknowns in any row i'. Choosing $i' = \sigma_1$, and substituting the resulting expressions of (10a) into (10b) the following systems of equations can be set up for the (m-1)n unknowns $A^r_{\sigma_1 K}$, $A^t_{\sigma_1 K}$, and $A^u_{\sigma_1 K}$*, (k=1,...,n)

---

* m=4 only

m=3	m=4	
$\sum_{k=1}^{n}\left[A^{s}_{\sigma_i k}\, A^{r}_{\rho k}\right]\left(\frac{1}{A^{r}_{\sigma_i k}}\right) = \delta_{\rho s}$	$\sum_{k=1}^{n}\left[A^{s}_{\sigma_i k}\, A_{\rho k}\right]\left(\frac{1}{A^{r}_{\sigma_i k}}\right) = \delta_{\rho s}$	
$\sum_{k=1}^{n}\left[A^{s}_{\sigma_i k}\, A^{t}_{\tau k}\right]\left(\frac{1}{A^{t}_{\sigma_i k}}\right) = \delta_{\tau s}$	$\sum_{k=1}^{n}\left[A^{s}_{\sigma_i k}\, A^{t}_{\tau k}\right]\left(\frac{1}{A^{t}_{\sigma_i k}}\right) = \delta_{\tau s}$	(14a)
$(n_r + n_t$ eqns)	$\sum_{k=1}^{n}\left[A^{s}_{\sigma_i k}\, A^{u}_{u k}\right]\left(\frac{1}{A^{u}_{\sigma_i k}}\right) = \delta_{u s}$	
	$(n_r + n_t + n_u$ eqns)	
$\sum_{k=1}^{n}\left[\frac{A^{s}_{\sigma k}}{A^{s}_{\sigma_i k}}\right]\left(A^{t}_{\sigma_i k}\right) = \delta_{\sigma t}$	$\sum_{k=1}^{n}\left[\frac{A^{s}_{\sigma k}}{A^{s}_{\sigma_i k}}\right]\left(A^{t}_{\sigma_i k}\right) = \delta_{\sigma t}$	
$\sum_{k=1}^{n}\left[A^{r}_{\rho k}\right]\left(\frac{A^{t}_{\sigma_i k}}{A^{r}_{\sigma_i k}}\right) = \delta_{\rho t}$	$\sum_{k=1}^{n}\left[A^{r}_{\rho k}\right]\left(\frac{A^{t}_{\sigma_i k}}{A^{r}_{\sigma_i k}}\right) = \delta_{\rho t}$	(14b)
$(n_s + n_r$ eqns)	$\sum_{k=1}^{n}\left[A^{u}_{u k}\right]\left(\frac{A^{t}_{\sigma_i k}}{A^{u}_{\sigma_i k}}\right) = \delta_{u t}$	
	$(n_s + n_r + n_u$ eqns)	
$\sum_{k=1}^{n}\left[\frac{A^{s}_{\sigma k}}{A^{s}_{\sigma_i k}}\right]\left(A^{r}_{\sigma_i k}\right) = \delta_{\sigma r}$	$\sum_{k=1}^{n}\left[\frac{A^{s}_{\sigma k}}{A^{s}_{\sigma_i k}}\right]\left(A^{r}_{\sigma_i k}\right) = \delta_{\sigma r}$	
$\sum_{k=1}^{n}\left[A^{t}_{\tau k}\right]\left(\frac{A^{r}_{\sigma_i k}}{A^{t}_{\sigma_i k}}\right) = \delta_{\tau r}$	$\sum_{k=1}^{n}\left[A^{t}_{\tau k}\right]\left(\frac{A^{r}_{\sigma_i k}}{A^{t}_{\sigma_i k}}\right) = \delta_{\tau r}$	(14c)
$(n_s + n_t$ eqns)	$\sum_{k=1}^{n}\left[A^{u}_{u k}\right]\left(\frac{A^{r}_{\sigma_i k}}{A^{u}_{\sigma_i k}}\right) = \delta_{u r}$	
	$(n_s + n_t + n_u$ eqns)	
$\left(\begin{array}{l} \rho = \rho_1, \ldots, \rho_{n_r} \\ \sigma = \sigma_1, \ldots, \sigma_{n_s} \\ \tau = \tau_1, \ldots, \tau_{n_t} \\ u = u_1, \ldots, u_{n_u} \end{array}\right)$	$\sum_{k=1}^{n}\left[\frac{A^{s}_{\sigma k}}{A^{s}_{\sigma_i k}}\right]\left(A^{u}_{\sigma_i k}\right) = \delta_{\sigma u}$	
	$\sum_{k=1}^{n}\left[A^{t}_{\tau k}\right]\left(\frac{A^{u}_{\sigma_i k}}{A^{t}_{\sigma_i k}}\right) = \delta_{\tau u}$	(14d)
	$\sum_{k=1}^{n}\left[A^{r}_{\rho k}\right]\left(\frac{A^{u}_{\sigma_i k}}{A^{r}_{\sigma_i k}}\right) = \delta_{\rho u}$	
	$(n_s + n_t + n_r$ eqns)	

The following observations concerning each of the sets of equations (14a), (14b), (14c), (14d) are obvious:

1) Each set of equations corresponds to one of the m columns r,s,t,u as noted by the second index of the delta functions in each set.

2) There can be at most one delta function equal to 1 in each set (no two rows can be the same)

3) If all delta's are zero in any set then the diagonal element has been measured in the column corresponding to that set.

4) All of the (m-1)n unknowns in row σ_i appear in each set.

If each of the equations (14) is devided by the unknown expression in the k_p term, the n(m-1) unknown coefficients A^{j}_{ik} on the left hand side of the equations will be replaced by (n-1)(m-1) unknown ratios $A^{j}_{ik_q}/A^{j}_{ik_p}$ $(q \neq p)$. The reciprical of the unknown expression in the k_p term will appear on the right hand side modified by the corresponding delta function so that the number of unknown expressions on the right hand side of each set is zero or one depending on whether a diagonal element has been measured or not in the corresponding column. Since the number of unknowns on the left hand side of each set has been reduced by (m-1), (m-1) independent unknowns must appear on the right hand side of the equations if a solution can be found. Since at most one delta function can be equal to 1 in each set, at least (m-1) of the m sets must contain a delta function equal to 1. In view of observation 3 above this means that not more than one diagonal

element can be measured. Moreover, since the unknown coefficient expressions modifying the (m-1) non-zero delta's must all be independent only certain sets of delta's lead to a complete solution. For example, if $\delta\rho^*s$ and $\delta\sigma^*t$ † are equal to 1, the unknowns $A^r_{\sigma_i K_p}$ and $1/A^t_{\sigma_i K_p}$ will appear on the r.h.s. of the equations. Since these two expressions are independent, a solution can be found if m=3. However, if $\delta\rho^*s$ and $\delta\sigma^*r$ are the only non-zero delta's for m=3, only $A^r_{\sigma_i K_p}$ and its reciprocal $1/A^r_{\sigma_i K_p}$ will appear on the r.h.s. and no solution can be found.

Notice that in each delta function two columns are in a sense represented since the row variable refers to the column in which it was measured. For example, $\delta\rho^*s$ refers to columns r and s. The delta $\delta\sigma^*r$ also refers to the same columns s and r but in reverse. The r.h.s. unknown coefficients of any two different delta's which refer to the same two columns are reciprocals of one another and are, therefore, dependent, i.e., their product is equal to 1. Hence, a "cyclic pair" of non-zero delta's such as $\delta\rho^*s$ and $\delta\sigma^*r$ does not provide two independent unknowns. (Note, however, that a solution is obtainable if in addition to the "cyclic pair" an additional delta (e.g. $\delta\sigma^*t$) is not zero thus forming a "non cyclic pair" with any of the two others.)

In view of the above, it can be seen that by excluding all such "cyclic pairs" only the following sets of (m-1) delta's (i.e., also their products) must be set equal to 1 if the independence requirement is to be met for m=3.

---

† ρ^* and σ^* are one of the rows measured in colums r and s respectively.

m=3

a) $\delta\rho^{*}s \cdot \delta\sigma^{*}t = 1$

b) $\delta\rho^{*}s \cdot \delta\tau^{*}r = 1$

c) $\delta\tau^{*}s \cdot \delta\rho^{*}t = 1$

d) $\delta\tau^{*}s \cdot \delta\sigma^{*}r = 1$

e) $\delta\sigma^{*}t \cdot \delta\tau^{*}r = 1$

f) $\delta\sigma^{*}t \cdot \delta\sigma^{**}r = 1$ ††

Since the labelling of columns is arbitrary, it can be seen that conditions a) through e) are equivalent. Thus the relations a) to f) can be reduced to the following two necessary conditions for solution where t and r are any two of the three injected compartments: (Each delta implies that a certain element must be measured as indicated in the table at the right of (15))

m=3

		necessary measured elements	
condition 1 :	$\delta\sigma^{*}t \cdot \delta\sigma^{**}r = 1$	T_{ts} , T_{rs}	(15a)
condition 2 :	$\delta\sigma^{*}t \cdot \delta\tau^{*}r = 1$	T_{ts} , T_{rt}	(15b)

If either condition is satisfied a complete solution can be determined. Condition 1 implies that the elements T_{ts} and T_{rs} are measured. Condition 2 implies that the elements T_{ts} and T_{rt} are measured. Either of these conditions also implies that

$\delta_{\tau t} = 0$ and $\delta_{\rho r} = 0$ for all values of τ and ρ

Therefore, the only diagonal element that can be measured is T_{ss}.

†† σ^{*} and σ^{**} are two different rows measured in the same column, s.

Compartment s can be referred to as the reference compartment in the sense that any measurements made in column t or r are linked to compartment s through the measurements T_{ts} and T_{rs} for condition 1 or are indirectly so linked in the case (condition 2) where r is linked to t through T_{rt} and is in turn linked to s through T_{ts} .

By considering the system of equations (14) for m=4, a corresponding set of conditions can be determined for the independence of the system. Here, at least three (m-1) delta's must be equal to one where, as in the case , m=3, "cyclic pairs" such as $\delta\rho^{*}s$, $\delta\sigma^{*}r$ are excluded. Sets such as $\delta\rho^{*}s$, $\delta\sigma^{*}t$, $\delta\tau^{*}r$ are also cyclically related and must be excluded for m=4 since as previously described the corresponding coefficient expressions of the k_p terms are dependent (i.e. their product is equal to one).

<u>m=4</u>

		necessary measured elements	
Condition 1 :	$\delta\sigma^{*}t \ \delta\sigma^{**}r \ \delta\sigma^{***}u = 1$	T_{ts} , T_{rs} , T_{us}	(16a)
Condition 2 :	$\delta\sigma^{*}t \ \delta\sigma^{**}r \ \delta\tau^{*}u = 1$	T_{ts} , T_{rs} , T_{ut}	(16b)
Condition 3 :	$\delta\sigma^{*}t \ \delta\tau^{*}r \ \delta\tau^{**}u = 1$	T_{ts} , T_{rt} , T_{ut}	(16c)
Condition 4 :	$\delta\sigma^{*}t \ \delta\tau^{*}r \ \delta\rho^{*}u = 1$	T_{ts} , T_{rt} , T_{ur}	(16d)

Each of these conditions imply that sufficient measurement measurements linking each injected compartment to the reference compartment s either directly or indirectly have been made.

The conditions 1 and 2 for m=3 and 1 to 4 for m=4 , can equally be applied to the cases where the n elements are selected from m

rows and no two elements are in the same column. The symbols s,t,r,u would then represent the m rows and the required measured elements (e.g. T_{ts} , T_{rs} for cond.1, m=3) would have their subscripts reversed (e.g. T_{st} , T_{sr}).

IV

An extension of the considerations of the previous section to the general case where n elements T_{ij} from m column's $j_p (p=1,\ldots,m)$ are measured can now be made, assuming as before that no two elements are measured in the same row.

A new symbolism is employed. The rows measured in each column j_p are labelled i_{pq} $(q=1,\ldots,n)$ where the subscript q numbers the different rows measured in column j_p and n_p is the number of rows measured in column j_p.

The values, $A^{j_p}_{i_{pq}k}$, $\begin{pmatrix} p=1,\ldots,m \\ q=1,\ldots,n_p \\ k=1,\ldots,n \end{pmatrix}$

are, therefore, the measured coefficients and $A^{j_p}_{i_{p'q'}k}$, $\begin{pmatrix} p=1,\ldots,m \\ p'\neq p \\ q'=1,\ldots,n_{p'} \\ k=1,\ldots,n \end{pmatrix}$

are the unknown coefficients to be determined. The latter must satisfy the initial conditions (10b) for the $(n-n_p)$ unmeasured elements $T_{i_{p'}j_p}$ $(p'\neq p)$ in each column j_p :

$$T_{i_{p'q'}j_p}(0) = \delta_{i_{p'q'}j_p}$$

or

$$\sum_{k=1}^{n} A^{j_p}_{i_{p'q'}k} = \delta_{i_{p'q'}j_p}, \quad \begin{pmatrix} p=1,\ldots,m \\ p'\neq p \\ q'=1,\ldots,n_{p'} \end{pmatrix} \tag{17a}$$

The total number of such equations equals nxm-n = nx(m-1).

Using the relationship between the coefficients (10a), we may arbitrarily choose a specific row $i' = i_{\bar{p}1}$; then, all unknowns $A^{j_p}_{i_{p'q'}k}$ $(p'\neq p)$ can be expressed in terms of the nxm coefficients

$A^{j_p}_{i_{\bar{p}1}k}$, $\begin{pmatrix} p=1,\dots,m \\ k=1,\dots,n \end{pmatrix}$ in row $i_{\bar{p}1}$ and columns j_p and the measured element $A^{j_{p'}}_{i_{p'q'}k}$ in each row $i_{p'q'}$

$$A^{j_p}_{i_{p'q'}k} = \left(\frac{A^{j_p}_{i_{\bar{p}1}k}}{A^{j_{p'}}_{i_{\bar{p}1}k}}\right) \cdot A^{j_{p'}}_{i_{p'q'}k} \quad , \quad (p \neq p') \tag{17b}$$

Substituting in (17a) the resulting system of equations for the nx(m-1) unknowns in row $i_{\bar{p}1}$ is:

$$\sum_{k=1}^{n} \left[A^{j_{p'}}_{i_{p'q'}k}\right] \cdot \left(\frac{A^{j_p}_{i_{\bar{p}1}k}}{A^{j_{p'}}_{i_{\bar{p}1}k}}\right) = \delta_{i_{p'q'}j_p} \quad , \quad \begin{pmatrix} p=1,\dots,m \\ p' \neq p \\ q'=1,\dots,n_{p'} \end{pmatrix} \tag{18}$$

The system of equations (18) represents m sets of $(n-n_p)$ equations corresponding to the m columns j_p . If p or p' is equal to $\bar{p}$, the unknown ratio in parenthesis will contain only one unmeasured constant.

Restating the considerations described in the previous section, if we devide each equation by the unknown ratio in, e.g., the k_1 term, the total number of independent unknowns on the left hand side of the equations will be reduced by (m-1) and (m-1) unknowns,

$$\left(A^{j_{p'}}_{i_{\bar{p}1}k_1} \Big/ A^{j_p}_{i_{\bar{p}1}k_1}\right) \quad , \tag{19}$$

where either p or p' but not both may be equal to $\bar{p}$, appear as coefficients of the delta functions on the right hand side of the

equations. Thus, the total number of unknowns on the right hand side of the resulting equivalent set of equations depends on the values of the delta functions, varying from 0 if all delta's are equal to 0 to (m-1) if at least (m-1) delta's having independent coefficients are equal to one. Further since we have assumed that no two elements in the same row are measured, at most one value of $\delta_{i_{p'q'} j_p}$ can be equal to one for each p. If the (m-1) non-zero delta's are numbered by the subscript μ, $(\delta_{i_{p'q'} j_p})_\mu$, $\mu = 1, \ldots, (m-1)$, the condition that at least (m-1) values of delta must be equal to 1 can be written:

$$\prod_{\mu=1}^{(m-1)} \left(\delta_{i_{p'q'} j_p}\right)_\mu = 1 \tag{20a}$$

where the coefficients of the (m-1) delta's must be independent. Considering that the coefficients of the $\delta_{i_{p'q'} j_p}$ are the unknown ratios (19) and that each also appears in reciprocal form as the coefficient of the delta having reversed p subscripts, $\delta_{i_{pq} j_{p'}}$, the product of two such coefficients is one, and therefore, two non-zero delta's will not have independent coefficients if their indeces p and p' are reversed. In fact, if the product of any μ' coefficients (19) is one so that $\prod_{\mu=1}^{\mu'} (p/p')_\mu$ is also one, they can only represent at most $(\mu'-1)$ independent unknowns. Thus, the condition for the independence of the (m-1) coefficients (19) modifying the (m-1) non-zero delta's in (20a) is

$$\prod_{\mu=1}^{\mu'} (p/p')_\mu \neq 1, \quad \text{for all } \mu' \leq m-1 \tag{20b}$$

In conclusion, if a solution can be found, conditions (20a) and (20b) must be satisfied for at least (m-1) measurements T_{ij}. Condition (20a) implies that of the n measured elements T_{ij} at least (m-1) measurements must be of the form $T_{j_p j_{p'}}$ $(p \neq p')$, where j_p is numerically equal to (m-1) of the measured columns. This means that (m-1) of the injected compartments j_p must be measured after injection in another compartment $j_{p'}$ (non-diagonal measurements), and the remaining injected compartment may or may not be measured diagonally. Since the ratios $(p/p')_\mu$ are independent (20b), if j_1 is measured with respect to j_2, j_2 must be measured with respect to a different compartment j_3 (assuming $n > 2$, $m > 2$), etc. This suggests a pictorial analog. If we represent the (m-1) necessarily measured elements $T_{j_p j_{p'}}$ (injected compartment $j_{p'}$, measured compartment j_p) by the representation:

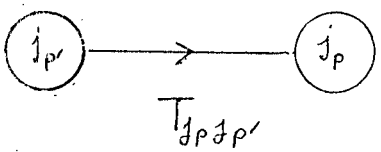

schematic representation of the measurement $T_{j_p j_{p'}}$

condition (20b) implies that no "cyclic connections" can be made in the representation of the (m-1) necessary measurements. For example, if $m > 3$ the following schemes are precluded.

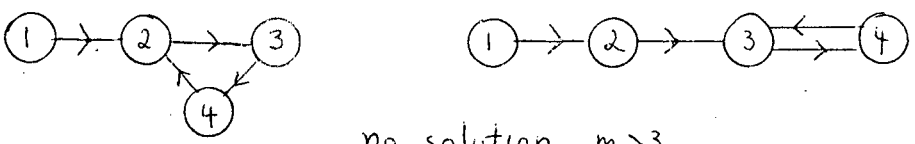

no solution, $m > 3$

whereas the schemes, e.g.,

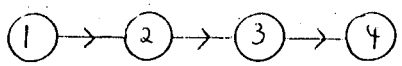

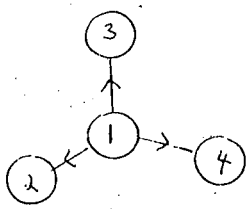

lead to a solution for m=4.

The diagramatic schemes for the necessary conditions (20) are given in section V for various values of m. It can be seen that all of the m compartments are measured either directly or indirectly with respect to a common reference compartment, (1). Since the remaining (n-m) compartments are all measured with respect to one of the m injected compartments, they are also measured with respect to the reference compartment, though indirectly. The above conclusions are, of course, valid with appropriate modification when m refers to the number of measured rows from which the n measured elements are selected so that no two are in the same column. The schemes in V will be identical except that all arrows are reversed.

The diagramatic schemes for the (m-1) necessary measurements of condition (20) are shown below for m=2,3,4, and 5 , ($n \geq m$). All m compartments are measured with respect to the reference injection compartment (1) . Since the reference compartment (1) may be measured with respect to any of the m compartments, this is indicated by the measurement (1) ← (m) . If (1) were a common reference-measurement compartment , all arrows would be reversed.

m = 2

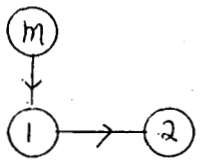

m = 3

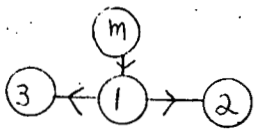

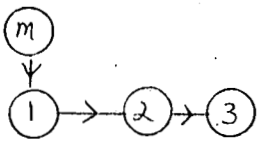

m = 4

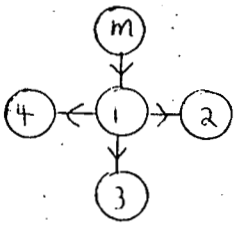

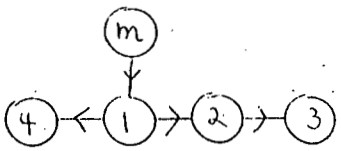

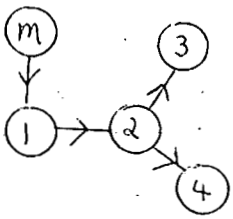

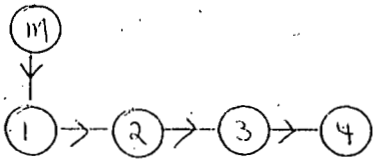

$m = 5$

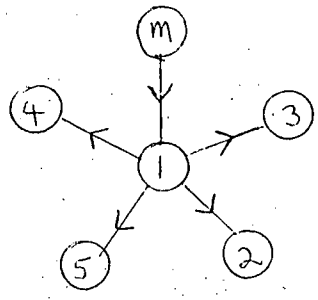
m
4
3
1
5
2

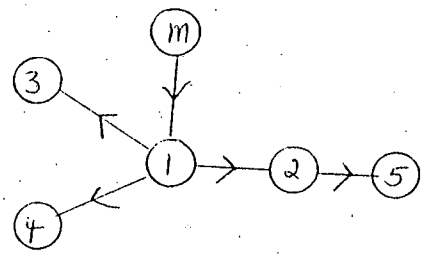
m
3
1
2
5
4

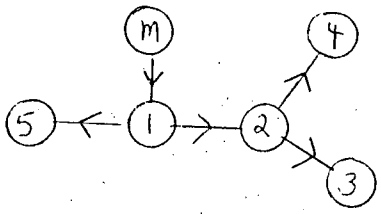
m
4
5
1
2
3

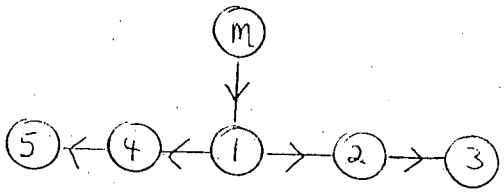
m
5
4
1
2
3

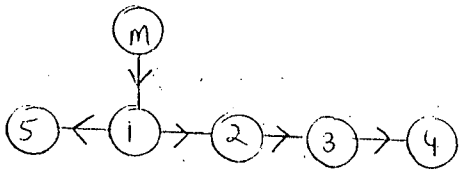
m
5
1
2
3
4

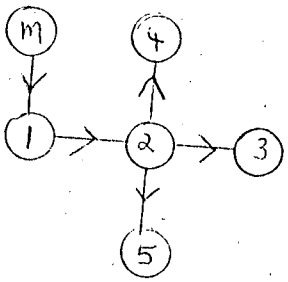
m
4
1
2
3
5

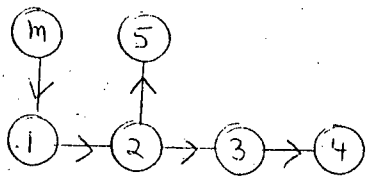
m
5
1
2
3
4

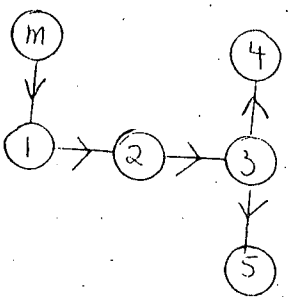
m
4
1
2
3
5

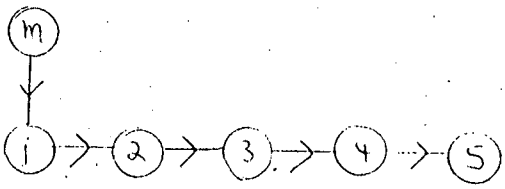
m
1
2
3
4
5

Appendix

Consider the case where n elements of $\underline{\underline{T}}$ are measured in m_c columns and m_r rows where $m_c < n$ and $m_r < n$. Clearly, at least two measured elements must be in the same row and at least two measured elements must be in the same column of $\underline{\underline{T}}$. Two distinct cases arise as indicated in fig.3, depending on whether one of the measured elements is in both a row and a column that contains another measured element (case1) or not (case 2).

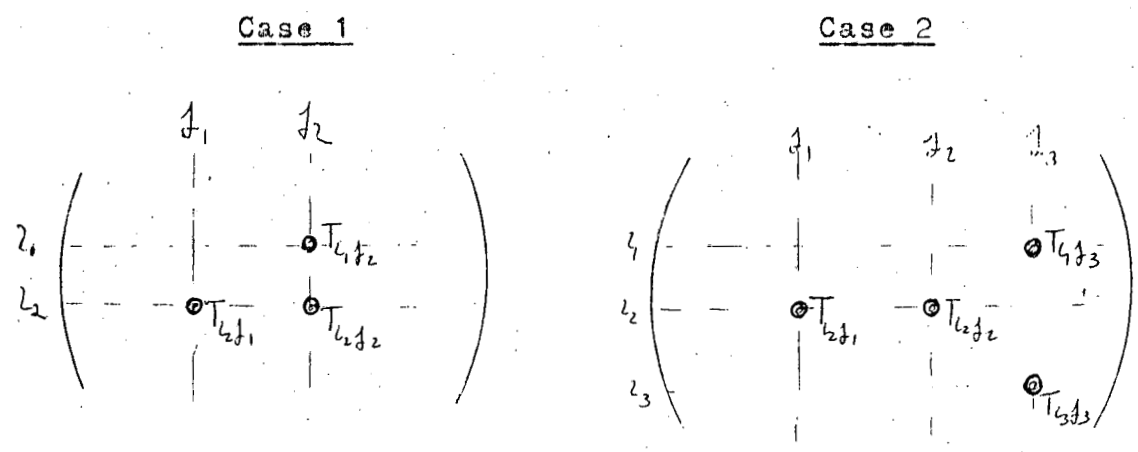

Fig. 3

Case 1: The measured elements in rows i_1 and i_2 and column j_1 or j_2 are: $T_{i_1 j_2}$, $T_{i_2 j_1}$, $T_{i_2 j_2}$

The element $T_{i_1 j_1}$ is unknown. The equations (10a) can be used to determine the unknown coefficients $A^{j_1}_{i_1 k}$ $(k=1,\dots,n)$

$$A^{j_1}_{i_1 k} = \left[A^{j_1}_{i_2 k} \left(\frac{A^{j_2}_{i_1 k}}{A^{j_2}_{i_2 k}} \right) \right] \quad , \; k = 1, \ldots, n \qquad (21)$$

Since the quantities in brackets are known, $T_{i_1 j_1}$ can be completely determined using the n equations (21). Therefore, the number of equations (10a) has been reduced by n and the number of equations (10b) has been reduced by one . Hence the total number of equations (10) has been reduced by (n+1), whereas the total number of unknowns has only been reduced by n. Clearly the system of equations (10) cannot be solved for all unknowns in case 1.

Case 2

The measured elements of $\underline{\underline{T}}$ in rows i_1 , i_2 , i_3 and columns j_1 , j_2 , or j_3 are: $T_{i_1 j_3}$, $T_{i_2 j_1}$, $T_{i_2 j_2}$, $T_{i_3 j_3}$

Unmeasured elements in these same rows and columns are:

$$T_{i_1 j_1}, \; T_{i_1 j_2}, \; T_{i_2 j_3}, \; T_{i_3 j_1}, \; T_{i_3 j_2}$$

The unknown coefficients $A^{j}_{i_k}$ corresponding to these unknown values of $\underline{\underline{T}}$ can be expressed using (10a) in terms of the n unknowns in the element $T_{i_2 j_3}$.

$$\begin{aligned}
A^{j_1}_{i_1 k} &= \left[A^{j_1}_{i_2 k} \; A^{j_3}_{i_1 k} \right] \left(\frac{1}{A^{j_3}_{i_2 k}} \right) \\
A^{j_2}_{i_1 k} &= \left[A^{j_2}_{i_2 k} \cdot A^{j_3}_{i_1 k} \right] \left(\frac{1}{A^{j_3}_{i_2 k}} \right) \\
A^{j_1}_{i_3 k} &= \left[A^{j_1}_{i_2 k} \; A^{j_3}_{i_3 k} \right] \left(\frac{1}{A^{j_3}_{i_2 k}} \right) \\
A^{j_2}_{i_3 k} &= \left[A^{j_2}_{i_2 k} \; A^{j_3}_{i_3 k} \right] \left(\frac{1}{A^{j_3}_{i_2 k}} \right)
\end{aligned} \qquad \begin{aligned} &(k = 1, \ldots, n) \\ &(4n \text{ equations}) \end{aligned} \qquad (22)$$

The 5 equations (10b) for the 5 unknown elements of $\underline{\underline{T}}$ in the specified rows and columns will therefore only contain the n unknowns $A^{j_3}_{i_2 k}$ (k=1,...,n).

$$
\begin{aligned}
&\sum_{k=1}^{n} A^{j_3}_{i_2 k} = \delta_{i_2 j_3} \\
&\sum_{k=1}^{n} [A^{j_1}_{i_2 k} \cdot A^{j_3}_{i_4 k}] \cdot \left(\frac{1}{A^{j_3}_{i_2 k}}\right) = \delta_{i_4 j_1} \\
&\sum_{k=1}^{n} [A^{j_2}_{i_2 k} \cdot A^{j_3}_{i_4 k}] \cdot \left(\frac{1}{A^{j_3}_{i_2 k}}\right) = \delta_{i_4 j_2} \\
&\sum_{k=1}^{n} [A^{j_1}_{i_2 k} \cdot A^{j_3}_{i_3 k}] \left(\frac{1}{A^{j_3}_{i_2 k}}\right) = \delta_{i_3 j_1} \\
&\sum_{k=1}^{n} [A^{j_2}_{i_2 k} \, A^{j_3}_{i_3 k}] \left(\frac{1}{A^{j_3}_{i_2 k}}\right) = \delta_{i_3 j_2}
\end{aligned}
\tag{23}
$$

Clearly Case 2 does not apply to $n < 4$. If n=4, the system of equations (23) consists of 5 equations in 4 unknowns. Using (23) a solution is at most obtainable for the 5n unknowns in equations (22), since the number of remaining independent equations (10) will be less than the number of remaining unknowns.

If n=5, (23) is only solvable for the 5 unknowns $A^{j_3}_{i_2 k}$(k=1,...n) if at least one of the delta functions is equal to one. This will be true if at least one of the 5 unknowns $T_{i_4 j_1}, T_{i_4 j_2}, T_{i_3 j_1}, T_{i_3 j_2}, T_{i_2 j_3}$, is diagonal in which case the 5n unknowns in (22) can be determined. If such a partial solution is obtainable, the number of additionally determinable unknowns depends on the location of the remaining (5th) measured element. It can either be selected so that it lies in one of the remaining columns j_4, j_5 and one of the remaining rows i_4, i_5, or so that only one row is i_4, i_5, or one column is j_4 or j_5.

In the latter case, two configurations similar to Case 1 result, and only two additional elements T_{ij} can be determined. For example, if the 5th measured element is $T_{i_2 j_4}$ then $T_{i_1 j_4}$ and $T_{i_3 j_4}$ can be determined using 2n equations (10a).

$$A^{j_4}_{i_1 k} = [A^{j_4}_{i_2 k} \cdot A^{j_3}_{i_1 k}] \left(\frac{1}{A^{j_3}_{i_2 k}}\right)$$

$$A^{j_4}_{i_3 k} = [A^{j_4}_{i_2 k} \cdot A^{j_3}_{i_3 k}] \left(\frac{1}{A^{j_3}_{i_2 k}}\right) \quad , \quad k=1,\ldots,n \tag{24}$$

where $A^{j_3}_{i_2 k}$ has been previously determined from equations (23), and the quantities in brackets are measured. The solution (24) reduces the available equations (10b) for the remaining unknowns by 2. Since the number of remaining equations (10) will be 2 less than the number of remaining unknowns, a complete solution is unobtainable.

In the remaining case where the 5th measured element lies in a different row i_4 and a different column j_4 a complete solution is still unobtainable. This can be seen since the 3n unknowns of the 3 elements T_{ij} in column j_4 and rows i_1, i_2, i_3, and the 3n unknowns of the 3 elements in row i_4 and columns j_1, j_2, j_3 can be expressed using (10a) in terms of the n unknowns in any one of the 6 elements, e.g. $T_{i_2 j_4}$. Hence 6 equations (10b) can be written to contain only the 5 previously undetermined unknowns $A^{j_4}_{i_2 k}$.

$$
\begin{aligned}
\sum_{k=1}^{n} A_{i_2 k}^{j_4} &= \delta_{i_2 j_4} \\
\sum_{k=1}^{n} \left[A_{i_4 k}^{j_3} / A_{i_2 k}^{j_3}\right] \cdot A_{i_2 k}^{j_4} &= \delta_{i_1 j_4} \\
\sum_{k=1}^{n} \left[A_{i_3 k}^{j_3} / A_{i_2 k}^{j_3}\right] \cdot A_{i_2 k}^{j_4} &= \delta_{i_3 j_4} \\
\sum_{k=1}^{n} \left[A_{i_4 k}^{j_4} \cdot A_{i_2 k}^{j_1}\right] \left(\frac{1}{A_{i_2 k}^{j_4}}\right) &= \delta_{i_4 j_1} \\
\sum_{k=1}^{n} \left[A_{i_4 k}^{j_4} \cdot A_{i_2 k}^{j_2}\right] \left(\frac{1}{A_{i_2 k}^{j_4}}\right) &= \delta_{i_4 j_2} \\
\sum_{k=1}^{n} \left[A_{i_4 k}^{j_4} \cdot A_{i_2 k}^{j_3}\right] \left(\frac{1}{A_{i_2 k}^{j_4}}\right) &= \delta_{i_4 j_3}
\end{aligned}
\tag{24}
$$

where the terms in brackets are either measured or previously determined This reduces the number of equations (10) so that there is one less equation for the remaining unknowns than the number of such unknowns. A complete solution is therefore, also unobtainable for n=5 in both cases 1 and 2.

For $n > 5$ similar reasoning can be used to show that a complete solution is generally unobtainable in Cases1 and 2.

REFERENCES

1) H.E. Hart: Analysis of Tracer Experiments in non-conservative steady-state Systems. Bulletin of Mathematical Biophysics Volume 17, 1955

2) J.Z. Hearon: Theorems of Linear Systems Annals of the New York Academy of Sciences, Volume 108, Art.1, 1963

3) M. Athans, F.L. Falb Optimal Control McGraw Hill, 1966 , p. 127

4) P. Bertrand, G. LeCardinal, E. Walter Reconstruction of the Transition Matrix From Experimental Data Submitted for publication

5) S.I. Rubinow, A. Winzer Compartment Analysis; An Inverse Problem Bulletin of Mathematical Bioscience: 11 (1971), 203-247

III

THREE DIMENSIONAL IMAGING OF MULTIMILLIMETER SIZED COLD LESIONS BY FOCUSING COLLIMATOR COINCIDENCE SCANNING (F.C.C.S.)

H.E. Hart and S. Rudin
Department of Physics
City College of New York
New York, N.Y. 10031

and

Section of Nuclear Medicine
Department of Oncology
Montefiore Hospital & Medical Center
Bronx, New York 10467

A twin probe high resolution focusing collimator coincidence scanning system has been developed which can tomographically image multi-millimeter structures. The three dimensional detection and imaging capabilities, the related off-focal suppression and the sensitivity are compared with standard techniques.

I. INTRODUCTION

In most radioisotope imaging, the information obtained constitutes essentially a 2-dimensional projection of the 3-dimensional radioisotope tissue distribution (1). That this is true even when focusing collimators are employed is evidenced by their isoresponse surfaces which characteristically exhibit sharp lateral discrimination but much less rapid variation in sensitivity along the longitudinal axis. In photographic terms, the resulting images can be characterized as having a relatively high lateral resolution with a large longitudinal depth of focus. The detection of a small cold lesion imbedded in a radioactive medium therefore normally involves not only identification of a continuous region wherein the count defect is statistically unlikely (i.e. more than three standard deviations removed from the average expectation in surrounding areas) but the ability to correctly attribute image variations arising from quite independent physiological and/or structural factors. For example, variations in overall organ thickness or bone shielding can result in substantial local changes in the image densities recorded. The above difficulties have contributed to limiting the effectiveness of radioisotope imaging as a means of detecting small lesions and in particular small cold lesions.

If the longitudinal depth of focus can be so reduced that only successive sections of interest are evidenced with off-focal plane contributions highly suppressed, then clearly the count excess or count defect arising from a small lesion within the relatively thin focal slab will be statistically much more significant and spurious interpretations arising from off-focal factors minimized. This can be done, of course, somewhat effectively in x-ray tomography by smearing off-focal plane contributions

and identifying high spatial frequency information as necessarily arising from structure within the plane of interest. In the equivalent form of radioisotope tomography, however, it appears that the considerably poorer statistics involved and the ghost images and other artifacts associated with discrete off-focal plane structure may tend to limit resolution and lesion detection.

Analytic methods, in general employing computers, have had more success in correlating inherently longitudinally insensitive information to obtain improved 3-dimensional representations (17). X-ray transmission tomography has, of course, been strikingly effective in characterizing tissue densities. Computer analysis has also been applied in Nuclear Medicine where the resulting 3-dimensional representation of the radioisotope distribution can characterize normal or pathological tissue function.

In most of these techniques (2), the raw data essentially reflects gamma-ray emission occurring throughout 3-dimensional radioisotope distributions. There is little if any rejection prior to analysis, of counts arising from off-focal plane sites. While such initial rather general acceptance of counts usually enables the subsequent analysis to successively "focus" on different planes, extraction of maximal information for any one plane is correspondingly restricted. Off-focal plane counts may so exceed the contributions from the focal region of interest that relatively minor fluctuations in statistics or off-focal structure may significantly degrade the focal plane image.

It follows from the above that any means whereby off-focal contributions can be suppressed or identified may improve the ultimate spatial resolution possible. This is in fact the rationale for the technique of Focusing Collimator Coincidence Scanning (FCCS). (Other approaches to this end are positron annihilation time-of-flight measurement, x-ray fluorescence scanning and computerized reconstruction (16). If the counts accepted at each

scan position are restricted a priori to those arising from radioactive decays within the focal volume, small variations in the radioisotope focal concentration should be more detectable. This is because the resulting changes in the count rate will then be a much larger fraction of the total and more likely to be statistically significant.

In FCCS, the emphasis on focal events is accomplished by using isotopes which decay by multiple gamma-ray emissions and by restricting the counts accepted to those coincidences arising from a single nuclear decay in which the emitted gamma-rays separately strike two of the angulated confocal probes. Since the fields of view of the separate probes only overlap within their common focal region, the coincidence requirement severely limits the volume being radioassayed at any one time.

The coincidence requirement of FCCS does, of course, significantly reduce the total number of gamma-ray events accepted. Therefore, the overall FCCS count rate is much lower than that for standard single gamma scanning and some of the tomographic techniques under development which continually accept counts from a much larger region (2). The time required for a complete three dimensional FCCS scan of large organs such as the liver or for obtaining total body cross sections is therefore likely to be long. In many potential applications, however, the tissue volume of genuine interest is actually quite restricted. In thyroid, cardiac and even possibly prostate or parathyroid scanning, for example, only a small volume of tissue is likely to be of concern and the time required for the scan should therefore be relatively short. Counts accepted from tissue more than a few centimeters away from the region of interest (or even as little as one centimeter away) might not contribute to and, in fact, might only serve to

degrade scan quality within the region of interest. The high resolution capabilities of FCCS demonstrated in this report may be required for such applications.

The capabilities of FCCS were first examined experimentally using ^{125}I. A single short focus large solid angle focusing collimator was used and coincidences detected simply by accepting only those "events" corresponding to the summed energy of the ^{125}I coincident gamma and K shell x-ray. Using this simple rather long resolving time, summed energy coincidence technique and a far from ideal collimator geometry, it was still possible to show that the image of a point source was significantly reduced in size over that obtained when the energy window was adjusted to accept single gamma-rays (3). A two probe experiment with low efficiency collimators, again using the summed energy technique, indicated the possibility of improved cold lesion detection (4). Since the general theory of FCCS (5) indicated the importance of a very short resolving time to minimize statistical coincidences and since superior collimators had become available, it was decided to carry out a two probe experiment in which summed energy coincidence gating would be replaced by modern much higher speed electronic pulse techniques and to employ a phantom with a simulated cold lesion somewhat smaller than could be detected by other current scanning techniques. The experiment together with related theory required for a qualitative discussion of results are reported below.

In Section II, the general theory of FCCS is particularized to reflect the experimental design parameters, and the concept of a three dimensional volume information density is introduced. In Section III the

experimental arrangement is detailed and the system point source response characterized. In Section IV, the results of scanning an experimental phantom are presented and discussed. System modifications for possible clinical applications of FCCS are considered in Section V.

II. THEORETICAL CONSIDERATIONS

A. Lesion Detectibility Using FCCS

In the general idealized theory of FCCS (5) a configuration was assumed such as appears in Fig. 1. This geometry is essentially equivalent to having N single channel collimator-detector assemblies so separated that their off-focus overlap can be neglected and with no septal or collimator penetration. It will be further assumed, purely for convenience, that the counting efficiencies are the same for each gamma ray energy. If the actual energy dependence were taken into account, this would not change the basic form of the resulting expressions below except for very simple multiplicative factors (11). Angular correlation is also neglected and for the isotopes considered the effect, in fact, would be quite small.

If the N detectors are operated in the summed energy mode and if statistical coincidences are neglected, the count rates of Table 1 (system configuration A) apply, where: λ is the average single channel efficiency; 2D is the number-of-gamma-rays/second emitted per unit volume; ν_1 and ν_2 are the single gamma-ray count rates from off-focal sites and focal sites, respectively; μ_1 and μ_2 are the coincident count rates from off-focal sites and focal sites respectively.

If there is a short summing time τ during which statistical coincidences

can occur and a dead time δ following, during which no events are recorded, modifications must be made. Again following the analysis of Hart (5), the resulting count rates for the N detector appear in Table 1 (system configuration B).

The N-channel detector in the twin probe configuration of the current coincidence experiment appears in Fig. 2. Since only coincidences activating both probes were accepted in the experiment being reported, $\mu_1 = 0$ (in configurations A and B, double gamma-ray coincidences impinging on a single probe were included as well). Note that while μ_1 in the idealized theory formally represents those very unlikely events for which both gamma rays go through the identical collimator channel, in practice neighboring and near neighboring collimator channels exhibit substantial off-focal overlap. However, the requirement that both probes be activated simultaneously almost completely eliminates the effect of off-focal overlap provided the single gamma count rate is sufficiently low and the resolving time sufficiently short to minimize statistical coincidences. This assures a reasonably effective division of the scanned tissue volume into an N channel overlapping focal region α and a single-channel accessible off-focal volume NV_{sc}, in accordance with the theoretical assumptions. An equivalent approach, using a higher moment analysis in a gamma camera system which permits the geometric separation criterion for rejection to be varied continuously, appears elsewhere (6). The experimental requirement that both probes be activated not only causes μ_1 to vanish but results in halving the other coincidence terms. The resulting count rate characteristics appear in Table 1 (system configuration C). The factor of 2 in the denominator of these focal and off-focal coincidence rates

is due to the rejection of coincidences in which both gamma rays strike the same probe.

In the experiment actually carried out each probe was gated to respond to only one of the two gamma ray energies and another modification in the theoretical count rates of Table 1, system configuration C is therefore indicated. It will be useful in carrying out this final adjustment to tabulate the different logical detection possibilities in Table 2. Both single gamma count rates (Table 1, columns 1 and 2, Row D) are halved because as is indicated in Table 2 each probe is gated to only one of the two possible energies. Referring to the accepted coincidence count rates in Table 2, it can be seen that the off-focal statistical coincidence rate (Table 1, column 3, row D) will be reduced by a factor of 4 since the single count rate for each energy gamma ray is halved. The factor of 4 also applies to statistical coincidences arising from the focal region as well [$(\nu_2^2+2\nu_1\nu_2)\tau$, in column 4, Row D] . For the true focal coincidence rate μ_2, however, the energies of the two coincident gamma rays are, of course, correlated and the resulting counts are reduced by only a factor of two. Alternatively numerical factors in the denominators of Table 1, Row D can be determined by inspection by noting the ratio of the accepted events to total possible events (accepted plus rected) in Table 2 for the three different categories considered.

To determine the extent to which the count rates of Table 1, Row D (i.e. those associated with the actual experimental design) are suitable for lesion detection, it is necessary to employ the criterion of Dewey and Sinclair (7). A lesion within the focal region of size $\beta_{\gamma 1}$, for

single gamma ray scanning and $\beta_{\gamma 2}$, for coincident scanning will probably be detected if the inequalities (1) hold.

$$\frac{\beta_{\gamma 1} \nu_2 t_1}{\alpha 2 \omega} > 3\left(\frac{\nu_1 t_1}{2\omega}\right)^{\frac{1}{2}}$$
$$\frac{\beta_{\gamma 2} \mu_2 t_2}{\alpha 4 \omega} > 3\left(\frac{\nu_1^2 \tau t_2}{8\omega}\right)^{\frac{1}{2}} \qquad (1)$$

where t_1, is the single gamma counting time and t_2 is the coincident counting time. In deriving inequalities (1) the expressions in Table 1 (system configuration D) were used. If it is assumed that the total focal efficiency, $N\lambda$, is only a few percent ($N\lambda \ll 1$), ν_2 can be approximated by $2DN\lambda\alpha$. For τ and δ sufficiently small, $\omega \approx 1$. The relative lesion detectability (r.l.d.) comparing the two scanning techniques, now defined as the ratio of the minimum detectable $\beta_{\gamma 1}$ (symbolized by $\beta_{\gamma 1m}$) to the minimum detectable $\beta_{\gamma 2}$ (symbolized by $\beta_{\gamma 2m}$) when $t_1 = t_2$, is then given by equation (2),

$$\text{r.l.d.} \triangleq \frac{\beta_{\gamma 1m}}{\beta_{\gamma 2m}} = \frac{3\left(\frac{V_{sc}}{DN\lambda t_1}\right)^{1/2}}{3\left(\frac{8 V_c^2 \tau}{(N\lambda)^2 t_2}\right)^{1/2}}$$

$$= (N\lambda)\left(\frac{1}{4\nu_1\tau}\frac{t_2}{t_1}\right)^{1/2} = \frac{N\lambda}{(4\nu_1\tau)^{1/2}} \qquad (2)$$

where the further assumption has been made that the single count rate is not excessive, $\nu_1\tau \ll N\lambda/2$. For typical values used in the experiment ($N\lambda \approx 0.02$, $\tau \approx 50\,ms$, $\nu_1 \approx 2\times10^3\ sec^{-1}$) the resulting r.l.d. $\approx$ 1 indicates no advantage for FCCS over single gamma ray scanning. If, however, the standard error associated with the uncertainty of source boundaries and non-uniformity is estimated conservatively to be 5% of the ambient count rate,

then a new term (6) must be added to inequalities (1), resulting in inequalities (1a).

$$\frac{\beta\gamma_1 \nu_2 t_1}{\alpha 2\omega} > 3\left[\frac{\nu_1 t_1}{2\omega} + (0.05)^2\left(\frac{\nu_1 t_1}{2\omega}\right)^2\right]^{\frac{1}{2}}$$

$$\frac{\beta\gamma_2 \mu_2 t_2}{\alpha 4\omega} > 3\left[\frac{\nu_1^2 \tau t_2}{8\omega} + (0.05)\left(\frac{\nu_1^2 \tau t_2}{4\omega}\right)\right]^{\frac{1}{2}} \qquad (1a)$$

If at least a few thousand counts are obtained during t_1, then the new term will dominate for single gamma ray counting whereas for coincident counting there is only a small (5%) correction factor. The effect on the r.l.d. of this new term is then indicated by equation (2a).

$$r.l.d._{(.05)} = \frac{\beta\gamma_{1(.05)}}{\beta\gamma_{2(.05)}}$$

$$= \frac{0.15 V_x}{(1.15)\left(\frac{8 V_x^2 \tau\omega}{(N\lambda)^2 t_2}\right)^{1/2}} = (0.052) N\lambda \left(\frac{t_2}{\tau}\right)^{\frac{1}{2}} \qquad (2a)$$

For the typical experimental values mentioned above, $r.l.d._{(.05)}$ now becomes about 40 in favor of FCCS.

This indicates that FCCS may be better adapted to deal with non-uniformities than single gamma scanning. The 5% correction factor was chosen somewhat arbitrarily since it represents a fluctuation of approximately one color step in the usual clinical color coded scan. Therefore, the resulting favorable r.l.d. ratio of 40 is not to be viewed as quantitatively valid in all applications. However, for most realistic tissue source materials, it would appear that the above analytic approach should be reasonably applicable.

In the experiment described below, the non-uniformities consist of the finite rather small dimensions of the phantom and its rather complex

configuration of a single spherical cold region with abutting hot spots imbedding in an otherwise homogeneous field. It is these non-uniformities which, as will be seen below, are rather faithfully represented by FCCS but completely distorted or masked in single gamma scanning.

It might be noted that by using radioisotopes with multiple gamma ray cascades (6) the $r.l.d._{(.05)}$ would be further increased.

The above theoretically predicted advantage and the experimental results described below can be contrasted with the negative theoretical conclusions and experimental results found for a focusing-slit collimator gamma-gamma coincidence system (8).

B. Information Density in Tomographic Scanning

In comparing the lesion detectability of FCCS and single gamma scanning in Section IIA it was appropriate to assume that the lesion was in each case located at the system focus. This configuration is necessarily artificial, of course, since in carrying out a scan the location of the lesion is, a priori, usually unknown. The actual evaluation of scans, involves a visual integration of the count density over continguous regions.

Because of the large depth of focus, the standard single gamma-ray scan is a two dimensional, planar, projection of the three dimensional radioisotope distribution and the planar information density P.I.D. (counts/unit area in a single scan) is a natural statistical measure. However, the information content of a whole sequence of scans is available for lesion detection in FCCS with correlative interpretation possible among contiguous or neighboring volume elements in the three dimensional scan space.

To analyse the statistical significance of structure in an FCCS image, it is necessary therefore to introduce the analogous concept of a volume information density (VID) i.e. counts/unit volume.

The possible presence of a lesion in an FCCS sequence is indicated by a statistically significant fluctuation in the counts observed in any three dimensional volume of the scan space (i.e. the volume integration of the VID over any three dimensional region of the scan space). The VID will be a useful statistical parameter in the discussions of system design and performance to follow.

III. DESCRIPTION OF EXPERIMENT

A. Isotope and Instrumentation

The energy of the coincident gamma rays of ^{75}Se used in this study are in two ranges: 97 to 136 keV and 265 to 280 keV (9).

Each probe used in this work consisted of a 1 inch thick cylindrical lead housing containing a 5 inch diameter, 2 inch thick Harshaw Co. NaI(Tl) crystal, an RCA 4525 bialkali photomultiplier tube and a 5 inch diameter 2.5 inch thick 1500 channel lead collimator (10). Figure 3 indicates the electronic configuration of the experiment, Table 2 above summarizes the detection logic and the scanning geometry appears in Fig. 4.

B. The System Response

Two families of single gamma ray isoresponse surfaces one for each energy range of gamma ray emission were obtained using a point source in air. These families differed significantly only for isoresponse surfaces of less than 5%. The coincident mode performance of the system was tested by verifying that the two probe coincidence response for a point source in air was consistently within a few percent of the product of the single gamma ray responses for a point source in air.

Referring to Fig. 5, the product response will decrease much more

rapidly in moving from the origin in the OX and OX' directions than in moving radially outward within the AB plane. The effective FCCS focal volume can be shown to approximate a very small flattened or oblate spheroid (not shown in Figure 5) with its minor axis in the XX' direction.

The effect of scatter and tissue attenuation upon the response of the system must be considered. Tissue attenuation and scatter for different energy gamma rays have been studied for single gamma detection by Beck (18) and isoresponse characteristics described. Isoresponse characteristics for a point source in air using FCCS have also been determined with plastic sheets of up to 4 cm interposed between the source and detectors and with large amounts of plastic backscattering material (11). While attenuation reduced the count rate as expected, the normalized FCCS point source response functions (except for the restricted regions along the individual collimator axes) were effectively unaltered by scatter. This is, of course, not too surprising since for an off-focal event to be accepted using FCCS, both gamma rays would have to be scattered appropriately.

To further study the effects of scatter and attenuation the absolute focal coincident count rate was measured for a homogeneous radioisotope distribution in water. The experimental result agreed to within 20% of the value calculated taking into account attenuation, the branching ratios, the detector efficiencies for different gamma ray energies and an effective focal volume estimated from the experimental point source response function (11).

Although the normalized isoresponse characteristics are little affected by scatter, the absolute coincidence count rates were observed to be significantly reduced by the effects of attenuation for focal depths of

several centimeters. If attenuation is severe, the focal signal can be masked by statistical coincidences and such considerations play an important role in radioisotope selection. For gamma ray energies below 100 keV and lesion depths > 2 cm, gamma ray absorption can therefore severely limit lesion detectability using FCCS.

For lesion depths of a few centimeters, energies above ~100 keV are required. For example, ^{75}Se could be selected for use in the experiment here reported because its coincident gamma ray energies were sufficiently high, 121, 136, 165, 280 keV, that attenuation would not compromise the focal signal. To detect deeper lesions, ~6 cm, gamma ray energies of between 300-600 keV are indicated. Since these gamma rays exhibit tissue half value layers of ~6-8 cm, the focal signal would still be statistically significant.

IV. RESULTS: SCAN OF VOLUME PHANTOM CONTAINING A COLD LESION

The test phantoms (Fig. 6) consisting of cold spherical defects imbedded in a homogeneous radioisotope distribution were placed in collars to insure that the gamma ray attenuation would be uniform for transverse scanning (Fig. 4). Coincidence and single gamma ray counts over a 2 mm spacing, 3-dimensional, cubic lattice were obtained and the results appear in Figs. 7 and 8.

Note that while the presence of a defect is apparent in plane sections 2, 3 and 4 of Fig. 7 there is no evidence of a central lesion in Fig. 8. Since the effective focal region in the coincidence mode is very small, the scan is unaffected by phantom boundaries ~1 cm away in the transverse and longitudinal directions. Note, however, that the effect of the phantom boundaries actually dominates the single gamma ray scans. There is

paradoxically maximal activity in the centers of sections 2, 3 and 4, right where the defect is, with gross attenuation near the periphery. This is a consequence of the long longitudinal depth of focus of each probe (~5 cm) when used in the single gamma ray mode. Therefore, in spite of the highly favorable count ratios for single gamma ray scanning as compared with PCCS (100/1), off-focal plane structural variation so distorts the single gamma ray scan that its inherently much greater statistical reliability is of little help in accurate lesion detection. This is consistent with the theoretical prediction of equation (2a) although the 5% effect of non-uniformity assumed arbitrarily in the derivation would of course, not be expected to apply precisely.

Referring to the scans in Fig. 7, it may be noted that there is an asymmetry with respect to the central defect. The regions labelled "A" on three successive serial scans consistently indicate a higher activity than the symmetrical areas "B". This unexpected increase in activity, upon inspection of the phantom, could be attributed to a 3 mm "diameter" glob of the epoxy used to cement the spherical bead in place. Upon separate testing, it was determined that this epoxy in fact tended to absorb ^{75}Se. Further examination of the scan of Fig. 7 also suggested the presence of a region of slightly increased, marginally detectable, activity just to the lower left of the central defect (Region C). This, in turn corresponded to a small 2 mm "diameter" epoxy glob in the phantom.

From the above it appears that Fig. 7 constitutes a reasonably valid tomographic representation of a 3-dimensional radioisotope volume distribution with a resolution of a few millimeters.

V. CONSIDERATIONS REGARDING CLINICAL APPLICABILITY

In order to adapt the type of experimental extremely high resolution device here described into a more generally useful clinical FCCS system, the system sensitivity scan speed would have to be increased. By employing a 6 probe system (a central probe and five surrounding probes) the number of combinations of probe pairs would be increased from one as in the experiment to 15 (C^6_2) with a corresponding increase in the coincidence count rate. In the experiment reported, each probe is sensitive to only one of the emitted ^{75}Se gamma ray energies. If both gamma energies are accepted by all probes the count rate would be increased by a factor of 2. The full width at half maximum of the present extremely high resolution probes was 6 mm. By using collimators, for example, with channel widths 3 times as large, the effective focal volume would be increased by a factor of $\sim (3)^3 = 27$ and the overall increase in system sensitivity for focal events would be approximately 800 fold (i.e. 15 x 2 x 27). For a "large" lesion (i.e. one that fills the enlarged focal volume) the lesion signal rate would therefore be increased by the full factor of ~ 27. For smaller defects which only partially occupy the enlarged focal volume, the increase in signal rate would, of course, be proportionately smaller. In choosing collimators it is therefore desirable to try to match the coincidence focal volume to the approximate size of the lesion suspected or sought. Too small a focal volume results in an unduly low sensitivity and long scan times. Too large a focal volume results in an unnecessary loss in resolution and an unnecessary increase in the statistical coincidences arising from the increase in the single gamma count rates.

To detect a 1 cm diameter lesion in a clinically feasible time the experimental collimator widths should be approximately doubled. The focal volume (and the effective fraction of the lesion being assayed) would increase by a factor of 8 and the 6 probe system detection sensitivity by $\sim 15 \times 2 \times 8 = 240$. At the experimental concentration used 7.5 μCi/ml and the VID obtained, $\sim 10^4$ counts/cm^3 (which is at least 1 order of magnitude larger than is likely to be clinically necessary), the 2 cm^2 scan of the phantom should take $\sim$1 min. The resolution, reduced by a factor of $\sim$2, (for the collimator channel width doubled, keeping the collimator thickness and focal length constant), should be adequate to detect variations in activity on a centimeter scale. This is suggested by the experimental results where detail on a 3-4 mm scale is readily observable. Since the collimator channel widths are doubled with the proposed "clinical" collimators, geometric scaling considerations indicate that equivalent detail on a 6-8 mm scale should be detectable.

Since the single gamma geometric efficiency is proportional to R^2, where R is the radius of the collimator field of view at the focal plane, doubling the collimator channel width would increase the single gamma count rate by a factor of 4 and therefore the statistical coincidences by a factor of 16. Commercially available electornics can now be obtained with resolving times $\tau \sim 15$ ns which will reduce the statisticals by a factor of $\sim$ 3 (11). The resulting increase in the statistical count rate would therefore be $\sim 15 \times 2 \times 16 \times 1/3 = 160$ and the focal signal to statistical noise ratio would increase by a factor of 240/160 or from the experimental value of the ratio 7/1 for the phantom used to 10.5/1. Since the statistical coincidences actually depend, of course, upon the nature of the

radioisotope distribution, the signal to noise ratio of 10.5/1 refers specifically to the phantom used. For a small sphere imbedded in a uniform slab of activity of thickness S and neglecting attenuation, the statisticals are proportional to S^2. For a slab 6 cm thick, the statisticals would therefore be increased by the factor $(6/2)^2$ over that observed with the phantom so that the signal to noise ratio is reduced to 1.2/1. For more clinically realistic isotope concentraitons of $\sim 1\,\mu Ci/cm^3$, the signal is reduced by the factor of 1/7.5 and the statisticals by $(1/7.5)^2$ with a revised focal signal to statistical noise ratio of 8/1. Again assuming a more clinically realistic VID of 10^3 counts/cm^3, the time taken for scanning 2 cm^2/min appears to be clinically satisfactory for scans of small organs or re-scans of suspicious regions within larger volumes.

The isotope here employed, ^{75}Se, is just one of several isotopes suitable for FCCS which are immediately available -- ^{192}Ir, ^{43}K, ^{130}I, and ^{82}Br. There are at least fifteen other isotopes which might be suitable subject to the development of more efficient methods of production and radiochemical processing including the preparation of radioisotope chelates with short biological half-lives: ^{194}Tl, $^{194m2}Ir$, ^{200m}Au, ^{196}Tl, ^{198}Tl, ^{178}Hf, ^{179}Hf, ^{180}Hf, ^{186}Ta, ^{190}Ir, ^{178}Ta, ^{144}Pm, ^{190}Au, and ^{101}Rh. Many of the above isotopes exhibit excellent branching ratios and N-fold multi-gamma cascade decay schemes. An N-fold cascade introduces a favorable factor of N(N-1)/2 in the focal coincidence count rate (6).

To improve the efficiency of detection of the high gamma ray energy emitters tungsten collimators may be required. By going to higher energy emitters less tissue absorption will occur for each coincident gamma ray and hence relatively more coincidences detected depending upon the

depth of the emitter. An additional benefit in going to higher energies is that the spectral resolution of NaI(Tl) crystals improves as the energy increases, so that compton scattered gamma rays may be better discriminated against.

Using various means, therefore, it may be possible to obtain a two to three order of magnitude increase in the experimental FCCS sensitivity here reported and still be able to detect 1 cubic centimeter cold lesions in three dimensions.*

The clinical applicability of FCCS may not be limited to static three dimensional imaging. The above general coincidence techniques are readily applicable to the measurement of dynamic response within a fixed interior volume.** This might be accomplished by using intersecting broad focus collimators. The much higher count rates required would be achieved, of course, at the expense of spatial resolution.

From the results of the high resolution FCCS studies here reported and from reasonable extimates as to the ongoing development of the method, it therefore appears that FCCS may be of clinical applicability in the near future.

* It has been shown by Smoak et al (12) that by proper positioning of the patient, motion artifacts will not compromise image detail on a centimeter scale. There is also active development of physiological triggering techniques to further reduce the effect of organ motion (13-15).

** The possibility of using the FCCS geometry to study tumor vascularization and blood supply has been proposed (19).

VI. SUMMARY

A tomographic determination of multi-millimeter detail within a radioisotope distribution has been achieved using FCCS.

The possible clinical applicability of FCCS has been reviewed and the development of a FCCS tomographic imaging device for clinical use proposed.

ACKNOWLEDGEMENT

We should like to thank Dr. Powell Richards of Brookhaven National Laboratory for supplying the experimental, high resolution collimators. It is also a pleasure to thank Mr. Richard Young for technical assistance in setting up the experiment, Dr. Philip Bardfeld for making available facilities of the Section of Nuclear Medicine, Mr. Steve Ostrow, Mrs. Mona Cohen and Mrs. Ann Rudin for help in preparing the manuscript. This work was carried out under Contract AT (11-1) 3253 from the U.S. Atomic Energy Commission, and Grant 10220 of the City University of New York Faculty Research Award Program.

Table 1. Expressions for count rates of FCCS Systems in Various Configurations

System configuration	Types of counting signal: Single gamma-ray off-focal	Single gamma-ray focal	Coincident gamma-ray off-focal	Coincident gamma-ray focal
A. N-channel detector	$\nu_1 = 2DN\lambda(1-\lambda)V_{sc}$	$\nu_2 = 2DN\lambda\alpha(1-N\lambda)$	$\mu_1 = ND\lambda^2 V_{sc}$	$\mu_2 = D(N\lambda)^2\alpha$
B. N-channel detector with a summing time, τ, and a dead time, δ, where $\omega = [1+(\tau+\delta)(\nu_1+\nu_2+\mu_1+\mu_2)][1+\tau(\nu_1+\nu_2+\mu_1+\mu_2)]$	$\frac{\nu_1}{\omega}$	$\frac{\nu_2}{\omega}$	$\frac{(\mu_1+\nu_1^2\tau)}{\omega}$	$\frac{[\mu_2+(\nu_2^2+2\nu_1\nu_2)\tau]}{\omega}$
C. Twin probe system where each probe can detect both gamma ray energies and $\mu_1 = 0$.	$\frac{\nu_1}{\omega}$	$\frac{\nu_2}{\omega}$	$\frac{\nu_1^2\tau}{2\omega}$	$\frac{[\mu_2+(\nu_2^2+2\nu_1\nu_2)\tau]}{2\omega}$
D. Twin probe system where each probe can detect only one gamma ray energy	$\frac{\nu_1}{2\omega}$	$\frac{\nu_2}{2\omega}$	$\frac{\nu_1^2\tau}{8\omega}$	$\frac{[\mu_2+(\nu_2^2+2\nu_1\nu_2)\frac{\tau}{2}]}{4\omega}$

Table 2. Experimental design.

	Probe 1 (Gate γ_A)	Probe 2 (Gate γ_B)
Single Gamma Ray Counting		
Accepted	γ_A	
Accepted		γ_B
Rejected (Energy Gating)	γ_B	
Rejected (Energy Gating)		γ_A
Coincidence Counting (True Focal Coincidence)		
Accepted	γ_A	γ_B
Rejected (Energy Gating)	γ_B	γ_A
Rejected (Separate pulse mode and energy gating)	$\gamma_A\gamma_B$	
Rejected (Separate pulse mode and energy gating)		$\gamma_A\gamma_B$
Coincidence Counting (Statistical Coincidence)		
Accepted	γ_A	γ_B
Rejected (Energy Gating)	γ_B	γ_A
Rejected (Separate pulse mode and energy gating)	$\gamma_A\gamma_B$	
Rejected (Separate pulse mode and energy gating)		$\gamma_A\gamma_B$
Rejected (Separate pulse mode and energy gating)	$\gamma_A\gamma_A$	
Rejected (Separate pulse mode and energy gating)	$\gamma_B\gamma_B$	
Rejected (Separate pulse mode and energy gating)		$\gamma_A\gamma_A$
Rejected (Separate pulse mode and energy gating)		$\gamma_B\gamma_B$

REFERENCES

1. R.N. Beck, "A theory of radioisotope scanning systems," in Medical Radioisotope Scanning. Vienna: IAEA, 1964, vol. I, pp. 35-55,1964.

2. G. Freedman, editor, Tomographic Imaging in Nuclear Medicine. New York: Society of Nuclear Medicine, 1973.

3. H.E. Hart, "Focusing collimator coincidence scanning," Radiology, vol. 84, p. 126, January, 1965.

4. B. Warshaw and H.E. Hart, unpublished work, 1968.

5. H.E. Hart, "Comparative resolution of single gamma counting and coincidence counting in focusing collimator scanning systems," Trans. N.Y. Acad. Sci., series II, vol. 30, no. 4, pp. 580-599, February 1968.

6. H.E. Hart, K.S. Rider, J. Korenthal, P. Spetsieris, and A. Bachman, "Lesion detection characteristics of a focusing collimator gamma camera coincidence system," IEEE Trans. Nucl. Sci., vol. NS-21, pp. 665-677, February 1974.

7. W.C. Dewey and W.K. Sinclair, "Criteria for evaluating collimators used in in-vivo distribution studies with radioisotopes," Int. J. Appl. Radiation and Isotopes, vol. 10, pp. 1-16, February 1961.

8. I. Schmitz-Feuerake, "Studies on three-dimensional scintigraphy with γ-γ coincidences," Phys. Med. Biol., vol. 15, pp. 649-656, October 1970.

9. L.J. Dillman, "Radionuclide decay schemes and nuclear parameters for use in radiation-dose estimation," J. Nucl. Med. suppl. no. 2, MIRD Pamphlet no. 4, p. 20, March 1979.

10. P. Richards and H.D. Atkins, "A collimator system for scanning at low energies," J. Nucl. Med., vol. 8, pp. 143-153, February 1967.

11. S. Rudin, "Three Dimensional Radioisotope Imaging using Gamma Ray Coincidence Scanning,"Ph.D. thesis, City College of the City University of New York, 1975.

12. W.M. Smoak, E.M. Smith and P.J.Kenny, "Reduction of physiologic degradation in imaging the liver," J. Nucl. Med., vol. 12, pp. 119-122, March 1971.

13. P.H. Deland and W. Mauderli, "Gating mechanism for motion-free liver and lung scintigraphy," J. Nucl. Med., vol. 13, pp. 939-941, December 1972.

14. S. Askienazi, P. Marti, B. Bok, M. Verel and L. Richard, "Non-radioactive hardware device for anatomical landmarks and patient motion correction," abstract, J. Nucl. Med., vol. 14, p. 378, June 1973.

15. V.P. Blings, C.B. Martin, I.G. Pollack and J.T. McClintock, "Electronic device corrects for motion in gamma camera images," J. Nucl. Med.,vol. 15, pp. 36-37, January 1974.

16. Phelps, M.E.; et al, "Application of annihilation coincidence detection to transaxial reconstruction tomography," J. Nucl. Med., vol. 16, pp. 210-224, March, 1975.

17. Cho, Z.H., "General views on 3-D image reconstruction and computerized transverse axial tomography," IEEE Trans. on Nucl. Sci., vol. NS-21 , pp. 44-71, June 1974.

18. Beck, R.N. et al, "Effects of Scattered Radiation on Scintillation Detector Response, Medical Radioisotope Scintigraphy," Vol. 1, pp. 595-615, Vienna:IAEA, 1969.

19. Robertson, J., private communcation.

FIG. 1. N channel focusing collimator where it is assumed that the fields of view intersect solely within a focal volume, α, with each channel field of view exhibiting an off-focal volume, V_{sc}. Note the total volume, V_{total}, of each field of view (focal and off-focal) is $V_{sc} + \alpha$ where V_{sc} was taken to be 1 in previous analysis.[5]

FIG. 2. The twin probe configuration where the N individual single channel detectors each of solid angle efficiency λ can be thought of as if they were two "single channel" detectors each subtending a solid angle of $N\lambda/2$ at the focus, F, and each including an off-focal volume, $NV_{sc}/2$, with the off-focal efficiency λ. The focal volume is α and the uniform tissue activity per volume is D. For simplicity in representation the umbra and penumbra characteristics of the experimental tapered channel collimators have been replaced by idealized cylindrical fields of view.

FIG. 3. The configuration of the experiment showing a circuit block diagram where cross-over timing was used. The coincidence module had a lower limit resolve time of 10 ns; however, in practice double delay line (DDL) amplifier noise made it necessary to employ a somewhat larger resolve time, 55 ns, so that true coincidence events would not be rejected.

FIG. 4. Scanning geometry. The scans were carried out by attaching the sources to an X-Y-Z traverse with positional reproducibility in all directions to better than 0.1 mm. The focal points of the two probes were aligned to better than 0.2 mm in the critical transverse, X, direction. A series of scans in the X-Y plane were obtained for incremental 2 mm intervals in the Z direciton.

FIG. 5. Two superimposed families of isoresponse surfaces of the two con-focal collimators whose axis are at right angles, along the BB' and AA' directions. The OA direction is into the plane of the figure. The isoresponse surfaces for the FCCS mode are the product of the individual probe responses -- a family of concentric oblate spheroids or ellipses of rotation with circular cross-section in planes parallel to the plane of the two collimator axes (plane AB).

FIG. 6. Phantom containing 160 μCi ^{75}Se with a single cold defect and two adjacent hot epoxy globs arising from selective concentration of the radioisotope. As a result of the ^{75}Se absorption, the phantom was more demanding than one with a single cold defect.

FIG. 7. Image using 10 contrast gradations resulting from FCCS scan of phantom of Fig. 6 where contrast enhancement (ratio of minimum to maximum activities observed) is 53%. Values obtained for each $(2\ mm)^3$ lattice point were corrected for background, statistical or "false" coincidences due to the 55ns resolve time (at no time more than 10 to 20% of the total, 1/7), and depth attenuation. The average scan VID was $\sim$20,000 true counts per cm^3 and each 12 mm x 18 mm plane took about 2 hours to scan.

FIG. 8. Single gamma ray scan (sum of count from both probes) obtained simultaneously with FCCS scan of Fig. 7. Contrast enhancement is 78%. Background was negligible and the depth attenuation factor was neglected since the single gamma ray isoresponse contours exhibit such a large depth of focus that over the scan region the effective average depth attenuation was essentially constant for the homogeneous medium concerned. The lesion signal would, of course, depend upon the lesion depth, but the correction factor can only be determined paradoxically after the lesion has been located and in fact no lesion could be detected.

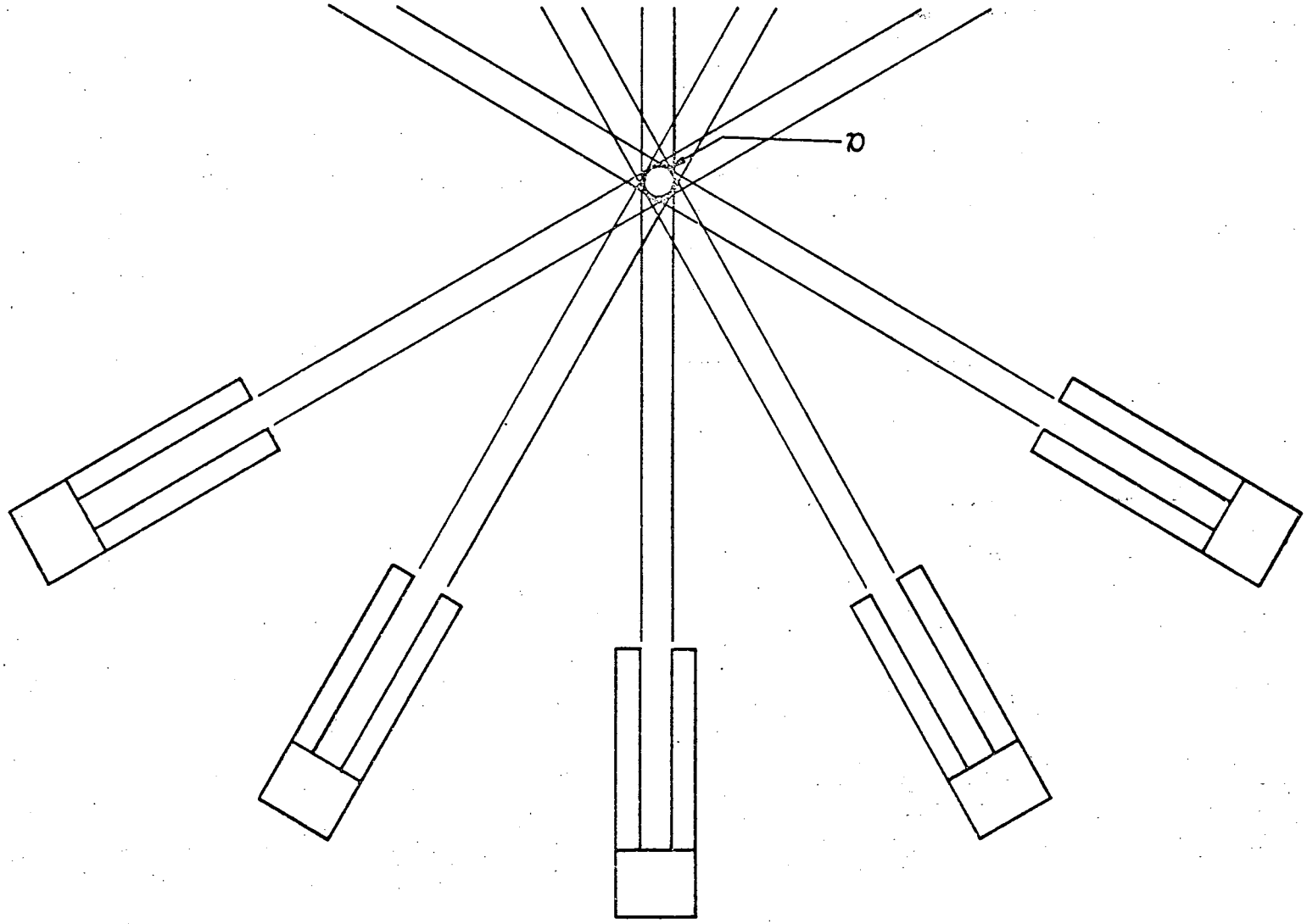
10

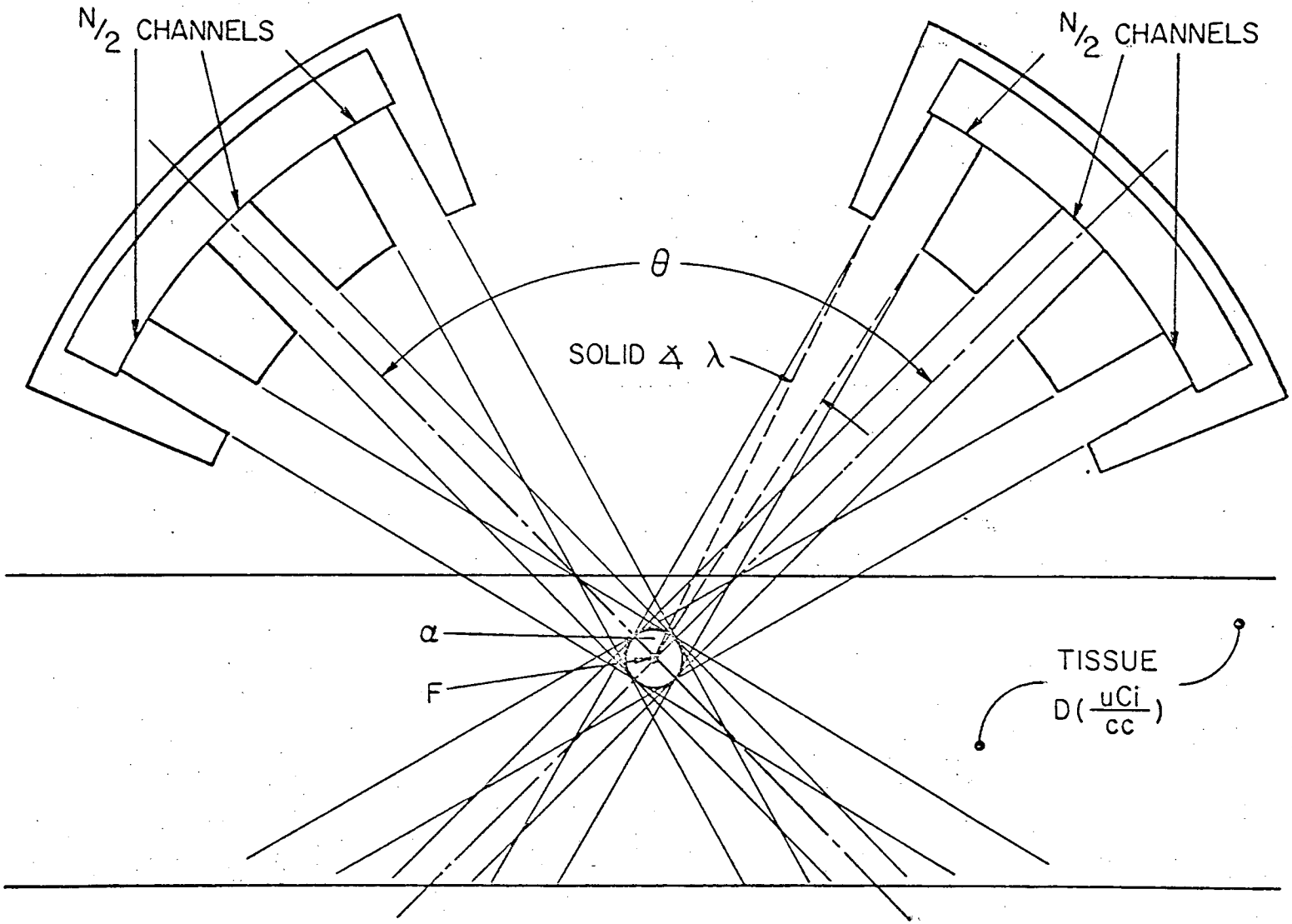
N/2 CHANNELS
N/2 CHANNELS
θ
SOLID ∡ λ
α
F
TISSUE
D(uCi/cc)

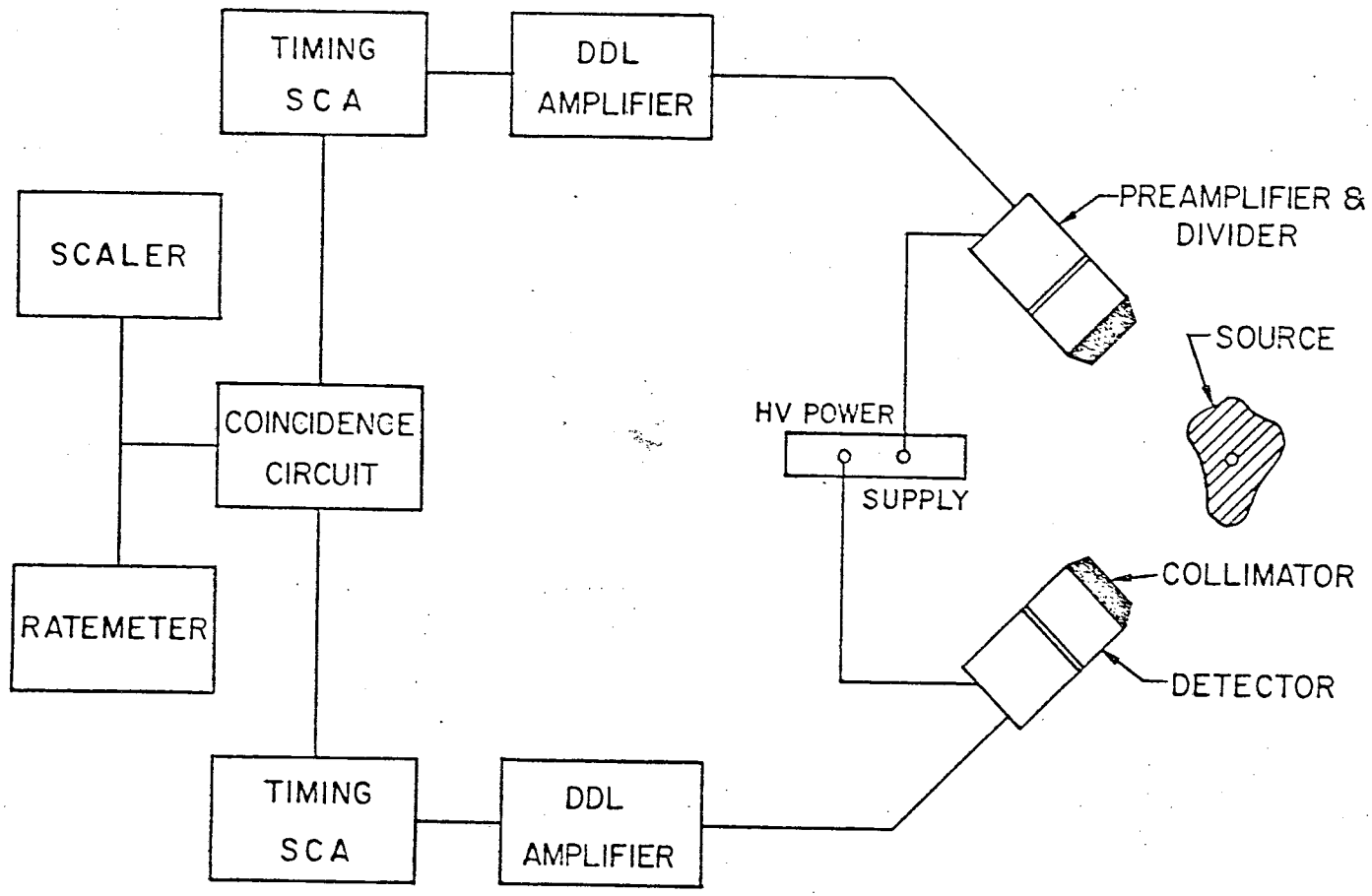
TIMING
SCA
DDL
AMPLIFIER
SCALER
PREAMPLIFIER &
DIVIDER
SOURCE
COINCIDENCE
CIRCUIT
HV POWER
SUPPLY
RATEMETER
COLLIMATOR
DETECTOR
TIMING
SCA
DDL
AMPLIFIER

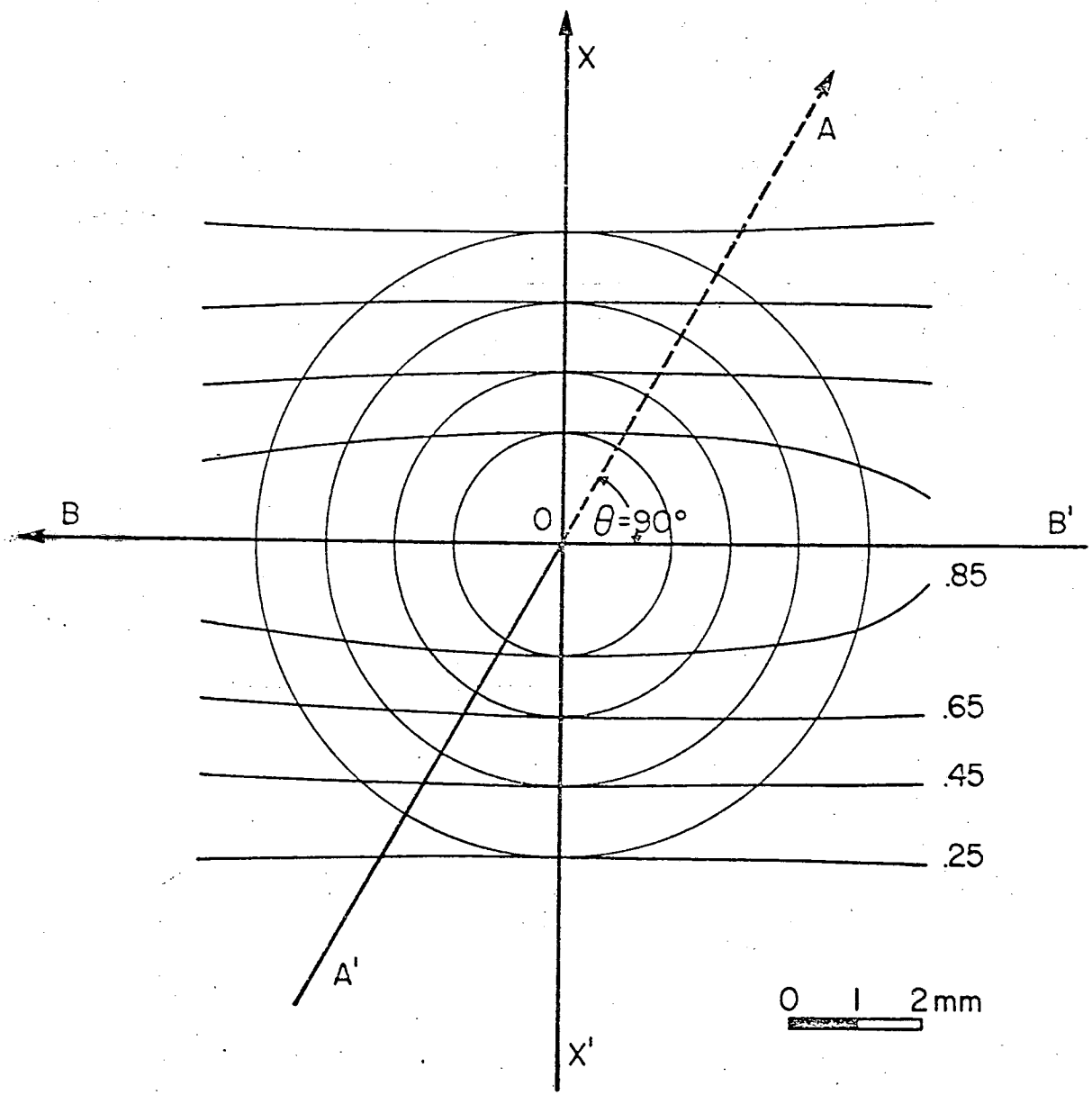
X
A
B
O
θ=90°
B'
.85
.65
.45
.25
A'
0 1 2mm
X'

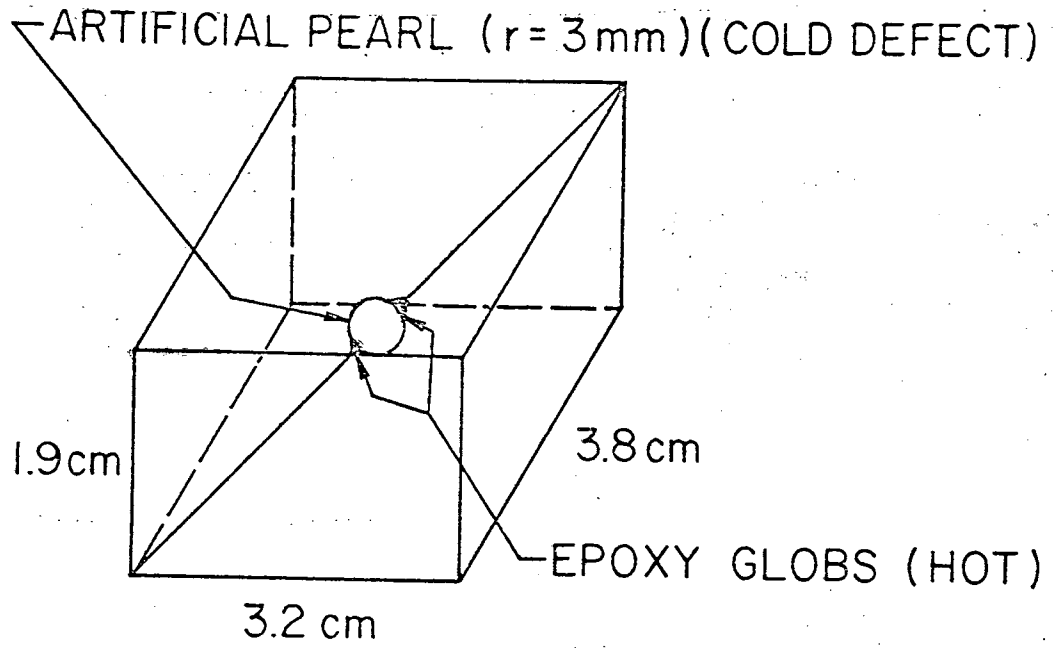

UNIFORM CONCENTRATION OF ^{75}SE

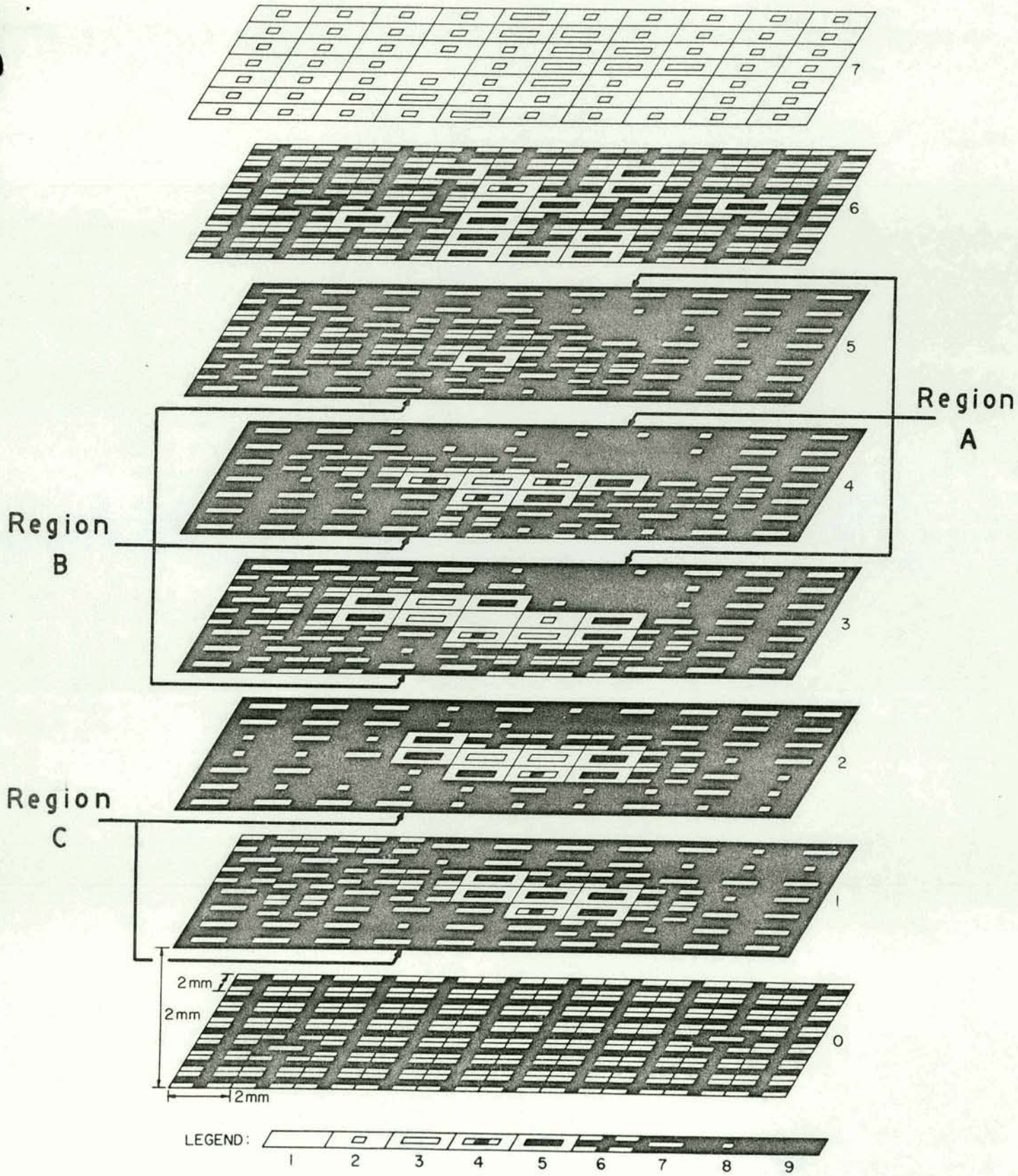
7
6
5
4
3
2
1
0
Region A
Region B
Region C
2mm
2mm
2mm
LEGEND:
1
2
3
4
5
6
7
8
9

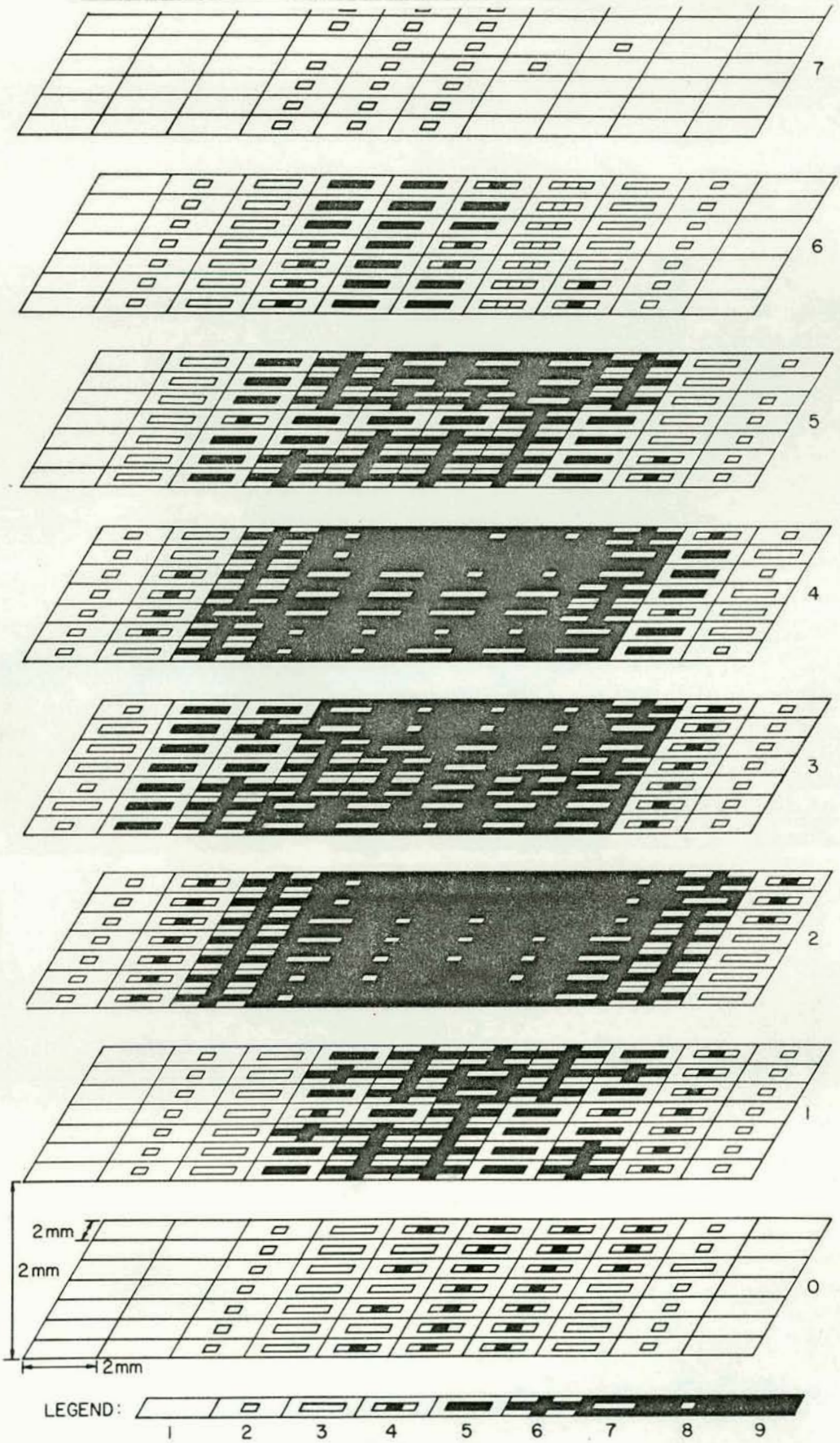
7
6
5
4
3
2
1
0
2mm
2mm
2mm
LEGEND:
1
2
3
4
5
6
7
8
9

APPENDIX IV

Current Status of FCCS Research:

The basic five probe focussing collimator coincidence scanning system (FCCS) employed has been rather completely detailed in last year's renewal proposal. The PhD dissertation of Dr. Stephen Rudin (CUNY '75) contains some additional material. Several changes and additions have been carried out in the last year or are currently being worked on.

The electronics and on line computer software has been modified[1] by augmenting the system with another scaler operating in a daisy chain with the existing scaler-timer. This arrangement allows for the future addition of yet another scaler should one be desirable. Using the additional data an isotope specific algorithm is being worked out which will more effectively recover the true coincidence count rate from the energy discriminated coincidence count rate and the raw timing coincidence count rate. In the future we will investigate the possibility of further reducing the resolve time by a combination of quicker timing discriminators and fast time to amplitude conversion. Such a system may provide effective resolve times of ~10 ns thereby reducing the statistical coincidence rate by a factor of ~4.

Data acquisition during the year was restricted to the determination of point source response functions and the imaging of phantoms. The five probe system was first equipped with broad focus high energy collimators (Raytheon 100/18B) which were chosen as initial equipment since they were available at nominal cost. The scan results were promising. However due to the extremely

broad field of views of the collimators, high resolution was of course not possible. Moreover the statistical coincidence rate which is proportional to the square of single gamma count rate was too high for distributed three dimensional sources at clinically typical tissue concentrations of radio-activity. The system has now been fitted with a new set of intermediate energy collimators (Raytheon FC 100/9B) which allow twice the resolution of the previous set (Table 1). The single gamma count rate is reduced by a factor of $\sim$ .36 and therefore the statistical coincidence count rate is only 1/8 that for the previous assembly. Since the new collimator has a focal efficiency 4/3 greater as well, there is a 11 fold improvement in the ratio of the true coincidence count rate to the statistical coincidence count rate.

A series of point spread functions (PSF), Fig. 1, has been obtained both in air and in tissue equivalent scattering medium at various depths using a point source of Se^{75} of 20 μCi activity and diameter 1 mm. The results indicate a FWHM of 7.5 mm for coincidence scanning in air at the focal plane. The FWHM is not significantly altered by the presence of the scattering medium (See Appendix III attached). The FWHM in the longitudinal direction is $\sim$ 8 mm, or roughly the same as the transverse FWHM. These well localized PSF's are ideally suited to a deconvolution procedure on the scan data from extended source phantoms. At present two methods of data analysis are being investigated, one a matrix inversion method and the other an apparently new direct iterative method whose efficiency is enhanced by the highly local nature of the PSF's. A transform matrix based on the PSF in air has been defined and software written to invert the matrix. The resulting matrix which transforms the image space to the object space is then used to deconvolute scan data. At present the program has only been used with

simulated data. Work on a program to implement the second method is just beginning.

The scanning of extended phantoms has just begun. A void (solid plastic sphere) of 1.15 cm^3 in 250 ml of a homogeneous solution of sodium selenite (Se^{75}) of actively ~ 0.5 μCi/Ml was scanned twice-once with the focal plane through the center of the void and again with the focal plane 12 mm above the center of the void (Fig. 2). The site of lowest activity was set to 0 and a simple smoothing carried out by giving the average of the 4 nearest neighbors equal weight with the central data point.

A linear density scale was then used to display the counts with a 4 mm lattice spacing. Note that the spherical void is clearly displayed in the "central" plane scan Fig. 2a. The scan of Fig. 2b through a plane only 1.2 cms above the center of the 1.3 cm diameter bead is essentially uniform, demonstrating the tomographic sharpness of the system.

The above results however, are in a sense just preliminary since the ultimate inherent resolution of the system is actually much greater. Three dimensional data averaging making appropriate use of the 14 nearest neighbors should further reduce the effect of statistical fluctuations while deconvolution should significantly reduce the loss of resolution arising from the finite extension of the PSFs. These two data handling approaches should permit cold lesion detection on a multi-millimeter scale.

For radioisotope imaging of small organs (~ 50 grams) or for rescanning suspicious regions observed on scans taken using faster, lower resolution

techniques, quite adequate three dimensional F.C.C.S. results should be obtainable in less than 1 hour with the current system. Further modifications in the collimators and electronics could easily reduce the time required by ~ 50%. It would appear that a variety of clinical applications for F.C.C.S. may exist.

TABLE 1

	HC 100/18B	FC 100/9B
Focal Efficiency	0.74%	1.0%
Holes	19	121
Focal Length	100 mm	100 mm
Thickness	80 mm	75 mm
Full Width Half Max. (singles)	18 mm	9 mm
Relative Sensitivity to an extended source	1	.36

Both collimators have tapered hexagonal channels.

FIG. 1a.

SCAN- FP1.

PT. SOURCE IN AIR.
FOCAL PLANE.

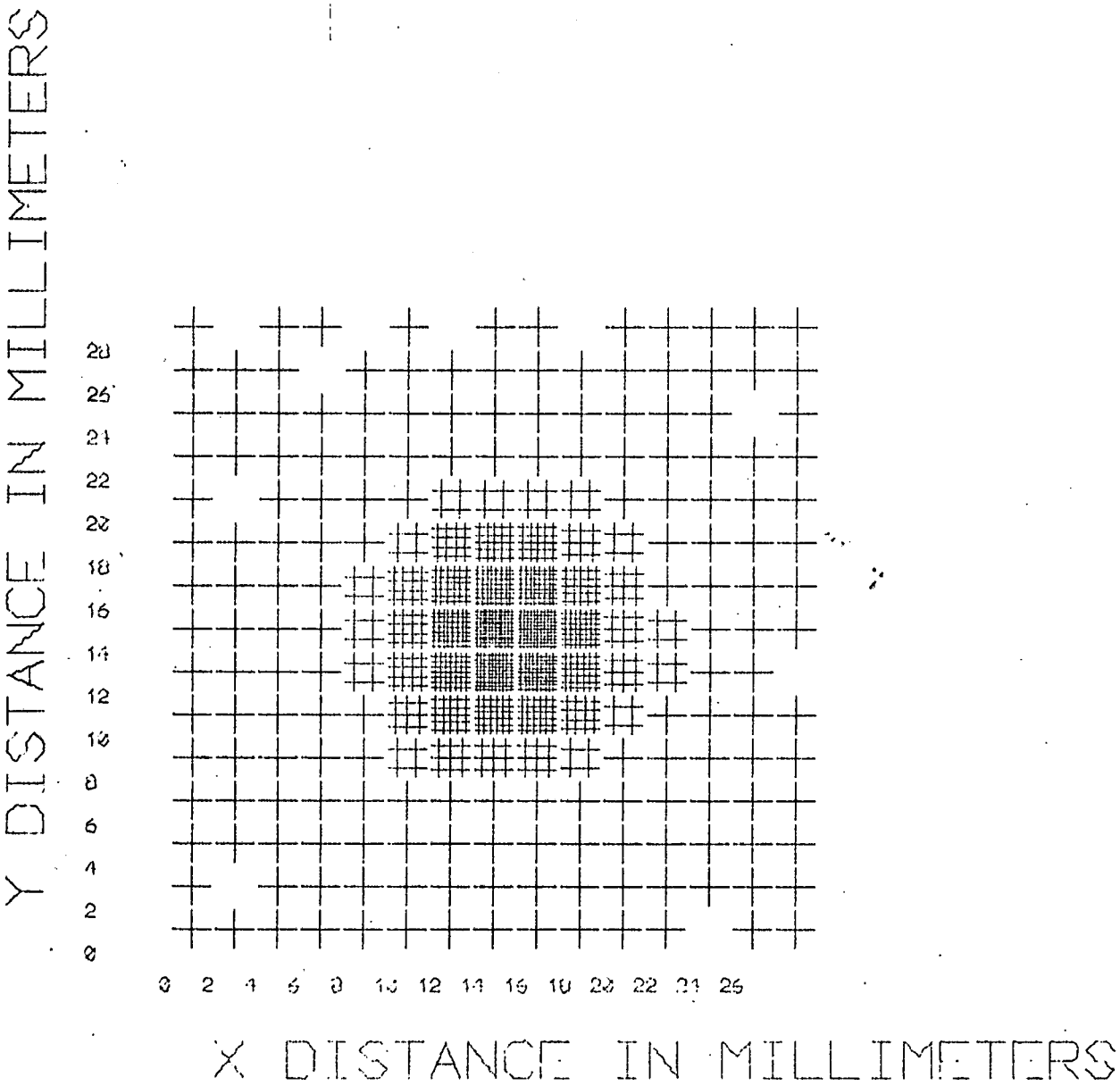

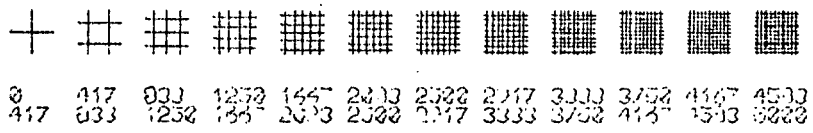

GREY SCALE

FIG. 1b.

SCAN- SC06

POINT SOURCE IN AIR.
4 MM. BELOW POCAL PLANE.

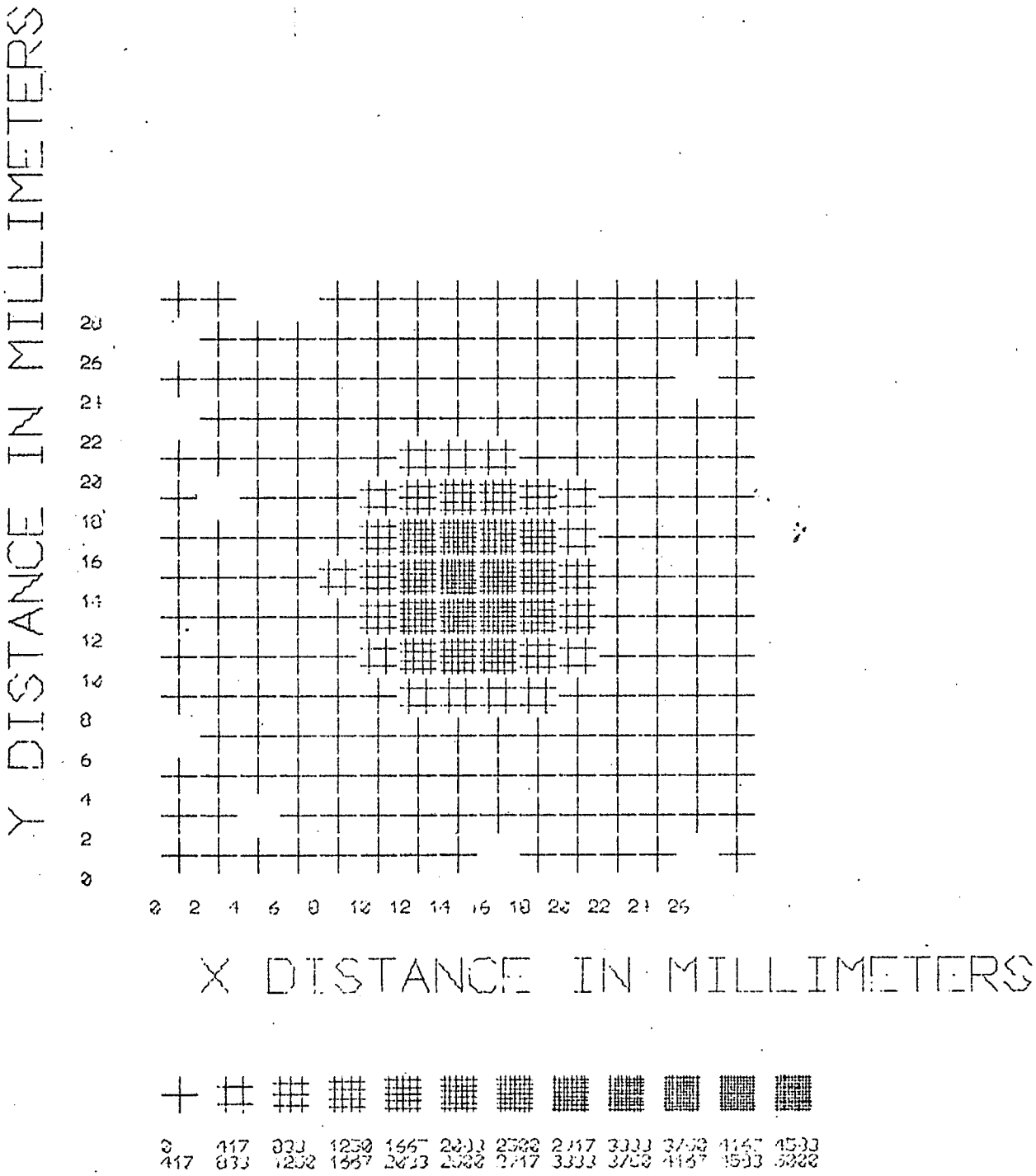

FIG. 1 c.

SCAN- SC15

PT. SOURCE IN AIR.
4 MM. ABOVE FOCAL PLANE.

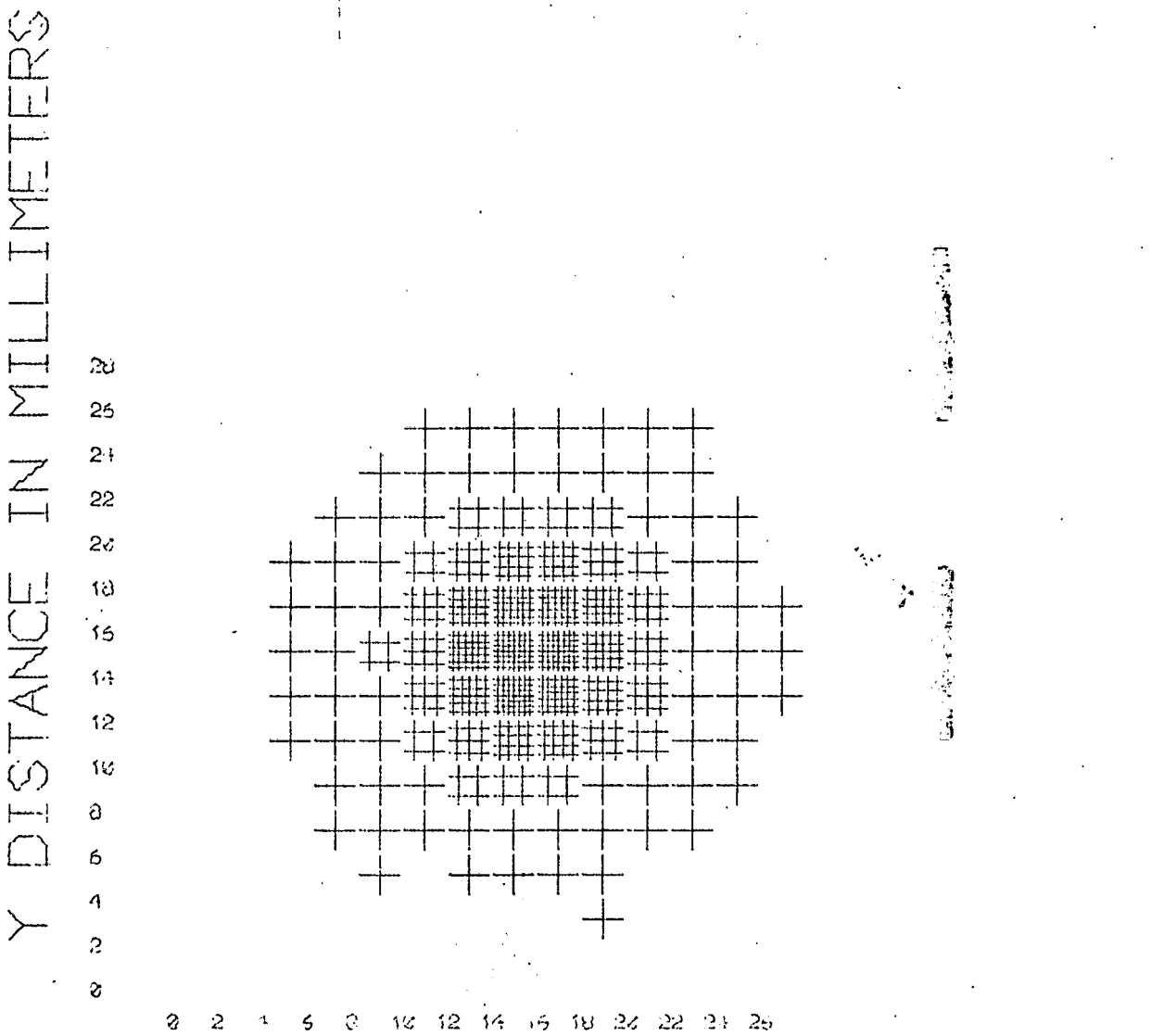

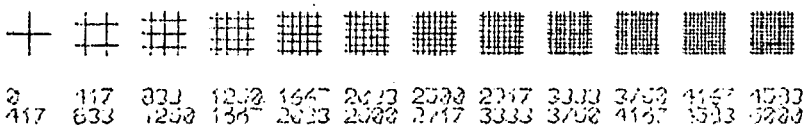

GREY SCALE

FIG. 1 d.

SCAN- SC17

PT. SOURCE IN AIR.
8 MM. BELOW FOCAL PLANE.

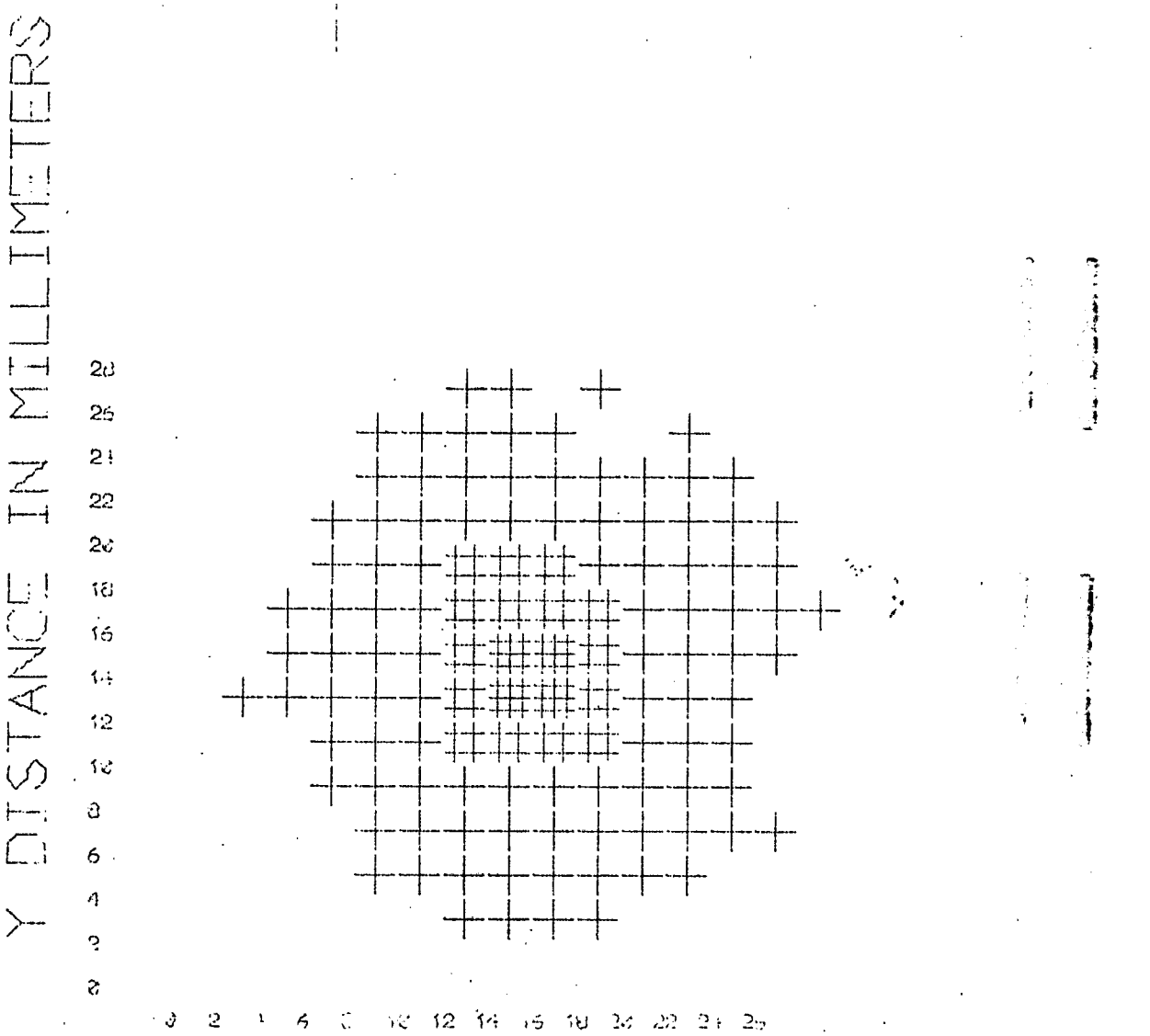

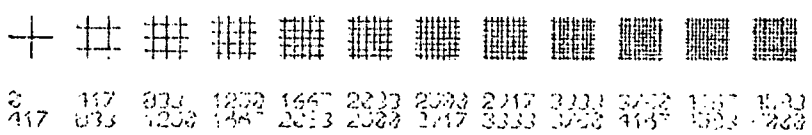

GREY SCALE

FIG. 1c.

SCAN- SC16

PT. SOURCE IN AIR.
8 MM. ABOVE FOCAL PLANE.

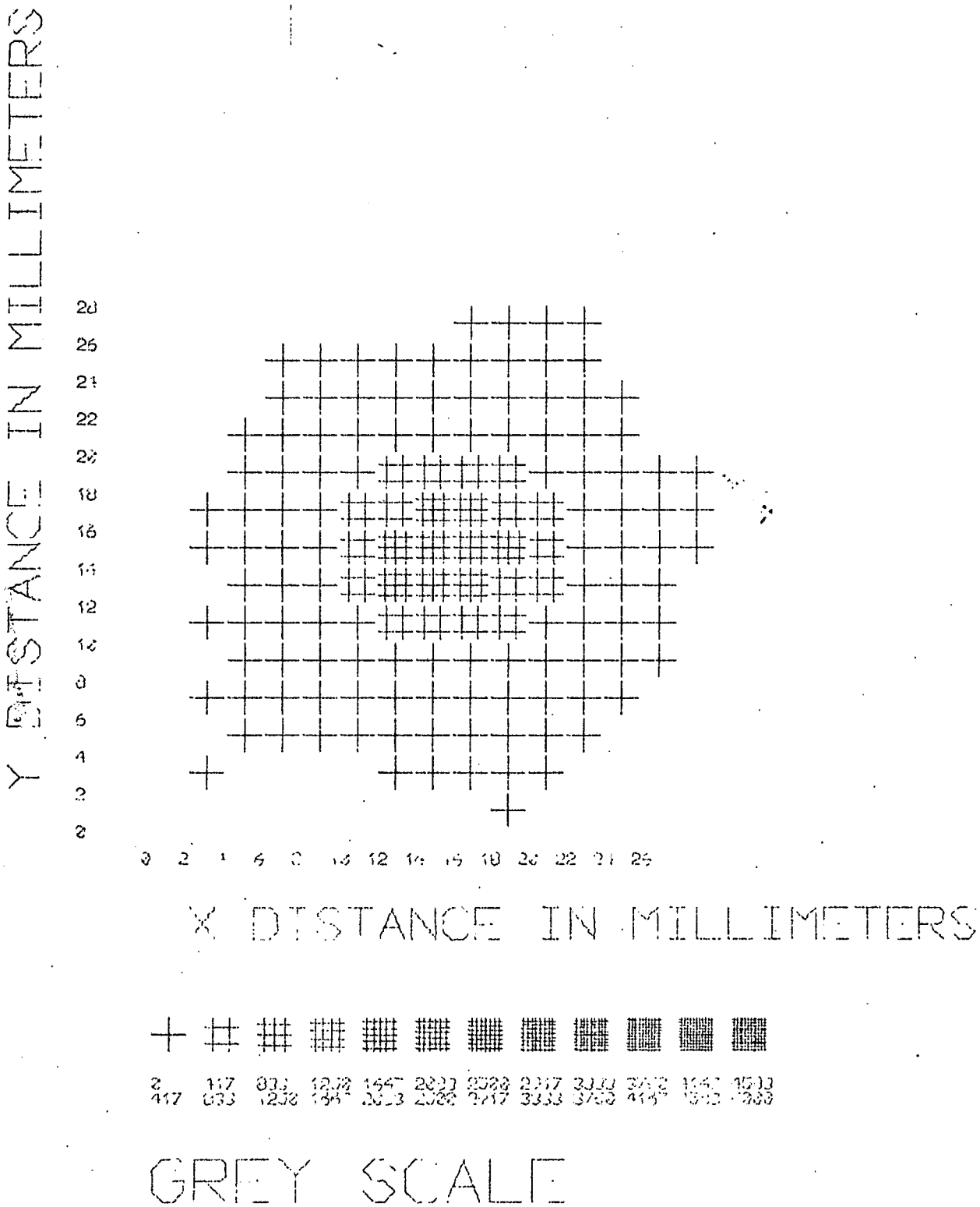

FIG. 1 f.

SCAN- C09.

FOCAL PLANE. SCATTERING MEDIUM 8MM. ABOVE DETECTOR.

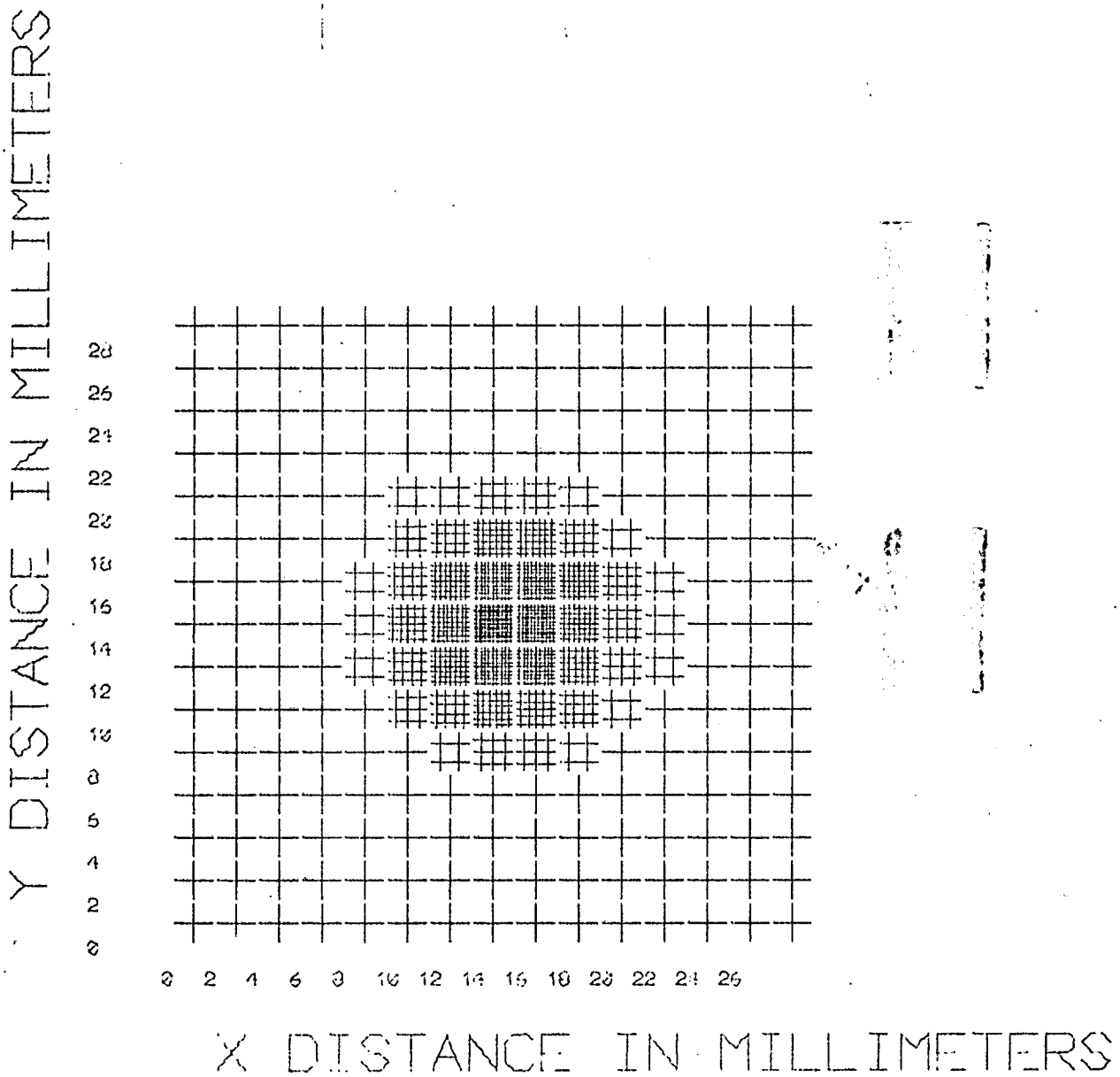

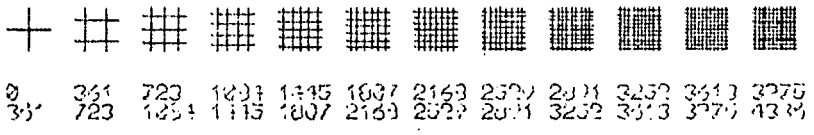

GREY SCALE

FIG. 19.

SCAN- C10.

4 MM. BELOW FOCAL PLANE. SCATTER MEDIUM 4 MM. ABOVE DETECTOR.

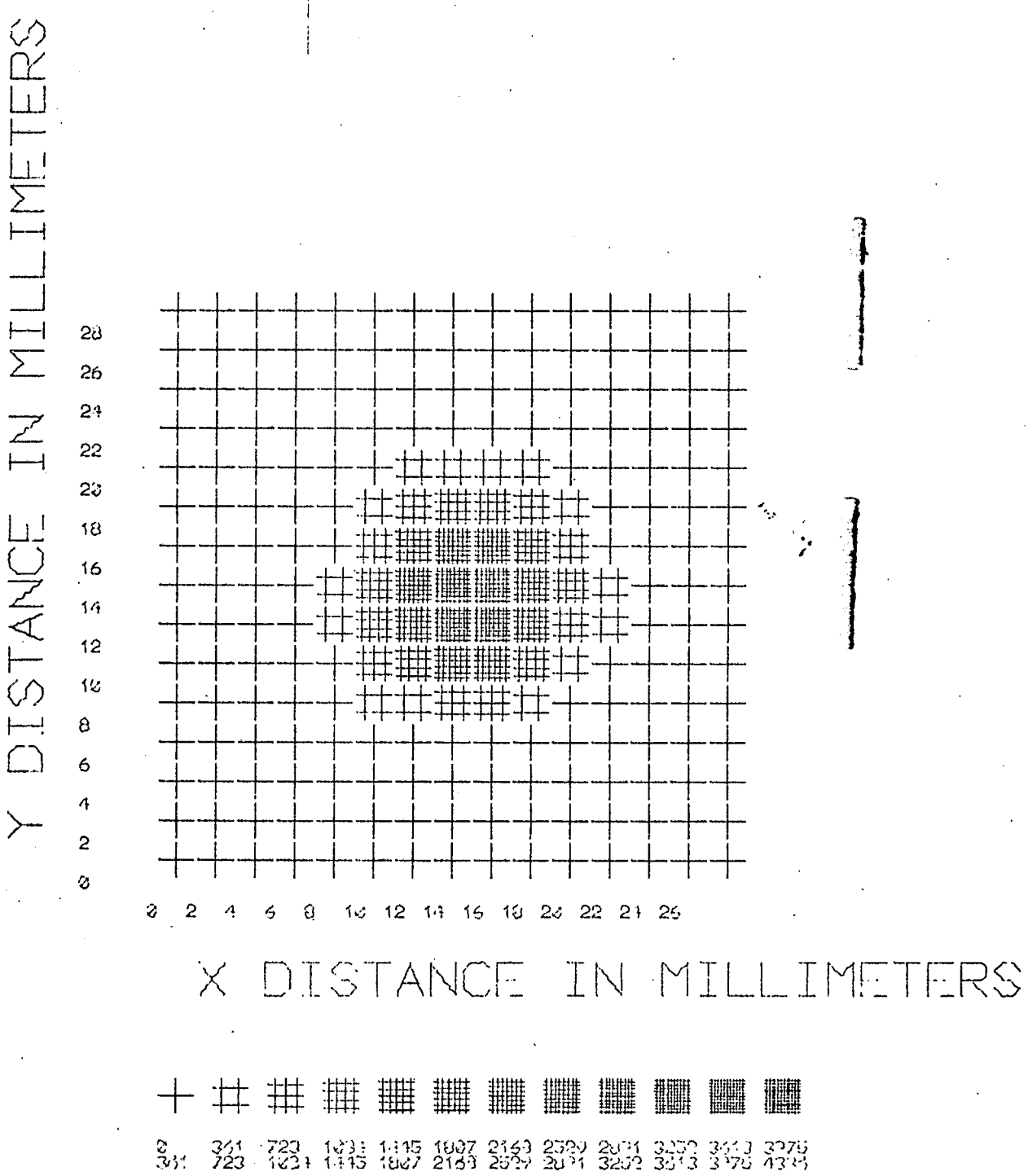

GREY SCALE

FIG. 1 h.

SCAN- SC11

4 MM. ABOVE FOCAL PLANE. SCATTER
MEDIUM 12 MM. ABOVE DETECTOR.

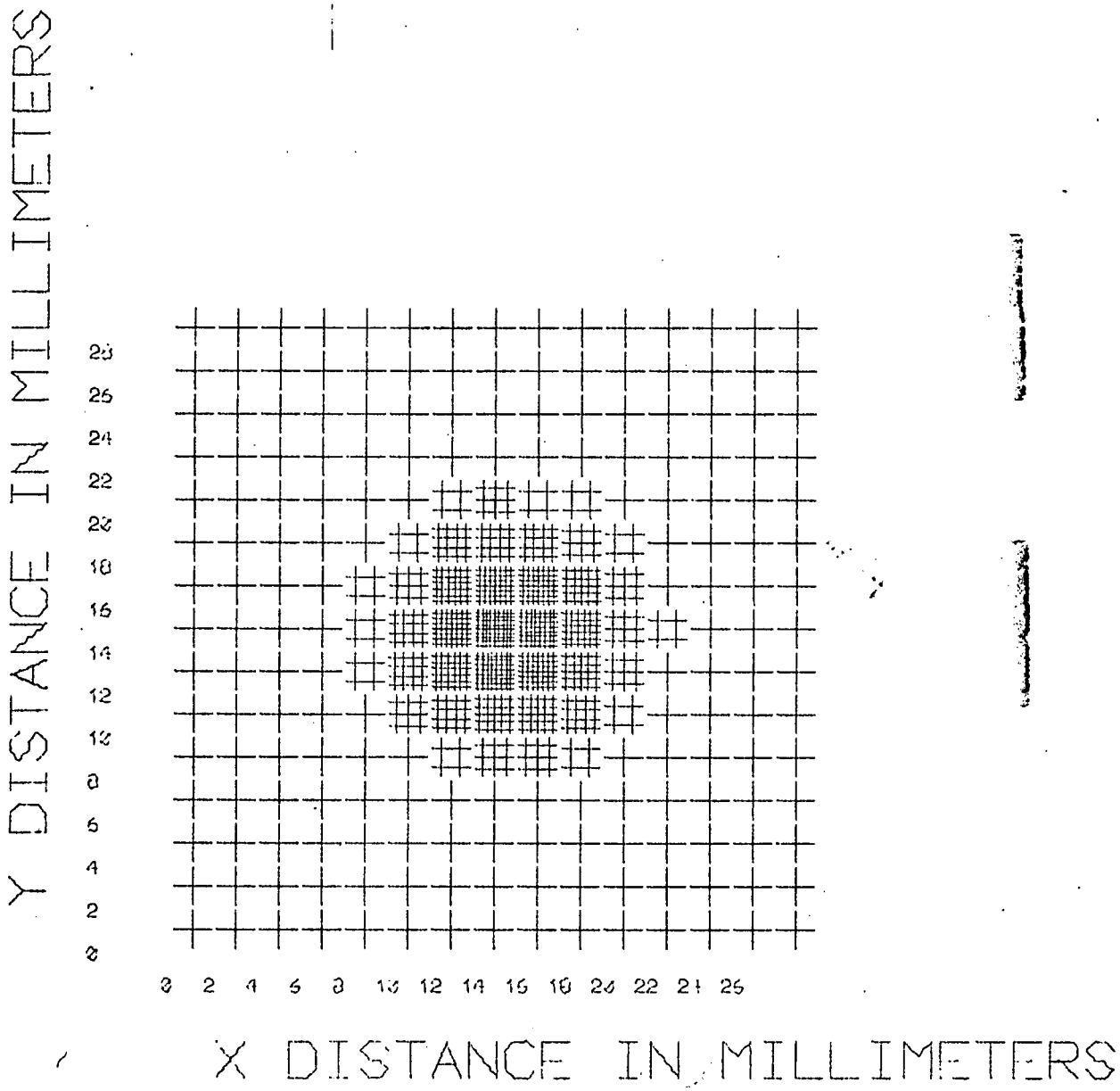

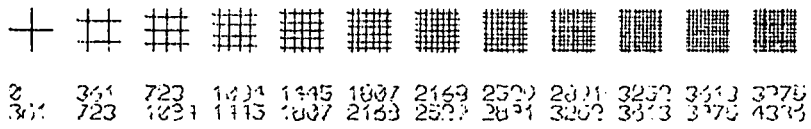

GREY SCALE

FIG. 1i.

SCAN- SC05

8 MM. BELOW FOCAL PLANE. MEDIUM
ADJACENT TO DETECTOR.

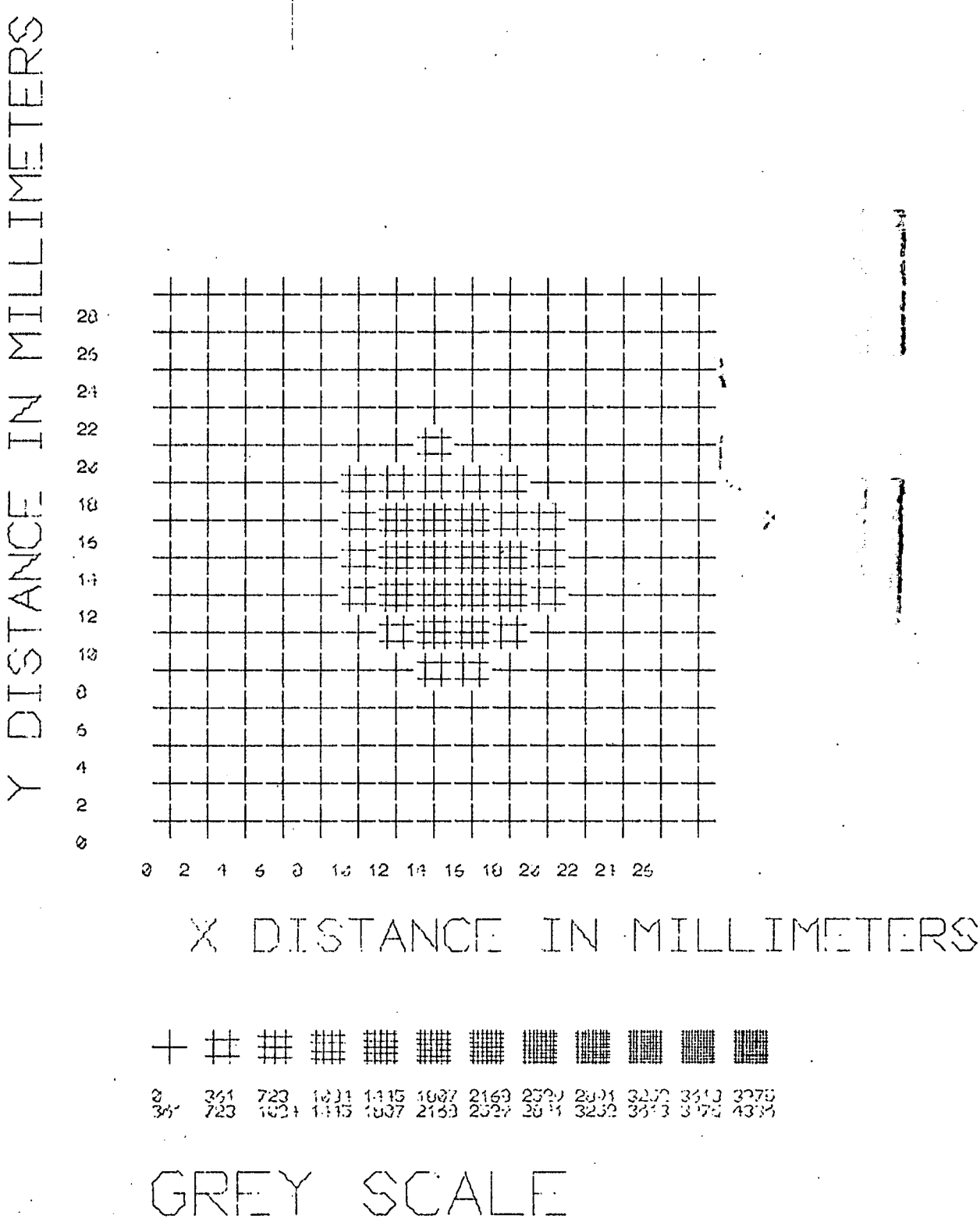

FIG 2a.

SCAN- D003

VOID IN FOCAL PLANE.
SIMPLE SMOOTHING.

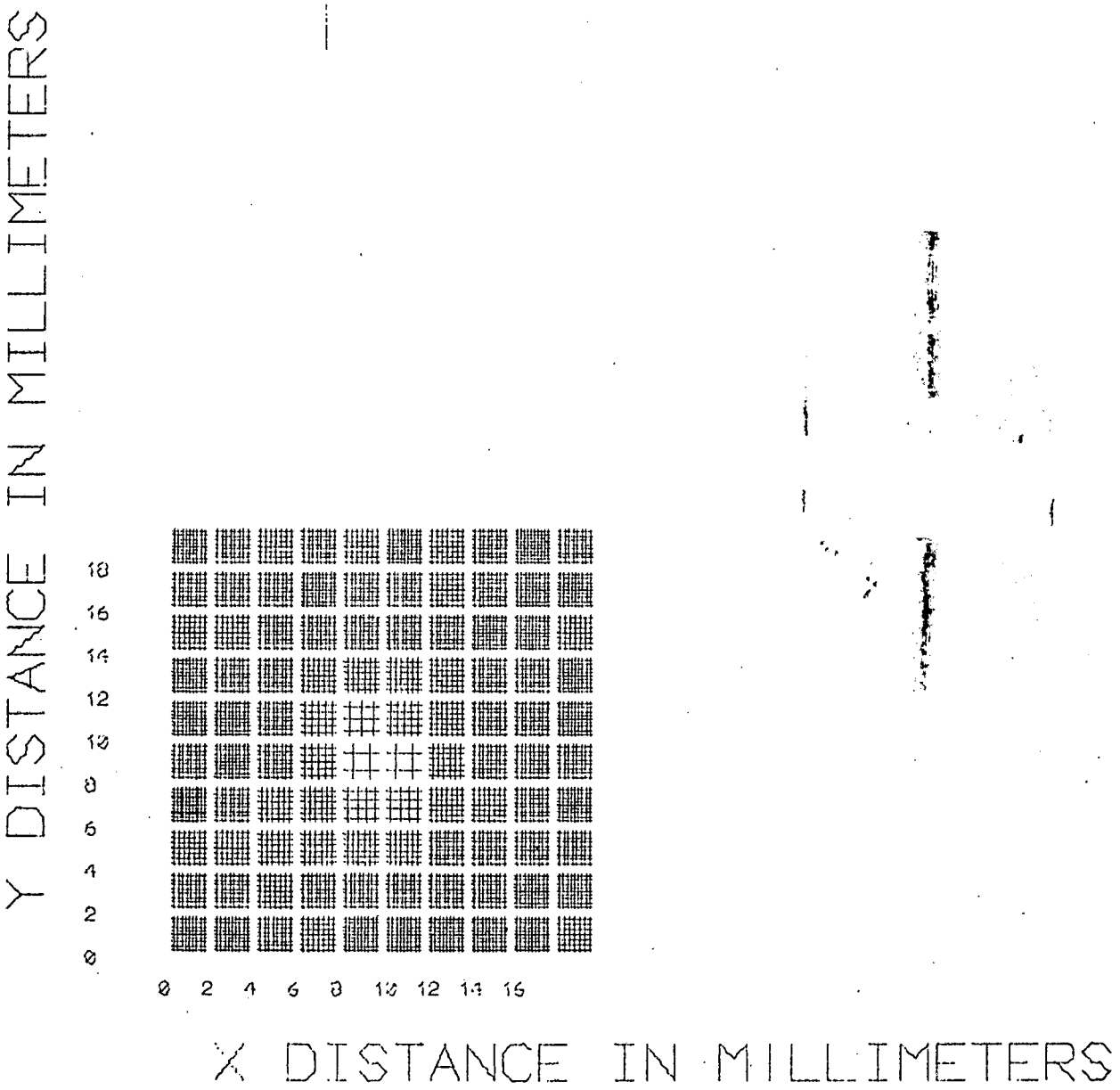

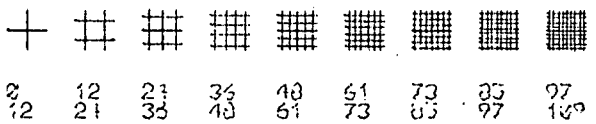

GREY SCALE

FIG. 2b.

SCAN- D002

VOID 12MM. ABOVE FOCAL PLANE
SIMPLE SMOOTHING.

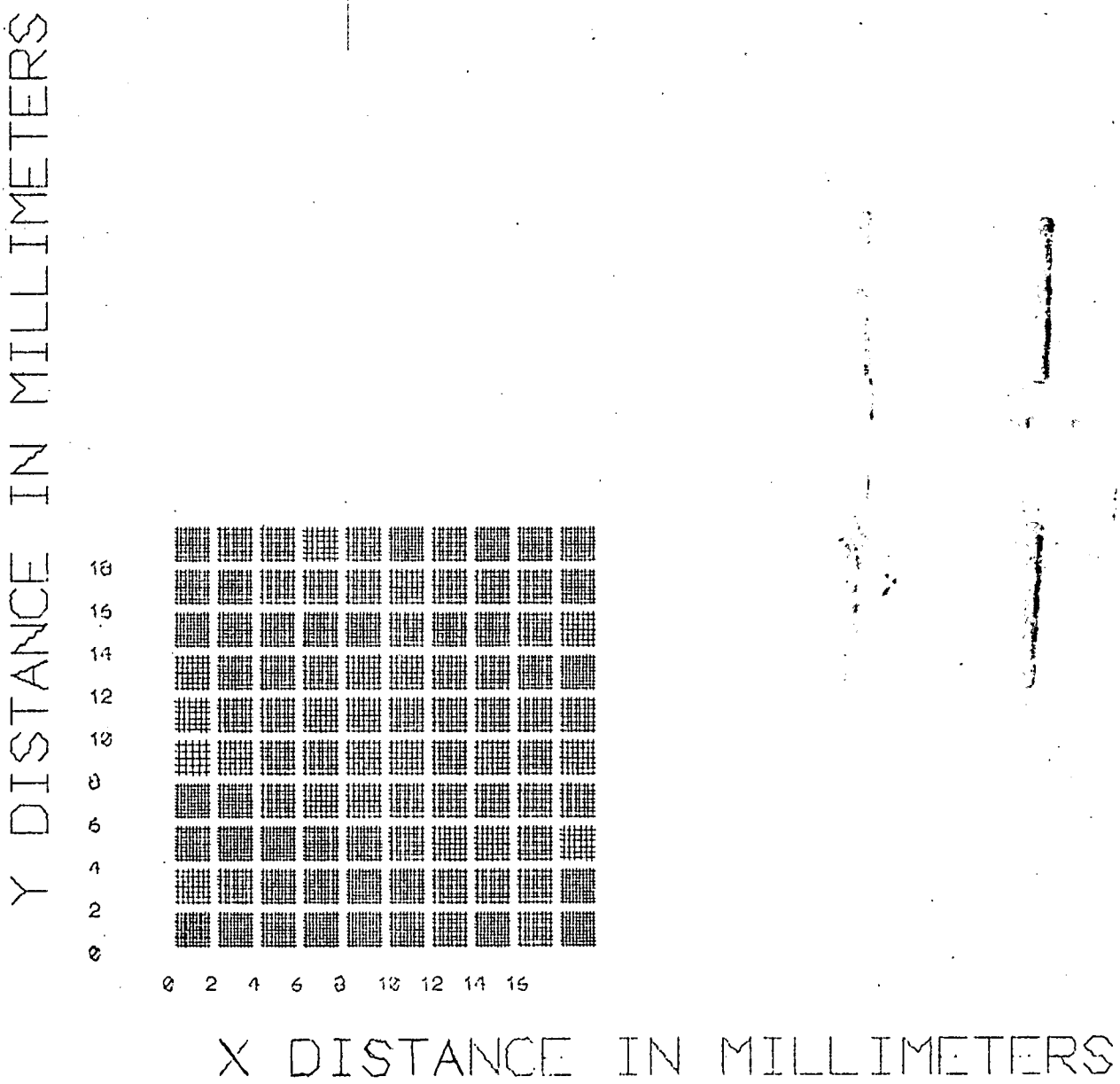

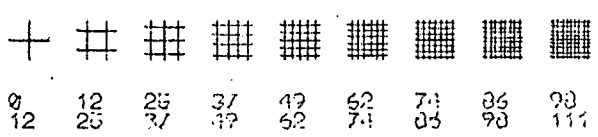

GREY SCALE